How Well Do We Understand the Land-Ocean-Atmosphere Carbon Cycle?

David Crisp[1], Han Dolman[2], Toste Tanhua[3], Galen A McKinley[4], Judith Hauck[5], Simon Eggleston[6], and Valentin Aich[6]

[1]Jet Propulsion Laboratory, California Institute of Technology
[2]Vrije Universiteit
[3]GEOMAR Helmholz Centre for Ocean Research
[4]Lamont Doherty Earth Observatory of Columbia University
[5]Alfred Wegener Institute Helmholtz Centre for Polar and Marine Research
[6]World Meteorological Organization

November 30, 2022

Abstract

Fossil fuel combustion, land use change and other human activities have increased the atmospheric carbon dioxide (CO_2) abundance by almost 50% since the beginning of the industrial age. These changes would have been much larger if natural sinks in the land biosphere and ocean had not removed over half of this anthropogenic CO_2. Here, we review the current state of knowledge of the ocean, land and atmospheric carbon cycles, identify emerging measurement and modeling capabilities, and gaps that must be addressed to diagnose the processes driving the carbon cycle and predict their response to human activities and a changing climate. The anthropogenic CO_2 uptake by the ocean has increased over this period, as the atmospheric CO_2 partial pressure (pCO_2) has increased. For the land carbon cycle, the emerging picture is more complicated. Over the past three decades, the uptake of CO_2 by intact tropical humid forests appears to be declining, but these effects are offset by a net greening across mid- and high-latitudes associated with afforestation, agricultural, and longer growing seasons. These studies have also revealed measurement gaps and other limitations in our understanding of the evolving carbon cycle. They show that continued ship-based observations combined with expanded deployments of autonomous platforms are needed to quantify ocean-atmosphere fluxes on policy relevant spatial and temporal scales. They also reinforce the urgent need for more comprehensive measurements of stocks, fluxes and atmospheric CO_2 in humid tropical forests and across the Arctic and boreal regions, which appear to be experiencing rapid change.

How Well Do We Understand the Land-Ocean-Atmosphere Carbon Cycle?

David Crisp[1], Han Dolman[2], Toste Tanhua[3], Galen A. McKinley[4], Judith Hauck[5], Simon Eggleston[6], Valentin Aich[6]

[1]Jet Propulsion Laboratory, California Institute of Technology, Pasadena, CA, USA.

[2]Department of Earth Sciences, Vrije Universiteit Amsterdam, Amsterdam, The Netherlands.

[3]GEOMAR Helmholtz Centre for Ocean Research Kiel, Marine Biogeochemistry, Kiel, Germany.

[4]Columbia University and Lamont Doherty Earth Observatory, Palisades, NY, USA.

[5]Alfred-Wegener-Institut, Helmholtz-Zentrum für Polar und Meeresforschung, Bremerhaven, Germany.

[6]Global Climate Observing System, World Meteorological Organization, Geneva, Switzerland.

Corresponding author: first and last name (David Crisp david.crisp@jpl.nasa.gov)

Key Points:

- Carbon dioxide (CO_2) emissions from fossil fuel use and other human activities have increased its atmospheric abundance by almost 50% during the industrial age.
- These increases would have been much larger if natural sinks in the ocean and on land had not removed over half of this CO_2, maintaining an airborne fraction < 45%.
- New measurements and models are providing insights into the carbon cycles as the land and ocean sinks continue to respond to human activities and climate change.

Abstract

Fossil fuel combustion, land use change and other human activities have increased the atmospheric carbon dioxide (CO_2) abundance by almost 50% since the beginning of the industrial age. These changes would have been much larger if natural sinks in the land biosphere and ocean had not removed over half of this anthropogenic CO_2. Here, we review the current state of knowledge of the ocean, land and atmospheric carbon cycles, identify emerging measurement and modeling capabilities, and gaps that must be addressed to diagnose the processes driving the carbon cycle and predict their response to human activities and a changing climate. The anthropogenic CO_2 uptake by the ocean has increased over this period, as the atmospheric CO_2 partial pressure (pCO_2) has increased. For the land carbon cycle, the emerging picture is more complicated. Over the past three decades, the uptake of CO_2 by intact tropical humid forests appears to be declining, but these effects are offset by a net greening across mid- and high-latitudes associated with afforestation, agricultural, and longer growing seasons. These studies have also revealed measurement gaps and other limitations in our understanding of the evolving carbon cycle. They show that continued ship-based observations combined with expanded deployments of autonomous platforms are needed to quantify ocean-atmosphere fluxes on policy relevant spatial and temporal scales. They also reinforce the urgent need for more comprehensive measurements of stocks, fluxes and atmospheric CO_2 in humid tropical forests and across the Arctic and boreal regions, which appear to be experiencing rapid change.

Plain Language Summary

Since the beginning of the industrial age in the mid-1700s, fossil fuel combustion, land use change and other human activities have increased the atmospheric carbon dioxide (CO_2) concentration to levels never before seen in human history such that CO_2 is now the primary driver of climate change. The atmospheric CO_2 abundance and its effect on the climate would have been much larger if natural processes in the ocean and on land carbon cycle had not absorbed over half of the CO_2 emitted by these human activities. Here, we review our understanding of anthropogenic CO_2 emissions and the processes controlling the emissions and uptake of CO_2 by the natural carbon cycle as it responds to continuing human activities a changing climate.

1 Introduction

Since the beginning of the industrial age, human activities have increased the atmospheric concentrations of carbon dioxide (CO_2) and other greenhouse gases (GHGs) to levels never before seen in human history. These large increases are driving climate change, because CO_2 is an efficient greenhouse gas with an atmospheric lifetime measured in centuries. Bottom-up statistical inventories indicate that fossil fuel combustion, industry, agriculture, forestry, and other human activities are now adding more than 11.5 petagrams of carbon (Pg C) to the atmosphere each year (Friedlingstein et al., 2019; 2020). Direct measurements of CO_2 in the atmosphere and in air bubbles in ice cores indicate that these and other human activities have increased the globally averaged atmospheric CO_2 dry air mole fraction from less than 277 parts per million (ppm) in 1750 to more than 410 ppm today. Measurements from Mauna Loa

Observatory show that over half of this increase has occurred since 1985 and over a quarter has happened within the past 15 years (Dlugokencky et al., 2018).

These increases would be much larger if processes operating in the natural carbon cycle had not removed over half of these anthropogenic CO_2 emissions. Carbon cycle measurements and modeling studies show that these anthropogenic CO_2 emissions are superimposed on an active natural carbon cycle that regulates CO_2 through photosynthesis and respiration on land and in the ocean (Beer et al., 2010), as well as temperature-driven solubility coupled with the ocean circulation (Takahashi et al., 2002; 2009). The land biosphere and ocean emit almost 20 times as much CO_2 into the atmosphere as human activities each year, but then reabsorb a comparable amount along with about half of the anthropogenic CO_2 emissions (Jones and Cox, 2005; Canadell et al., 2007; Raupach et al., 2008; Knorr 2009; Bennedsen et al., 2019, Friedlingstein et al., 2020). While the fraction of the anthropogenic CO_2 that stays in the atmosphere (the "airborne fraction") is remarkably constant, at about 0.45 for the multi-year average (e.g. Ballantyne et al., 2012; Raupach et al., 2008; 2014), it can change substantially from year to year. In some years, the airborne fraction can be as high as 80%, while in others, it can be as low as 30% (Raupach et al., 2008; 2014). Some of the largest changes in this airborne fraction appear to be associated with changes in uptake of CO_2 by the land biosphere (the land sink) in response to large-scale temperature and precipitation anomalies, like those associated with major El Niño events or large volcanic aerosol injections into the stratosphere (Frölicher et al., 2013). The ocean uptake also responds to El Niño events and large volcanic eruptions (Eddebbar et al., 2019; McKinley et al., 2004; 2020), but has a smaller impact on the amplitude of variability in the airborne fraction (Chatterjee et al., 2017). The relative roles of these and other processes that link the land, ocean and atmospheric carbon cycles with the climate are less well understood, compromising our ability to predict how the atmospheric CO_2 growth rate might change as the carbon cycle responds to climate change (Ballantyne et al., 2012, McKinley et al., 2017).

Over the past two decades, our understanding of the natural and anthropogenic contributions to the carbon cycle has grown steadily with the deployment of progressively more sophisticated ground-based, oceanic, airborne, and space-based carbon cycle measurement systems. These advances have been accompanied by the development of far more comprehensive diagnostic and prognostic carbon cycle modeling tools. On time scales of a decade or longer, "bottom-up" measurements of changes in carbon stocks on land and in the ocean provide a reliable indicator of the stability of these reservoirs and a useful integral constraint on their fluxes of carbon to the atmosphere. On shorter time scales, stock measurements are less reliable for estimating atmospheric emissions because land and ocean stock changes that are too small to be accurately quantified can produce large changes in the atmospheric CO_2 concentration. On these scales, direct measurements of CO_2 fluxes at the surface, fluxes derived from vertical gradients in pCO_2 across the air-sea interface or "top-down" fluxes estimated from spatial and temporal gradients in atmospheric CO_2 concentrations can provide more reliable results.

Both bottom-up stock and flux estimates and "top-down" atmospheric estimates are providing key insights into the carbon cycle. Bottom-up methods use empirical or process-based models of the land biosphere and ocean to estimate fluxes, or to upscale in situ measurements of the time change of stocks or of direct flux observations (e.g. Sabine et al., 2004; Doney et al., 2004; Gruber et al., 2019a; Pan et al., 2011; Sitch et al., 2015; Hubau et al., 2020; Piao et al., 2020; Jung et al., 2020; Long et al., 2013; Landschützer, et al., 2013; Rödenbeck et al., 2014;

2015; Gregor et al., 2019; Watson et al., 2020; Hauck et al., 2020; Carroll et al., 2020). "Top-down" models use inverse methods to estimate the surface CO_2 fluxes from the land or ocean needed to maintain the observed atmospheric or ocean CO_2 concentrations in the presence of the prevailing winds and ocean circulation (e.g. Enting et al., 1995; Mikaloff-Fletcher et al., 2006; Jacobson et al., 2007; Khatiwala et al., 2009; Chevallier et al., 2010; 2019; DeVries 2014; Crowell et al., 2019).

Both bottom-up and top-down methods benefit from remote sensing as well as in situ data. For example, a bottom-up forest stock inventory might use in situ measurements to estimate the above ground biomass from an ensemble of specific plots and then use remote sensing measurements to upscale those measurements to larger areas. Similarly, a top-down approach might combine in situ and remote sensing observations of atmospheric CO_2 along with models of atmospheric transport constrained by both in situ and satellite meteorological measurements to estimate regional-scale fluxes. In practice, top-down and bottom-up methods can be combined. For example, top-down methods for estimating net biospheric exchange (NBE) may use fossil fuel emissions derived from bottom-up inventories as a static (i.e. not optimized) input (i.e. Crowell et al., 2019).

As the world embarks on efforts to monitor and control CO_2 emissions, there is growing evidence that the natural carbon cycle is evolving in response to human activities, severe weather, disturbances and climate change. In this context, an improved understanding of both the anthropogenic and natural processes in the land biosphere and ocean that control the emissions and uptake of CO_2 is critical to our ability to predict its rate of increase in the CO_2 in the atmosphere and its impact on the climate. To address this need, advanced measurement capabilities are being deployed and their results are being analyzed with more comprehensive diagnostic and prognostic modeling tools. While these advances do not yet provide the full capabilities of the policy-relevant carbon observing system advocated by Ciais et al. (2014) or envisioned by the WMO Integrated Global Greenhouse Gas Information System (IG3IS), they are providing substantial new insights with respect to the anthropogenic and natural processes operating in the carbon cycle.

Here, we review the current state of knowledge of the anthropogenic and natural processes driving the land, ocean and atmospheric carbon cycles. We summarize advances in each domain and identify ongoing efforts to exploit this new information to create a more accurate and complete baseline and to identify trends. We also identify critical measurement and modeling gaps that must be addressed to produce an effective carbon monitoring system.

2 A Note on Units

Because the bottom-up and top-down land, ocean and atmospheric carbon communities focus on different aspects of the carbon cycle, they have developed a sometimes confusing array of units to quantify stocks and fluxes of carbon and CO_2. For example, the land carbon community typically quantifies the mass of stocks and fluxes carbon, the atmospheric community typically measures and reports the CO_2 dry air mole fraction, X_{CO2} and the ocean community uses the partial pressure, pCO_2, fugacity, fCO_2, and the air-sea carbon flux. To relate these units, it is useful to note that one petagram of carbon (1 Pg C) in the atmospheric CO_2 is equivalent to a concentration of ~ 2.124 ppm (c.f. Ballantyne et al., 2012; Friedlingstein et al., 2020). Table 1 summarizes these and other commonly used quantities and units used by the carbon cycle community and describes their relationships.

Table 1: Quantities and Units Describing the Carbon Cycle

Quantity	Acronym	Typical units	Comment
carbon dioxide dry air mole fraction	CO_2, xCO_2 or X_{CO2}	parts per million by volume (ppm)	Number of CO_2 molecules relative to each million (10^6) molecules of dry air. If CO_2 is assumed to be an ideal gas and its dry air mole fraction is increased by 1 ppm at constant temperature, the CO_2 partial pressure will increase by one micro atmosphere (µatm).
partial pressure of carbon dioxide	pCO_2	µatm	At sea level, $pCO_2 = (P - pH_2O) \times X_{CO2}$, where P is the total atmospheric pressure and pH_2O is the water vapor saturation vapor pressure (see Woolf et al., 2016). 1 µatm = 10^{-6} atmospheres = 0.10325 Pascals.
carbon dioxide fugacity	fCO_2	µatm	Effective ideal gas partial pressure of CO_2 that has the same temperature and Gibbs free energy as the real gas. At the surface, $fCO_2 = X_{CO2} \times \varphi_{CO2}$, where $\varphi_{CO2} \approx 0.0002$/K is the fugacity coefficient for CO_2 and K is the temperature in Kelvin.
column averaged carbon dioxide dry air mole fraction	XCO_2	ppm	This vertically-averaged quantity used by the atmospheric remote sensing community is derived from the ratio of the CO_2 column abundance and the dry air column abundance. The dry air column abundance is estimated from the measured molecular oxygen (O_2) column abundance, assuming an O_2 dry air mole fraction of 0.20955.
carbon stock or stock change		petagrams of carbon per year (Pg C yr^{-1})	1 Pg C = 10^{15} g C. 1 PgC = 10^{12} kg C = 10^9 tons of carbon = 1 Gt C. When oxidized to form CO_2, 1 Pg C generates 3.664 Pg CO_2.
Gross Primary Production	GPP	Pg C yr^{-1}	Total flux of carbon fixed through photosynthetic reduction of CO_2 by plants in an ecosystem.
Net Primary Production	NPP	Pg C yr^{-1}	Net flux of organic carbon produced by plants in an ecosystem. NPP equals GPP minus autotrophic respiration by plants, R_a.
Net Ecosystem Exchange or Net Ecosystem Production	NEE or NEP	Pg C yr^{-1}	Net primary production, NPP, minus carbon losses by heterotrophic (non plant) respiration, R_h. NEE and NEP are generally interchangeable, with NEE used more often to refer to fluxes measured in the atmosphere, while NEP is more often used for fluxes inferred from measurements of carbon stock changes.
Net Biospheric Exchange or Net Biome Exchange	NBE	Pg C yr^{-1}	Change in mass of carbon stocks after episodic carbon losses due to natural or anthropogenic disturbance.

3 Anthropogenic Contributions to the Carbon Cycle

Atmospheric CO_2 emissions from fossil fuel combustion, cement production, land use change and other human activities are currently being tracked by the regulatory, commercial and scientific communities (e.g. Andrew, 2020). International organizations such as the International Energy Agency (IEA) originally compiled fossil fuel statistics to avoid disruptions in the world's oil supplies, but now provide annual reports on a range of technologies to support sustainable energy development (IEA 2020). Those from national organizations, such as the U.S. Energy Information Administration (EIA) serve a similar purpose, tracking short-term and long-term trends in supply and demand around the world to support the energy industry, while those from national regulatory organizations such as the U.S. Environmental Protection Agency (EPA) compile statistics for regulating and reporting national emissions to other government agencies or organizations such as the United Nations Framework Convention on Climate Change (UNFCCC). Commercial organizations, such as British Petroleum, produce inventories to track trends in energy markets (BP 2020).

Similarly, to track emissions from land use change, international organizations such as the United Nations Food and Agriculture Organization (FAO) collect and disseminate global information on agriculture, forestry and other land use (AFOLU). Two methods are typically used to track emissions from land use change. In the first, data collected by FAO are used in so-called bookkeeping models that prescribe carbon loss per pool over time (Hansis et al., 2015, Houghton and Nassikas, 2017). In the second, satellite remote sensing data are used to determine the amount of land cover change and associate emission losses with the change by emission factors or more detailed biogeochemical models (van der Werf et al., 2017). For tracking historical land use changes, a map of historical land use is required such as LUH2-GCB2020 (Hurrt et al., 2020; see also Friedlingstein et al., 2020). Using this information, it is possible to project land use change impact on the carbon cycle using the new generation of dynamic global vegetation models (DGVMs). At the national level, land use change emissions are compiled and delivered to the UNFCCC by country level organizations such as the U.S. EPA, Japan's Ministry of the Environment and the European Union's European Environment Agency.

Scientific inventories, such as those compiled by the Carbon Dioxide Information Analysis Center (CDIAC; Boden et al., 2017) and the annual reports compiled by the Global Carbon Project (GCP), combine information from all of these sources to support scientific investigations of the energy and carbon cycles as well as other applications. The science community has also produced high resolution gridded inventories such as EDGAR (Janssen-Maehout et al., 2019), ODIAC (Oda et al., 2018), and Hestia (Gurney et al., 2019). These inventories use other data (population, night lights, etc.) to disaggregate national scale emissions to support carbon cycle investigations on spatial scales spanning individual forest plots or urban areas to full biomes. These gridded inventories also provide more actionable information on anthropogenic CO_2 emissions for policy makers working on urban to sub-national scales.

3.1 Regulating Greenhouse Gas Emissions - the Paris Agreement

The primary international regulatory framework for tracking anthropogenic CO_2 emissions is the UNFCCC. This treaty was established in 1994 to stabilize "greenhouse gas concentrations in the atmosphere at a level that would prevent dangerous anthropogenic interference in the climate system." To implement this treaty, parties to the 2015 UNFCCC Paris Agreement resolved to define Nationally Determined Contributions (NDCs) to a global GHG

reduction effort and to report progress toward these NDCs, at 5-year intervals through Global Stocktakes, the first of which is scheduled for 2023. The NDC reports are to be compiled based on the Intergovernmental Panel on Climate Change (IPCC) Guidelines for National Greenhouse Gas Inventories (IPCC 2006; 2019) and consist of bottom-up emission inventories, compiled from a statistical analysis of emissions reported from sources in specific sectors, including Energy, Industrial Processes Product use, Agriculture, Forestry, and Other Land Use (AFOLU), and Waste. Each sector is subdivided into a series of categories. For example, AFOLU is divided into six categories, including Forest Land, Cropland, Grassland, Wetlands, Settlements, and Other Land categories.

While CO_2 emissions from fossil fuel combustion in the energy sector constitute the largest direct anthropogenic contribution to the global carbon cycle, emissions of CO_2 and other greenhouse gases from managed lands tracked under the AFOLU sector are responsible for almost one quarter of all anthropogenic GHG emissions (Smith et al., 2014). These emissions originate primarily from deforestation and forest degradation, but also include contributions from agricultural land and livestock management. The IPCC Guidelines only require reporting of emissions on managed lands, but they acknowledge that natural disturbances (wildfires, insects, severe weather) contribute a significant source of interannual variability and uncertainty in this sector. The concept of natural and anthropogenic changes are becoming more diffuse as climate change itself affects "natural disturbances". A comprehensive understanding of the processes operating in the natural carbon cycle is therefore essential for tracking and attributing observed interannual changes in atmospheric CO_2 concentrations, and for linking bottom-up inventories with top-down monitoring, recording, and verification (MRV) strategies (Janssens-Maenhout et al., 2020).

3.2 Carbon Cycle Insights from Scientific Inventories

The Global Carbon Budget (GCB) compiled annually by the Global Carbon Project document the globally-averaged budget of anthropogenic carbon fluxes for five key components: atmosphere, fossil fuel emissions, land use change, uptake by the terrestrial biosphere ("land sink") and uptake by the ocean ("ocean sink"). From 2000-2006 to 2019, emissions from fossil fuel use and cement production increased from 7.6 to 9.7 Pg C yr^{-1}, with a peak of 10 Pg C yr^{-1} in 2018. The ocean and land sinks increased during the same time from 2.2 to 2.6 and 2.8 to 3.6 Pg C yr^{-1} respectively (Friedlingstein et al., 2020). The anthropogenic sinks are defined as their perturbation caused by direct effects of increasing atmospheric CO_2 and indirect effects by climate change.

In addition to these flux estimates, the GCBs document uncertainties, expressed as one standard deviation around the mean. Figure 1 shows the relative error of these estimates (uncertainty/mean) as they progress along the years for the 2006-2019 budgets. The estimates refer to each individual year for which the budget was prepared. As such, they indicate the progression in understanding of the uncertainties in the budget at that time (as opposed to an *a posteriori* analysis of the uncertainties of all years in a similar manner). The relatively low, stable uncertainties associated with both the fossil fuel emissions and atmospheric CO_2 concentrations result from two factors (Ballantyne et al., 2012). The first is the precision of the atmospheric in situ CO_2 measurements and efficient mixing of CO_2 throughout the atmosphere, although analytical errors and sampling bias do play a role. Second, while fossil fuel combustion is the primary source of anthropogenic CO_2 emissions, the relative error on this contribution is

relatively small because the fossil fuel industry provides reliable numbers on their sales, which are well correlated with the amount of fossil fuel burned. The highest relative errors are associated with land use change emissions. These estimates are based on either bookkeeping methods (Houghton, 2003; Houghton and Nassikas, 2017), and since 2018, also on DGVMs (Friedlingstein et al., 2019, 2020). Compared to the early period, 2000-2006, the relative error has not substantially decreased, nor has the mean value of the land use change emissions of 1.5 to 1.8 Pg C yr^{-1}, respectively.

In the GCB published in 2016 and before, the land sink was calculated as a residual: land sink = emissions - atmosphere - ocean sink. Since 2017, the land sink in the Global Carbon Budget has been calculated directly from DGVMs with a corresponding increase in relative error due to the divergence of the individual DGVM estimates. Since then, the ocean sink estimate from models is no longer normalized to a data-based estimate from the 1990s (Denman et al., 2007), which was previously applied to ensure the land sink estimate from the budget residual

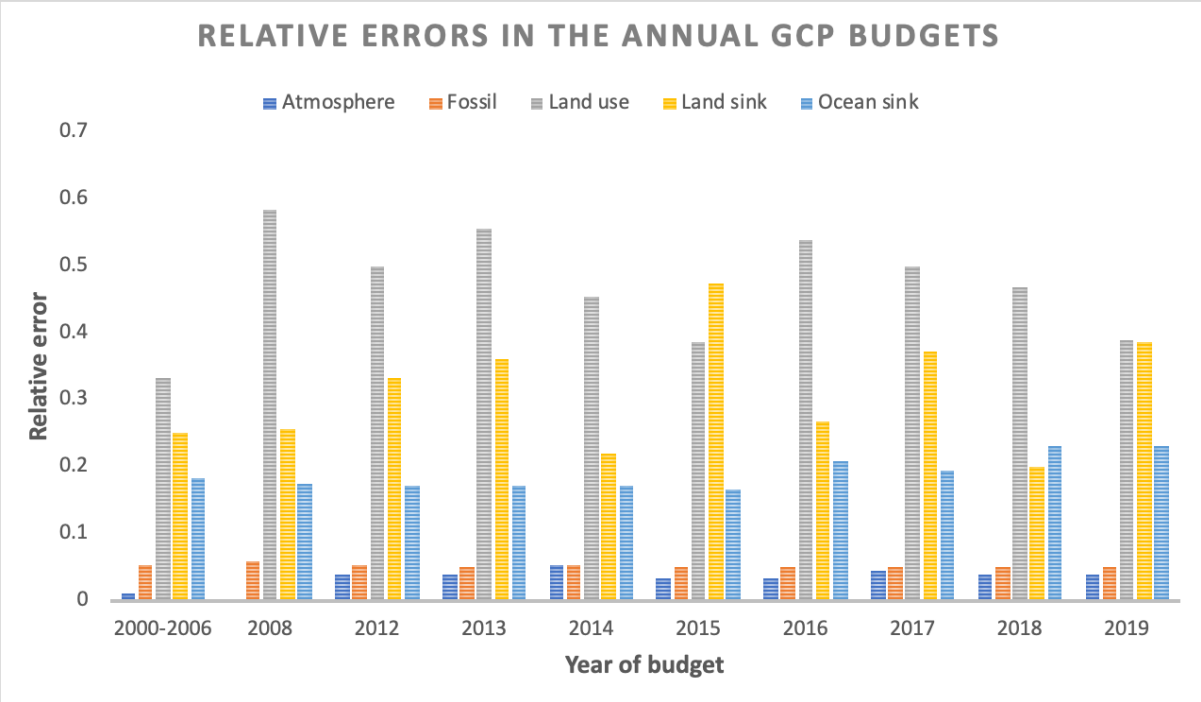

Figure 1. Relative error (1 standard deviation uncertainty / mean) for the Global Carbon Budget estimates since 2000. Numbers are taken for the individual year(s) reported each year from Canadell et al. (2007), LeQuéré et al. (2009) and LeQuéré et al. (2013-2018) and Friedlingstein et al. (2019-2020) and refer to the annual estimates.

had a realistic mean value. This change in methodology also affected the ocean sink uncertainty, which slightly increased from 17% in 2015 to 19% in 2016. The fact that the ocean sink was no longer scaled to the mean 1990s value led to a smaller ocean sink estimate that, together with the same absolute uncertainty, resulted in the slightly higher relative uncertainty. The ocean sink uncertainty had also varied between 17 and 19% for the years 2006 to 2015.

With the advent of a direct estimate of the land sink from DGVMs, it is now possible to assess the degree to which the overall global carbon budget can be closed, i.e., the difference

between the sum of the fluxes and the atmospheric accumulation. This budget imbalance was estimated at 0.3 Pg C for 2018 and 2019, or approximately 10% of the magnitude of the land and ocean sinks (Friedlingstein et al., 2019, 2020). The budget imbalance indicates that there remains substantial uncertainty in global annual mean fluxes.

4 The Ocean Carbon Cycle

The ocean holds a large natural reservoir of carbon that exchanges with the atmosphere on short (non-geological) time-scales. Superimposed upon the cycling of this natural reservoir, the increasing atmospheric CO_2 concentration is causing the ocean to absorb a significant fraction of anthropogenic carbon emissions. Due to the natural carbon cycle of the ocean, 39,000 Pg C is stored in the ocean, which amounts to ~90% of the carbon contained in the combined land, ocean and atmosphere domains (Bolin 1983; Sundquist 1993; Sabine and Tanhua, 2010). The natural carbon cycle is driven by ocean circulation, seasonal heating and cooling, and biological processes (Figure 2, left).

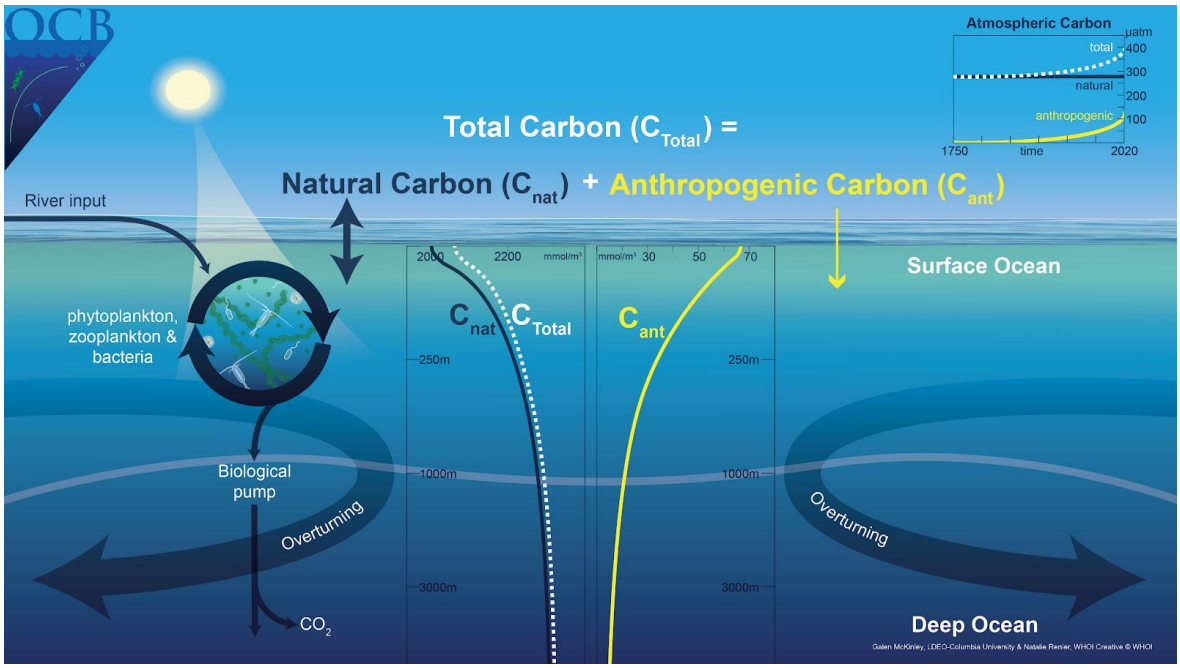

Figure 2: The total carbon cycle in the ocean (C_{Total}) is the sum of the natural carbon cycle (C_{nat}) and the anthropogenic carbon cycle (C_{ant}). The natural carbon cycle is quantitatively dominant, as shown in the observed data (GLODAPv2, Olsen et al., 2016) plotted in the center, and includes contributions from biological activity and the large-scale circulation of the ocean. Overlain is the uptake of additional carbon due to anthropogenic emissions to the atmosphere that occurs in the present ocean as atmospheric pCO_2 continues to rise.

The ocean carbon budget can be quantified as the storage of inorganic and organic carbon in the ocean, the fluxes of carbon across the air-sea interface, river input, and a small term for sedimentation. The natural carbon inventory is very large compared to the anthropogenic component and is believed to have been in an approximate long-term steady state in preindustrial times, such that there was zero global mean air-sea flux of natural carbon (F_{nat}). The

anthropogenic uptake flux (F_{ant}) is the additional ocean uptake due to the direct effect of increasing atmospheric CO_2 concentration and occurs as a perturbation to the vigorous natural cycle (Figure 2, right), with the column inventory of anthropogenic carbon (C_{ant}) from the latest data-based estimates mapped in Figure 3 (bottom).

The downward increase in natural carbon (C_{nat}) from surface to depth (Figure 2) is largely due to the biological carbon pump (BCP) (Sarmiento & Gruber, 2006). If the BCP did not operate, the atmospheric CO_2 concentration would be around 200 ppm higher (Maier-Reimer et al., 1996). During the last glacial maximum, changes in the efficiency of the BCP may have played an important role in lowering atmospheric CO_2 (Galbraith and Skinner, 2020; Sigman et al., 2010). Biological feedbacks may accompany anthropogenic climate change (Sabine & Tanhua, 2010, Hauck et al., 2015, Moore et al., 2018), but there is significant spread in model projections (Laufkötter et al., 2015, 2016; Frölicher et al., 2016). To date, observed timeseries are too short to provide evidence for long-term biologically-driven trends in the ocean carbon cycle (Henson et al., 2016). Thus, the ocean carbon sink for anthropogenic carbon over the industrial era is currently understood as a physical and chemical process (Figure 2, right). The contemporary (or 'net') air-sea CO_2 flux (F_{net}) is the sum of F_{nat} and F_{ant}. The surface ocean partial pressure of CO_2, pCO_2, CO_2 flux and interior ocean inventory of anthropogenic carbon (C_{ant}) are shown in Figure 3.

The ocean surface layer carbon content equilibrates with the atmosphere on time-scales of months. The ocean continually removes C_{ant} from the atmosphere because the ocean circulation transports C_{ant}-laden waters away from the surface layer and into the ocean interior, while the water that returns to the surface tends to have low C_{ant} content. Thus, the ocean circulation is essential to continued CO_2 uptake. At the global scale, the ocean overturns relatively slowly, on timescales of 1000 years. Because of this, 75% of all anthropogenic carbon attributable to the industrial age remains in the upper 1000m (Gruber et al., 2019a). Because carbon is highly soluble in ocean water, the fundamental limit on the rate of anthropogenic carbon uptake by the ocean is the rate of overturning, as it determines how fast waters with C_{ant} uptake capacity are exposed to the surface.

Since the beginning of the industrial era, the uptake of C_{ant} by the land carbon sink has been largely offset by emissions associated with land use change. The ocean has therefore been the primary cumulative net C_{ant} sink over this period (Friedlingstein et al., 2019; 2020). Looking forward, the behavior of the ocean carbon sink is expected to continue playing a critical role in determining how much anthropogenic carbon remains in the atmosphere (Randerson et al., 2015, Zickfeld et al., 2016, Schwinger and Tjiputra, 2018).

313 The following sections describe the approaches used to study the ocean carbon sink. A
314 mechanistic understanding of this sink is essential for diagnosing its state and for making reliable
315 future predictions. This requires quantification of carbon stocks and fluxes at higher spatio-
316 temporal resolution than is available from interior data alone. Air-sea fluxes on monthly to
317 decadal timescales are quantified using surface ocean observations and ocean models of varying

318 complexity. Agreement between independent estimates for mean fluxes and temporal variability
319 indicates growing confidence in global-scale mechanistic understanding. Yet, key uncertainties
320 remain and must be resolved to support better predictions for future ocean carbon sink and to
321 allow for reduced diagnostic uncertainty for the global carbon cycle as it evolves. Substantial
322 advances in observing systems, quantification of land-to-ocean fluxes of carbon, and models of

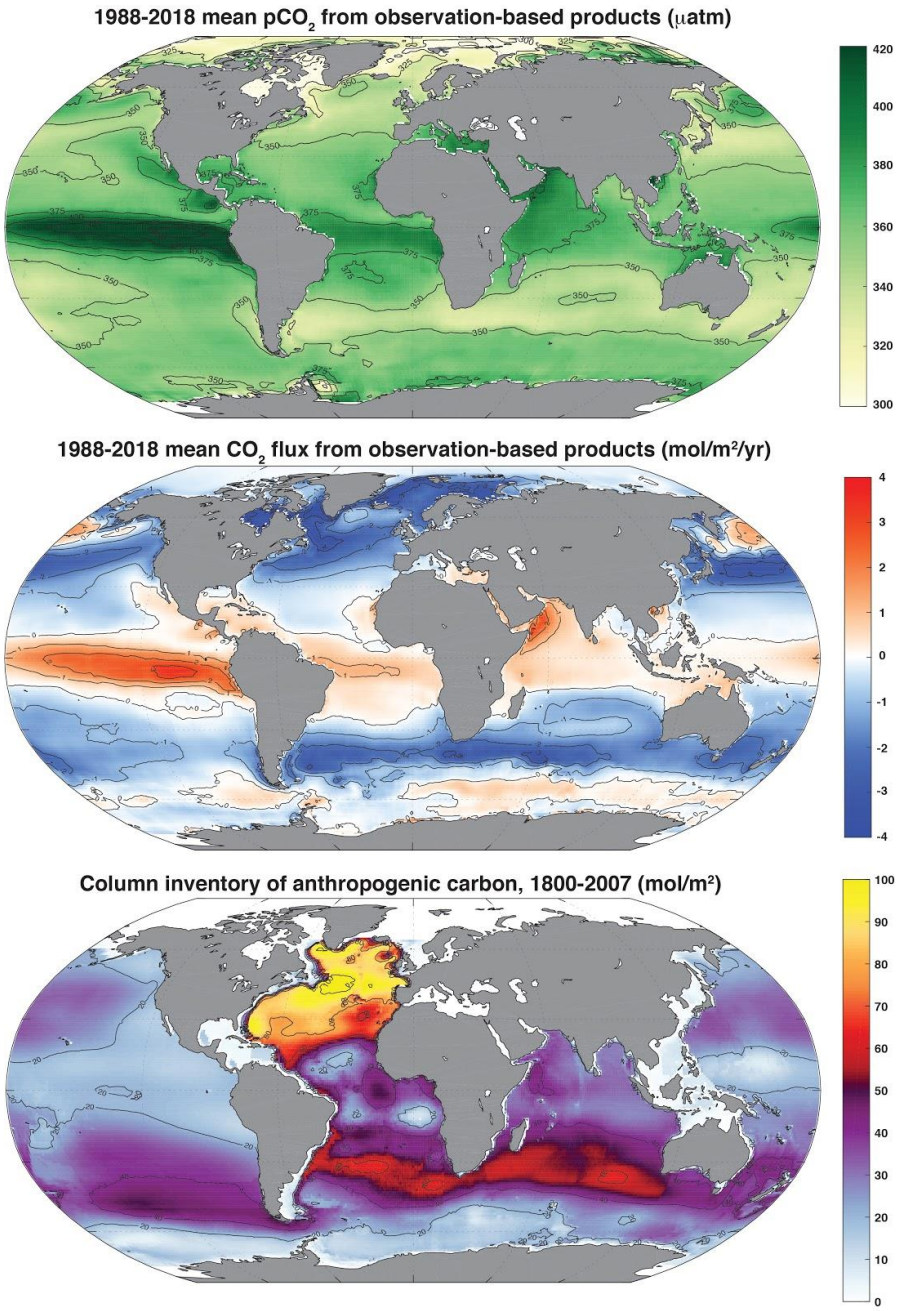

Figure 3: Surface ocean pCO_2 (top); and air-sea CO_2 flux (F_{net}), positive flux to the atmosphere (middle), 1988-2018, mean of 6 observation-based products (Fay et al., in prep); column inventory of anthropogenic carbon (C_{ant}, bottom), 1800-2007 (Sabine et al., 2004, Gruber et al., 2019).

ocean circulation are needed to reduce these uncertainties. In addition, as nations implement substantial reductions in carbon emissions, we need to assess the near-term response of the ocean carbon sink to reduced atmospheric pCO_2 growth rates.

4.1 Bottom-up Estimates of Anthropogenic Carbon Accumulation In The Ocean From Interior Observations

Based on a bottom-up accounting using interior ocean data, Gruber et al. (2019a) find a total ocean C_{ant} accumulation of 152 ± 20 Pg C for the industrial era through 2007. By combining evidence from top-down and bottom-up approaches, Khatiwala et al. (2013) find an inventory of 160 ± 26 Pg C in 2010. Consistent with previous inventories (Sabine et al., 2004), these studies find that the ocean has cumulatively absorbed excess carbon equivalent to 45% of industrial-era fossil fuel emissions until 2010, or 30% of the total emissions including LUC. The column inventory of ocean C_{ant} accumulation from Gruber et al. (2019a) is shown in Figure 3 (bottom).

The amount of C_{ant} estimated for 2010 (160 ± 26 Pg C) represents only about ~0.4% of the ocean carbon stock, indicating the significant challenge of directly observing the temporal change in carbon stock over time. Direct measurements are only possible in areas with rapid change in dissolved inorganic carbon (DIC; e.g. Tanhua and Keeling, 2012). Instead, it is more practical to infer ocean storage of C_{ant} against the large natural background, and then to calculate the change in storage over time. A few different methods have been used to estimate the storage of C_{ant}, either based on observations of biogeochemistry variables, or by transient tracers (see Sabine and Tanhua (2010) for a review).

On a global scale, different methods converge within the uncertainties, but significant differences persist regionally (e.g. Waugh et al., 2006, Khatiwala et al., 2009). Multivariate techniques (e.g. Friis et al., 2005, Clement and Gruber, 2018) can be used to disentangle variability and calculate decadal-scale trends. A global estimate of the storage of anthropogenic carbon finds an increase of 34 ± 4 Pg C between 1994 and 2007 (Gruber et al., 2019a), indicating a mean F_{ant} uptake of -2.6 ± 0.3 Pg C (negative flux into the ocean) annually over this time frame. This relatively accurate (~12%) estimate provides an important benchmark for the ocean's role in sequestering anthropogenic carbon, and acts as a direct constraint on the net magnitude of the land flux given low uncertainty on fossil fuel emissions and atmospheric carbon accumulation. The magnitude of the uptake implies that the ocean is continuing to take up anthropogenic carbon at a rate proportional to anthropogenic carbon emissions.

A critical element to the success of global estimates of anthropogenic carbon stocks and changes in carbon storage is the GLODAP data product (Key et al., 2004), which collects all carbon-relevant interior ocean data into a product that has undergone the extensive quality control (Tanhua et al., 2010) required to quantify small changes over a large background. This data product is now being released on an annual basis and the GLODAPv2.2020 version contains data from over 1.2 million water samples collected during 946 cruises (Olsen et al., 2020).

4.2 Bottom-up Estimates of Ocean-Atmosphere CO_2 Fluxes from Observations of Surface Ocean pCO_2

In order to understand the ocean carbon sink on annual to interannual timescales relevant to climate change policy, more frequent estimates of the sink are required than those produced from decadal timescale interior ocean observations. These data come from observations of the surface ocean partial pressure of CO_2 (pCO_2), and are used to directly estimate net air-sea CO_2 fluxes (F_{net}). The reported variable is surface ocean fugacity of CO_2 (fCO_2) which equals the partial pressure of CO_2 corrected for the non-ideal behavior of the gas (Pfeil et al., 2013). The fugacity of CO_2 is 0.3-0.4% smaller than the partial pressure of CO_2 (Zeebe and Wolf-Gladrow, 2001). For simplicity, we use the terminology pCO_2 to refer to these data for the remainder of this paper. Over the past decade, the number of publicly available observations of pCO_2 has increased rapidly from 6 million in the first release of the Surface Ocean CO_2 Atlas (SOCAT) database (Pfeil et al., 2013, Bakker et al., 2014, 2016, 2020) in 2011 to 28 million in 2020 (www.socat.info). These observations and their automated organization into a consistent database have enabled scientists to create a variety of new observationally-based estimates of the ocean carbon sink that use correlated data (sea surface temperature, salinity and height, chlorophyll, mixed layer depth) to drive upper ocean extrapolation techniques and machine-learning algorithms so as to fill the observational gaps (Rödenbeck et al., 2014; 2015, Landschützer et al., 2013; 2014; 2020; Denvil-Sommer et al., 2019, Gregor et al., 2019).

As the SOCAT database currently offers pCO_2 data for only ~2% of all 1° x 1° locations across the surface ocean, the extrapolation is quite significant. Nonetheless, comparisons of the extrapolated, observationally-based products to independent data indicate relatively low bias and convergence of the independent estimates (Gregor et al., 2019). Root mean square errors (RMSE) range from 10 to 35 µatm. The fact that bias and RMSE comparisons are largely consistent across the variety of approaches suggests that it is data sparsity rather than extrapolation methodology that is now a fundamental limitation on further error reduction (Gregor et al., 2019). Additional tests of the machine-learning based extrapolation approaches using an Earth System Model testbed indicate that they generally have low bias and are skillful in representing the amplitude and timing of seasonality across the global ocean. However, higher and lower frequency variations are more poorly represented because of inadequate sampling on these timescales (Gloege et al., 2020, Stamell et al., 2020). Several challenges remain in using these data, including the uneven distribution of data over time, methodological differences in the calculation of air-sea flux from pCO_2 (Fay et al., 2021, Woolf et al., 2019, Zavarsky and Marandino, 2019), and the potential need for adjustments to pCO_2 data to account for near-surface temperature and salinity gradients (Watson et al., 2020).

Despite the significant extrapolation and remaining uncertainties, it is a major advance for ocean carbon cycle science to have spatially-resolved, data-based estimates of air-sea CO_2 fluxes on monthly timescales. This allows for new investigation into the magnitudes and mechanisms of interannual and decadal variability in the ocean carbon sink, and a key point of comparison to ocean models that were previously the only basis for this analysis. Models are discussed in the next section, and results are compared in the following.

4.3 Bottom-Up Estimates of Ocean-Atmosphere CO_2 Fluxes from Ocean Models

Global ocean biogeochemical hindcast models estimate interior ocean carbon cycling and, from this, air-sea CO_2 fluxes. Models simulate the carbon distribution in the ocean with currents, water mass formation and mixing, and for biological carbon turn-over. The bottle-neck for ocean carbon uptake in the models, as in the real world, is the carbon transport across the mixed layer depth. As a result, the models' carbon uptake is sensitive to simulated physics (Doney et al., 2004; Goris et al., 2018; Huber and Zanna, 2017). Models can also provide air-sea flux estimates prior to the 1990s when surface pCO_2 observations were rare.

Models are routinely evaluated against observations or observation-derived estimates that characterize the physical and biogeochemical state of the ocean for the last several decades (Doney et al., 2004; Schourup-Kristensen et al., 2014; Aumont et al., 2015; Schwinger et al., 2016; Stock et al., 2020). For the suite of models used in the Global Carbon Budget, comparison of pCO_2 at observed locations from SOCAT reveals the models' ability to capture variability and trends on annual (RMSE <10 μatm) and decadal timescales (RMSE <10 μatm). However, large model-data mismatches on the seasonal timescale also exist (RMSE of 20–80 μatm; Hauck et al., 2020). Despite concurrence on annual and decadal timescales, ocean carbon sink estimates diverge (Hauck et al., 2020), indicating the available data do not fully constrain the models' emergent carbon sink.

Global ocean biogeochemical models are routinely used to quantify the ocean sink in the GCB. For example, for 2019, they find that the ocean sink accounted for 22% of 2019 anthropogenic CO_2 emissions (Friedlingstein et al., 2020). Models have also shed light on processes behind observed variability such as the weakening of the Southern Ocean carbon sink in response to increased westerlies (LeQuéré et al., 2007), and to explore the role of stationary Rossby waves in subduction of anthropogenic carbon (Langlais et al., 2017). As a component of Earth System Models, ocean models are the single tool for future projections. In the future, on timescales from decadal to centennial, models project a decreased carbon sink efficiency due to changes in the air-sea pCO_2 gradient, ocean circulation and reduced buffer capacity (Schwinger et al., 2014, Randerson et al., 2015, Zickfeld et al., 2016, Schwinger and Tjiputra, 2018, Ridge and McKinley, 2020b).

4.4 Reconciling Air-Sea Flux Estimates from Different Methods

We must accurately quantify the ocean sink and understand its mechanisms so that the sink can be monitored as it evolves, and so that reliable projections can be developed. The best window into our current understanding is the degree to which the above-mentioned independent estimates of the present-day sink's magnitude agree. We discuss the degree of agreement in this section, where a negative flux refers to a flux from atmosphere to ocean, and we discuss mechanistic understanding in the next section.

Surface ocean carbon observations indicate the net air-sea flux of carbon into the ocean (F_{net}~ -1.6 Pg C yr^{-1}), while interior measurements offer estimates of the anthropogenic uptake and storage (F_{ant}~ -2.6 Pg C yr^{-1}). Dynamic hindcast models as used in the GCB estimate the total of anthropogenic perturbations, that is the sum of anthropogenic uptake (F_{ant}) and anthropogenic climate change induced natural carbon fluxes ($F_{nat, ns}$). Closure terms of significant net magnitude (~1 Pg C yr^{-1}) are required to bridge the gap between F_{net} and F_{ant}.

To reconcile flux estimates from pCO_2-based data products with ocean models and estimates from interior data, it is well established that an adjustment due to the riverine input of

natural carbon that outgasses from the ocean ($F_{nat,riv}$) must be applied (Sarmiento and Sundquist, 1992; Aumont et al., 2001; Lacroix et al., 2020). Unfortunately, high quality direct estimates of $F_{nat,riv}$ do not exist, and so the closure between surface flux estimates of F_{net} and F_{ant} remains a significant uncertainty. Lacking better evidence, values typically used are between 0.45 and 0.78 Pg C yr^{-1} (Jacobson et al., 2007, Resplandy et al., 2018), with uncertainty estimates that are approximately 100% of these mean values. Anthropogenic changes to the riverine input of carbon are an additional closure term not usually considered with no temporally-resolved estimates available and one estimate for 2000-2010 suggesting it to be small (0.1 Pg C yr^{-1}, Regnier et al., 2013). No estimates on anthropogenic changes to the outgassing of the riverine carbon in the ocean are available.

It has also been proposed that climate change is having an effect on the natural carbon cycle ($F_{nat,ns}$, Le Quéré et al., 2010; Gruber et al., 2019a). The magnitude of this non-steady state component of the natural carbon cycle is still highly uncertain. $F_{nat,ns}$ has been estimated with one model for the period 1981-2007 (Le Quéré et al., 2010) and with a back-of-the-envelope calculation for the period 1994-2007 (Gruber et al., 2019a), suggesting a reduction of F_{ant} by 10 to 15%. Gruber et al. (2019a) estimate $F_{nat, ns}$ by assuming that the accumulation of anthropogenic carbon in the ocean follows a strictly linear scaling with the atmospheric load. However, this assumption is known to hold only when the atmospheric growth is strictly exponential, which has not been the case (Raupach et al., 2014, Ridge and McKinley 2020b), and thus the resulting estimate of +0.38 Pg C yr^{-1} is likely an upper-bound. Another approach for estimating $F_{nat, ns}$ is to use ocean models that represent the natural carbon cycle, and to make a reasonable assumption that the total carbon cycle response to climate variability is dominated by the natural component. With this assumption, models indicate $F_{nat, ns}$ for 1994-2007 of +0.06 to +0.31 Pg C yr^{-1} (DeVries et al., 2019; McKinley et al., 2020). Better quantification of this term is clearly needed.

Numbers for the ocean sink efficiency relative to emissions vary between 22% and 45% in the literature (Friedlingstein et al., 2020; Khatiwala et al., 2013; Sabine et al., 2004). These seemingly contradicting numbers are explained by different components of the ocean sink compared to different components of the emissions. Quantitatively the most important choice is the denominator used. For studies of the interior ocean cumulative ocean sink, efficiency is calculated relative to anthropogenic fossil emissions: 45% for the industrial era through 2010 (Khatiwala et al., 2013), and 41% for the industrial era through 2007 (Sabine et al., 2004). GCB estimates compare the ocean sink to total anthropogenic CO_2 emissions, which includes emissions to the atmosphere from land-use change. From the GCB, a lower number with an efficiency of 22% compared to total anthropogenic emissions is estimated for 2010-2019. The GCB's approach also includes climate perturbation effects ($F_{nat,ns}$), which reduces the magnitude of the ocean sink.

The choice to compare studies of interior ocean accumulation to fossil fuel emissions is motivated by the fact that these numbers are cumulative over the industrial era, and over this time, the land use source and land sink have been in approximate balance. Thus, this approach also circumvents the higher uncertainties associated with land-use changes emissions and the land sink. The GCB's approach, on the other hand, acknowledges that fossil fuel and land-use change emissions increase the atmospheric CO_2 concentration indistinguishably, and this determines the magnitudes of the ocean and land carbon sink.

4.5 Recent Evidence for Decadal Variability of the Ocean Carbon Sink

In the mid-2000s, studies using ocean hindcast models suggested a slowing of the ocean carbon sink from the mid-1990s and attributed this change to processes in the Southern Ocean (Lovenduski et al., 2007; 2008; Le Quéré et al., 2007). In the following decade, the release of both the LDEO pCO_2 database and the development of the international SOCAT database allowed for new analyses of trends in air-sea CO_2 fluxes directly from observations (Le Quéré et al., 2009; McKinley et al., 2011; Fay and McKinley 2013). Additionally, a variety of extrapolations of these data to global monthly coverage were developed (Rödenbeck et al., 2015), and a recovery of the ocean carbon sink following the low near the year 2000 was noted (Fay and McKinley, 2013; Landschützer et al., 2015; DeVries et al., 2017; Gruber et al., 2019b). The Southern Ocean was generally identified as a key regional driver of these trends. A number of studies agreed that the stagnation of the Southern Ocean carbon sink in the 90s was related to a trend towards a more positive Southern Annular Mode (SAM) index associated with stronger westerly winds leading to more upwelling of natural carbon and hence dampened net air-to sea CO_2 flux (Le Quéré et al., 2007; Lovenduski et al., 2007; Lenton and Matear, 2007; Hauck et al., 2013).

Increasing nutrient concentrations in surface waters of all sectors of the Southern Ocean provide further evidence of strengthened upwelling during the late 1990s (Iida et al., 2013; Ayers and Strutton, 2013; Hoppema et al., 2015; Pardo et al., 2017; Panassa et al., 2018). However, the same driving mechanisms cannot explain the reinvigoration of the sink in the 2000s, as the trends towards a more positive SAM and stronger winds in the 2000s continued. Asymmetric changes in atmospheric circulation (Landschützer et al., 2015), a weaker upper ocean overturning circulation (DeVries et al., 2017) and regional wind variability (Keppler and Landschützer, 2019) were proposed as possible explanations, but no consensus was reached on the driving mechanisms of the reinvigoration. Several studies concluded that ocean models were substantially underestimating the magnitude of decadal variability in the ocean carbon sink (De Vries et al., 2019; Gruber et al., 2019b).

In the last few years, more observation-based estimates have become available (Denvil-Sommer et al., 2019, Gregor et al., 2019), and now the size of the ensemble of observation-based estimates and of hindcast models is more comparable. With similar size ensembles for both observation-based and hindcast models, estimates of decadal variability are more similar in magnitude and phase, and not as large as the initial observation-based products had suggested (McKinley et al., 2020; Hauck et al., 2020). Both the ensemble of hindcast models and observation-based products indicate a larger ocean carbon sink in the early 1990s, then a slowing of the sink through about 2000, and then a strong and steady recovery through 2018 (Figure 4). In both the products and models, flux variability is largely homogenous across the globe (McKinley et al., 2020). The mechanism driving this variability is still unknown.

By representing the surface ocean as a single abiotic box that exchanges water with the deep ocean at a constant rate, McKinley et al. (2020) are able to reproduce the variability of the ocean carbon sink with two external forcings (Figure 4). The two external forcings are the observed atmospheric pCO_2 and surface ocean temperature anomalies caused by eruptions of large volcanoes (El Chichon, 1982; Mt Pinatubo, 1991). This result emerges because the globally-averaged air to sea pCO_2 gradient - the fundamental driver of the flux - is only 6-10 µatm, and thus anomalies in the atmospheric growth rate of a few µatm over several years can rapidly modify the global air-sea gradient. Large volcanic eruptions, such as Mt Pinatubo in

1991, cause a rapid surface ocean cooling, which increases solubility and creates an uptake pulse (Eddebbar et al., 2019). Then, as the ocean warms from this rapid cooling, solubility is lowered and the sink is damped for 5-7 years beyond the eruption (Figure 4).

This model of McKinley et al. (2020) is arguably simple. Yet, it can reproduce the ocean carbon uptake that occurs in the ensemble mean of much more complex models and observation-based products. What does this mean? It can be interpreted simply as Henry's Law operating at the global scale, wherein the partial pressure in the water is moving toward equilibration with the partial pressure in the air. Since the atmospheric pCO_2 continues to increase, the ocean continues to adjust toward equilibrium. In other words, McKinley et al. (2020) demonstrate that the ocean carbon sink temporal variability today is likely dominated by the external forcing from an ever-growing atmospheric pCO_2 concentration. This perspective is consistent with recent analysis that shows heat uptake and interior redistribution in the ocean is far more sensitive to the details of the ocean circulation than is the pattern and magnitude of carbon uptake and storage (Bronselaer and Zanna, 2020).

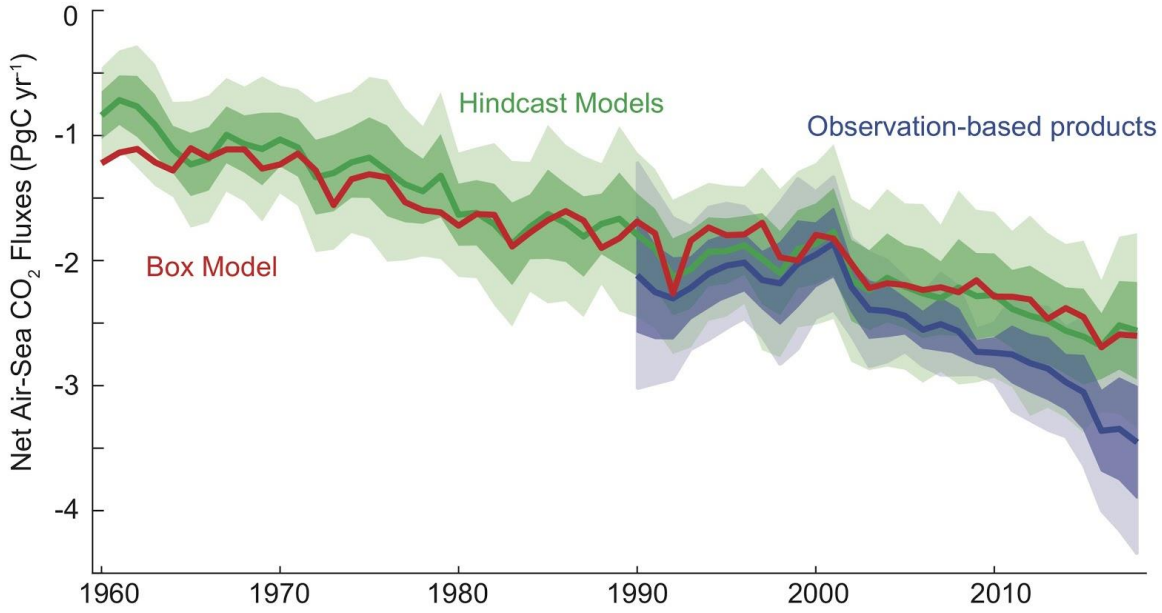

Figure 4. Air-sea CO_2 flux of carbon (F_{ant} + $F_{nat,ns}$) from observationally-based products (blue), hindcast models (green) and upper ocean diagnostic box model (red); negative flux into the ocean. Global ensemble means (bold), with 1 sigma and 2 sigma of individual members (shading). Hindcast ocean models from Global Carbon Budget 2020 (Friedlingstein et al., 2020). Observationally-based product pCO_2 fields have missing ocean areas filled with a full-coverage climatology (Landschützer et al., 2020) and air-sea flux calculated as average of 3 wind reanalyses (CCMP, ERA5, JRA55) with a quadratic parameterization (Wanninkhof 2014, Fay et al., 2021); to this F_{net} estimate, $F_{riv,nat}$= 0.62 Pg C yr^{-1} (Jacobson et al., 2007, Resplandy et al., 2018) is added. The upper ocean diagnostic box model (McKinley et al., 2020) is forced with observed atmospheric pCO_2 and surface ocean temperature changes associated with the eruptions of three large volcanoes (Agung 1963, El Chichon 1982, and Mt. Pinatubo 1991; Eddebbar et al., 2019).

4.6 Advancing Understanding of the Current and Future Ocean Carbon Sink

In order to continue to quantify the global carbon cycle, the constraint provided by the relatively low-uncertainty estimates for decadal anthropogenic carbon accumulation must be maintained. To better quantify fluxes on monthly to decadal timescales, increased observational capacity at the surface and higher fidelity models are needed. In order to be prepared to support climate management efforts in the near-term, the likely behavior of the ocean sink under emissions mitigation must receive increased attention.

Observations of ocean interior carbon require measurements with high accuracy and precision due to the small perturbations on a large background signal. For example, in 2010, the C_{ant} content was ~160 Pg C out of a total inorganic carbon content of ~39,000 Pg C. For the surface ocean flux estimates, the high spatiotemporal variability in pCO_2 and a low average deviation from air-sea equilibrium concentration needed to drive the observed net flux, i.e. a net flux of ~2.5 Pg C yr^{-1} over a total flux of ~90 Pg C yr^{-1}, indicates that accuracy and data coverage are possibly the most important components of the observing system. There is a seasonal bias in the observing system, with fewer observations being made in winter at high latitudes. This is particularly important for observations of surface fluxes, which tend to be high in winter, but less so for the interior ocean observations where seasonality tends to be low below the winter mixed layer.

4.6.1 Expanding autonomous observations:

Although ship-based observations remain a central resource for the carbon observing system, these are expensive and tend to be seasonally biased. Driven by these demands, there is a continuous development of sensors for inorganic carbon system measurements with at least some of these attributes; increased precision and accuracy, lower power consumption and lower instrument drift (Johnson et al., 2016; Sabine et al., 2020; Seelmann et al., 2019; Sutton et al., 2014). Similarly, there is a continuous development of autonomous platforms capable of carrying sensors for ocean carbon. These include moorings (Sutton et al., 2014), profiling floats (e.g. BGC Argo, Claustre et al., 2020), underwater gliders (Rudnick, 2016), and autonomous surface vehicles powered by wind or waves (Sabine et al., 2020). These developments are rapidly changing the capability to monitor ocean carbon with higher spatial and temporal resolution. For instance, observations from Biogeochemical (BGC) Argos floats enable the calculation of surface pCO_2 (from pH and alkalinity estimates) with reasonable accuracy and precision, ~11 µatm (Takeshita et al., 2018; Williams et al., 2017). Although not as good as the 2 µatm target for the ship-based observations, this system has shown potential to fill spatiotemporal gaps in the observations, with important implications for the carbon flux estimates. For example, Bushinsky et al. (2019) report on significantly lower uptake of carbon in the Southern Ocean by including winter time pCO_2 from BGC-Argo floats using a neural network interpolation.

4.6.2 Improved constraints on carbonate chemistry:

Although individual components of the ocean carbon observing system have high technical readiness levels, the new capabilities have not yet been integrated with existing, well-tested technologies to provide an observing system that can quantify ocean carbon uptake to within 10%. One key need is an improved understanding of the ocean inorganic carbonate system. There are four measurable inorganic carbon variables in the ocean - total alkalinity (TA), total dissolved inorganic carbon (DIC), pH and fCO_2. By measuring two out of those, the complete

inorganic carbon system can, in theory, be calculated. Small errors in the dissociation constants, the boron-salinity ratio, and small contribution to the total alkalinity from unknown bases, can cause significant discrepancies in directly measured and calculated carbon variables (Fong and Dickson, 2019, Takeshita et al., 2020). A recent study by Álvarez et al. (2020) shows that inconsistencies between calculated and measured pH has decreased during the last decade, and they conclude that improved standard operating procedures for measurements and calculation of pH are urgently needed. An improved understanding of these issues is essential to fully utilize data from, for instance, BGC Argo floats equipped with pH sensors.

4.6.3 High-quality, timely data:

As noted above, the anthropogenic perturbation in the global ocean is more than an order of magnitude smaller than the background natural state. Thus, if we are to track the changing anthropogenic carbon uptake by the ocean, we must maintain very high standards for accuracy and precision of carbon system data. New autonomous technologies offer great promise for expanding the observing system, but cannot be incorporated into the observing system if this substantially increases overall uncertainties. For the foreseeable future, ship-based measurements will continue to be required to calibrate and validate autonomous observations. Cross-over evaluations should occur both with deployment and post-deployment (Fay et al., 2018). At the same time, ocean carbon data should be ingested into publicly-released databases (SOCAT, GLODAP) in a timely manner that supports at least annual diagnoses of the ocean carbon sink. It is essential that these data be carefully quality controlled. As the timescales at which the user community requires these diagnoses become shorter, these data will need to be available more quickly.

4.6.4 Improved quantification of closure terms to link estimates of surface flux and interior C_{ant} accumulation:

In order to reduce uncertainties in the global and regional ocean carbon cycle, we need to understand how interior-based estimates of F_{ant} and surface flux estimates of F_{net} are quantitatively linked. A key barrier to this is the significant magnitude and high uncertainty in current estimates for natural fluxes of carbon in rivers ($F_{nat,riv}$) and interannual variability in the natural carbon cycle ($F_{nat, ns}$).

4.6.5 Constraining mechanisms of surface flux variability:

Though recent work has identified the important role of external forcing from atmospheric pCO_2 and volcanoes in driving ensemble-mean estimates of recent variability of the ocean carbon sink, individual models and individual observation-based products deviate from the mean of the ensembles (Hauck et al., 2020, McKinley et al., 2020). These deviations are due to internal variability of the ocean circulation and biology in each individual ensemble member. We do not currently have understanding of which of these individual estimates best represent the real ocean. To understand the actual total variability of the real ocean carbon sink (total = forced + internal), we need to select the observation-based products and models of highest fidelity. More stringent application of observational constraints can allow for focused analysis of the mechanisms driving variability in the highest-fidelity models and help improve others.

Another approach for combining observations and models is through data-assimilation that constrains the model ocean state and fluxes using observations, and closes data gaps by model dynamics rather than extrapolation. While assimilation applications so far have not provided annually updated global ocean sink estimates with full spatial and temporal

resolution (e.g., Mikaloff Fletcher et al., 2006; DeVries 2014; Verdy and Mazloff, 2017; DeVries et al., 2019), the first spatially and temporally resolved global data-assimilated models are starting to become available (Carroll et al., 2020).

4.6.6 Potential change in the natural carbon cycle:

Climate change induced modifications of the ocean, such as ocean acidification, warming and ecosystem composition could significantly influence the transport of particulate and dissolved organic carbon from the surface to the interior ocean, i.e. the "biological pump". The efficiency of this transport is a key factor regulating the atmospheric CO_2 concentration and is thought to play a role in regulating glacial / deglacial atmospheric CO_2 (e.g. Galbraith and Skinner, 2020). For instance, Marsay et al. (2015) suggest that a warmer ocean might lead to reduced sequestration of CO_2 by the biological pump. Complex interactions in the marine ecosystem will affect carbon export in a changing climate in ways that are difficult to predict and currently inadequately quantified (Laufkötter et al., 2015, 2016, Frölicher et al., 2016).

4.6.7 The future ocean sink under scenarios of emission mitigation:

On centennial timescales under high emissions scenarios, slowing of the overturning circulation and reduced buffer capacity will significantly slow the rate of ocean carbon uptake (Randerson et al., 2015, Ridge and McKinley 2020b). But how will the ocean sink evolve under the increasingly more likely scenario of emission mitigation (Hausfather and Peters, 2020)? Given that the long-term growth and interannual variability of the ocean sink observed to date is driven by the exponential growth of atmospheric pCO_2 (Joos, 1996, Raupach et al., 2014, McKinley et al,. 2020, Ridge and McKinley, 2020b), the ocean sink can be expected to slow in parallel to slowing in the growth rate of atmospheric pCO_2. In effect, the anthropogenic carbon stuck in the near-surface ocean will begin to equilibrate with the atmosphere and the sink will be significantly reduced in response to the mitigation of emissions. This will occur simply due a change in the growth of atmospheric pCO_2 - no change in the ocean circulation or buffer capacity is required (Ridge and McKinley, 2020b). Slowing of the ocean sink will feedback on the atmosphere, reducing the effectiveness of mitigation actions and increasing climate warming.

Though a series of idealized studies have established the general fact that the ocean sink will be reduced with mitigation (Joos et al., 1996, Raupach et al., 2014, Zickfeld et al., 2016, Schwinger and Tjiputra, 2018, MacDougall et al., 2020, Ridge and McKinley, 2020b), the spatially and temporally resolved response of the ocean sink to emission mitigation has received little attention. Thus, we do not know how rapidly the ocean sink will slow, nor where surface flux changes will be most substantial. We do not know what will be required from our monitoring systems to detect these changes.

Current uncertainties in ocean models suggest despite the fact that the current ensemble of models largely agrees as to the recent evolution of the sink (Figure 4), there may be substantial divergence in feedback strength and ocean sink response to emission mitigation. Since the majority of the anthropogenic carbon is held in the ocean's thermocline (Gruber et al., 2019a), the circulation here is critical to the ocean sink's near-term response to mitigation (Iudicone et al., 2016, Rodgers et al., 2020, Ridge and McKinley 2020b). There is substantial spread in the regional distribution of ocean carbon uptake in current models (McKinley et al., 2016, Hauck et al., 2020), and major differences in representations of seasonality (Mongwe et al., 2018), which illustrates knowledge gaps with respect to physical and biological processes and their representations in models. In addition, circulation in these critical upper-ocean regions

is not consistently represented in state-of-the-art models (Bronselaer and Zanna, 2020). Uncertainties in the ocean sink under mitigation need first to be assessed, and then they need to be reduced by model development efforts so that robust projections can be made. Especially in these first decades of climate management via emission mitigation, there will be great public interest in how emission cuts are changing atmospheric CO_2. Scientists need to be prepared to explain ocean carbon sink changes as they occur.

5 The Terrestrial Carbon Cycle

The terrestrial carbon cycle is characterized by large, spatially diffuse fluxes that should generally balance on multi-year time scales. Its primary stocks and fluxes are summarized in Figure 5. The Gross Primary Production (GPP) was estimated to be 123 Pg C yr^{-1} from an analysis of direct flux observation made by a network of eddy covariance towers (Beer et al., 2010). Roughly one third of this (40.8 Pg C yr^{-1}) is produced in the tropical forests, and one quarter (31.3 Pg C yr^{-1}) in the tropical savannas, making the tropics by far the largest contributor to global GPP. Temperate and boreal forest are estimated to have a GPP of only 9.9 Pg C yr^{-1} and 8.3 Pg C yr^{-1}. When integrated over the globe, the GPP of croplands contributes an estimated 14.8 Pg C yr^{-1}.

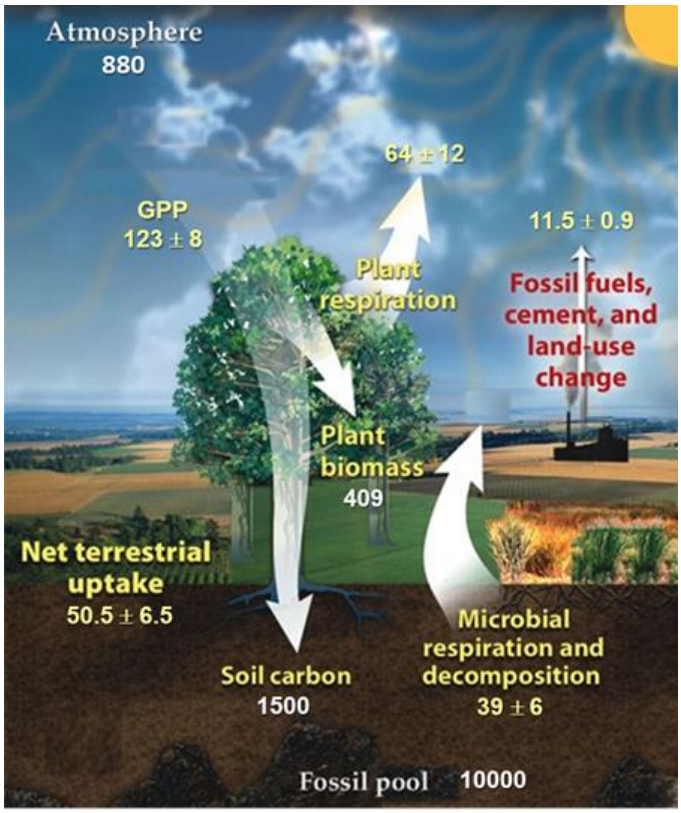

Figure 5: the land carbon cycle, showing the primary fluxes and reservoirs. The sources for the fluxes, shown in yellow, are listed in Table 2. Stock estimates are shown in white. Atmospheric carbon stocks were calculated assuming 410 ppm CO_2 and 1.884 ppm methane. Plant biomass stocks were taken from Spawn et al. (2020). Soil carbon stocks are from Scharlemann et al. (2014). Fossil pool stocks are from Ajani et al. (2013). (Adapted from U.S. Department of Energy Genomic Science program - https://genomicscience.energy.gov).

699 Welp et al. (2011), using oxygen isotopes, suggest that this value of Global GPP may be
700 too low and would be closer to 150 -175 Pg C yr^{-1}. However, Anav et al. (2015) argue that Welp
701 et al. used a limited number of observations and a simple model that included gross
702 photosynthesis, but neglected photorespiration by land plants . They note that plants immediately
703 respire away 20-40% of the carbon fixed by photosynthesis. When photorespiration is included,
704 they note that these GPP values are more in line with those obtained from other methods.

705 Global Autotrophic Respiration is estimated at 64 (±12) Pg Cyr^{-1} (Ito, 2020). This is the
706 term that is also called maintenance respiration and consists mainly of dark respiration. Precise
707 determination is difficult as it also involves a substantial below ground component. It is expected
708 to vary with biome and climate (Ito, 2020). Estimates of Net Primary Production (NPP), GPP
709 minus autotrophic respiration, are generally assumed to be of the order of 50% of GPP (i.e. Ito,
710 2020), but Ciais et al. (2020) suggest values in the range of 44-57 Pg C yr^{-1}. They suggest that
711 decomposition of organic matter or soil (heterotrophic) respiration (SHR) produces 39 Pg C yr^{-1}
712 within an interquartile range of 33-46 Pg C yr^{-1}. This estimate is lower than conventionally
713 assumed but agrees with recent large-scale estimates based on site soil respiration measurements
714 (e.g. Jian et al., 2020). An additional flux to the atmosphere of 8.3 ± 9 Pg C yr^{-1} is due to a series
715 of processes listed Table 2. The remainder of GPP-NPP-SHR and these additional losses
716 constitutes how much carbon is currently taken up by the land, and yields a value of the Net
717 Ecosystem Exchange (NEE) of 2.2 ± 0.6 Pg C yr^{-1}. This value is derived from a combination of
718 methods such as close analysis of stock changes, flux measurements and inventories at the
719 continental scale obtained during the Regional Carbon Cycle Assessment and Processes
720 (RECCAP) Project. It is clear from the above description that the terrestrial carbon cycle is
721 complex, composed of many, sometimes interacting elements, that often are not easy to
722 quantify.

Table 2: Land Carbon Fluxes (Note: numbers without uncertainties are assumed to have uncertainties comparable to their stated values.)

Quantity	Flux (P C yr^{-1})	Reference
Gross Primary Production (GPP)	123 ± 8	1
Net Primary Production	~50.5 (44 - 57)	2
Autotrophic Respiration	~64 ± 12	3
Soil Heterotrophic Respiration	39 (33 - 46)	2
Outgassing by Rivers, Lakes and Estuaries	0.8 to 2.3	2
Fires	1.6	2
Consumption of Harvested Crops	1.5	2
Land Use Change	1.1	2
Grazing	1.0	2
Biogenic Reduced Carbon	0.8	2
Decay and Burning of Wood Products	0.7	2
[1]Beer et al. (2010); [2]Ciais et al. (2020); [3]Ito (2020)		

5.1 Bottom-up Estimates of CO_2 Emissions from Land

Fluxes of carbon between the land biosphere and atmosphere have traditionally been inferred from changes in land carbon stocks. To create a "bottom-up" estimate of the CO_2 emissions or uptake due to deforestation, reforestation, disturbance, or land use change requires information about the area affected, the corresponding carbon stock per unit area, and the fraction of carbon exchanged with the atmosphere due to the observed change. In practice, all three of these properties are challenging to quantify accurately (e.g., Saatchi et al., 2011; Ramankutty et al., 2007; Pearson et al., 2017), but all have benefited from new in situ and remote sensing measurement techniques and more advanced bottom-up modeling techniques.

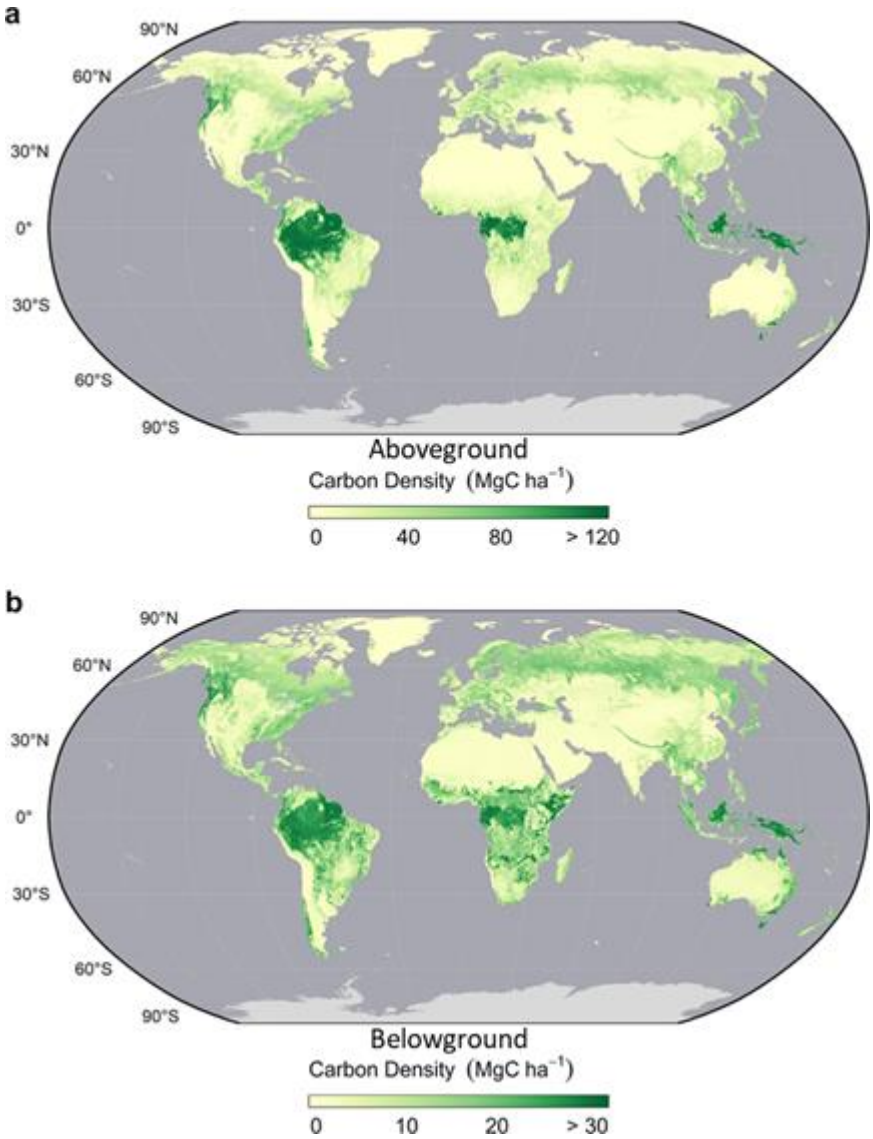

Figure 6. Maps of above and belowground living biomass carbon densities. (a) Aboveground biomass carbon density (AGBC) and (b) belowground biomass carbon density (BGBC). Maps have been aggregated at 5 km spatial resolution (Spawn et al., 2020).

Improved estimates of the area affected by the change have been facilitated by the availability of high-resolution space-based remote sensing observations from sensors such as LandSat, Moderate Resolution Spectroradiometer (MODIS) and Sentinel-2. Until recently, estimates of the carbon stocks per unit area associated with above-ground and below ground biomass still relied primarily on in situ measurements collected from a limited number of dedicated research plots at regular intervals (e.g. Pan et al., 2011). However, the increasing availability of above-ground biomass estimates derived from light detection and ranging (Lidar) and radio detection and ranging (radar) sensors on airborne and space-based platforms is providing improved spatial coverage and temporal sampling frequency. Soil carbon inventories still rely exclusively on in situ measurements, that are often characterized by limited spatial coverage and infrequent (decadal) repeat intervals (Ciais et al., 2014).

Figure 6 shows a map of global biomass (Spawn et al., 2020). This map was produced by combining and harmonizing several satellite products and site information. This involved using the satellite products of biomass with land cover with machine learning techniques to produce aerial estimates, and link this to below ground carbon density information (see Spawn et al., 2020 for more detail). These estimates yield a total living biomass of 409 Pg C, composed of an above ground biomass of 287 Pg C and a below ground biomass carbon density of 122 Pg C. Note that this is several orders of magnitude smaller than the ocean carbon reservoir, and in fact more comparable to the amount of total anthropogenic carbon stored in the ocean (160 Pg C).

CO_2 exchanged between the land and the atmosphere can be measured in situ using networks of eddy covariance flux towers, such as those deployed by FLUXNET (Baldocchi et al., 2001). The global network of eddy covariance sites have grown substantially over the past 25 years, with some records spanning that full period. These data provide unique constraints on the CO_2 fluxes from a broad range of vegetation types, climate regions and disturbance types. Globally, this network still has large gaps, particularly in the tropics, and each flux tower has a limited spatial footprint. Thus, early efforts to upscale results from local to regional scales often introduced large uncertainties (Baldocchi, 2003; Jung et al., 2009; Beer et al., 2010; Xiao et al., 2012; Keenan and Williams, 2018).

More recent methods that combine flux tower data with other remote sensing data in machine learning algorithms to produce upscaled fluxes (see Jung et al., 2020 for a review) yield global GPP estimates that agree well with those obtained from other methods, while providing insights into the processes controlling the carbon cycle of the land biosphere and their changes over time, particularly in the temperate Northern latitudes. Using radar derived estimates of biomass and soil carbon data from the harmonized world soil database and other sources combined with flux estimates of the global product of Beer et al. (2010), Carvalhais et al. (2014) calculated residence times of carbon. They found that the sensitivity of the residence time to soil moisture and temperature did not agree with the sensitivity of a set of DGVMs, while the overall pattern of increasing residence time at higher latitudes was reproduced. The following sections summarize recent results from bottom-up inventories that combine plot-based in situ measurements and remote sensing observations to constrain the carbon uptake and emissions from the land biosphere.

5.2 Indications of a Declining Tropical Land Sink from Bottom-up Inventories

The carbon sink associated with intact tropical forests has been a major focus of bottom-up inventory methods like those described above. For example, Pan et al. (2011) estimated the intact tropical forest carbon sink to be approximately 1.2 Pg C yr^{-1} over 1990–2007 using an in situ inventory derived from up-scaled plot measurements. Hubau et al. (2020) present a more up-to-date assessment of the carbon sink in African and Amazon forest and conclude that while the African sink strength showed no trend (0.66 Mg C ha^{-1} yr^{-1}), the Amazon forest sink slowed down –0.034 Mg C ha^{-1} yr^{-2} between 1983 and 2010, citing Brienen et al. (2015). The results presented in Figure 7 show that this trend has persisted. Hubau et al. (2020) attribute the downward trend in the sink strength by intact forest primarily to increased mortality of live biomass. Disentangling the compound effects of CO_2 fertilization (i.e. the increased rate of photosynthesis resulting from increased levels of CO_2 in the atmosphere), increased temperature and drought, they imply that chronic long-term environmental change factors, temperature and CO_2, rather than simply the direct effects of drought, underlie longer-term trends in tropical forest tree mortality. Temperature increases enhance respiration and a reduce growth by increasing the vapor pressure deficit (VPD).

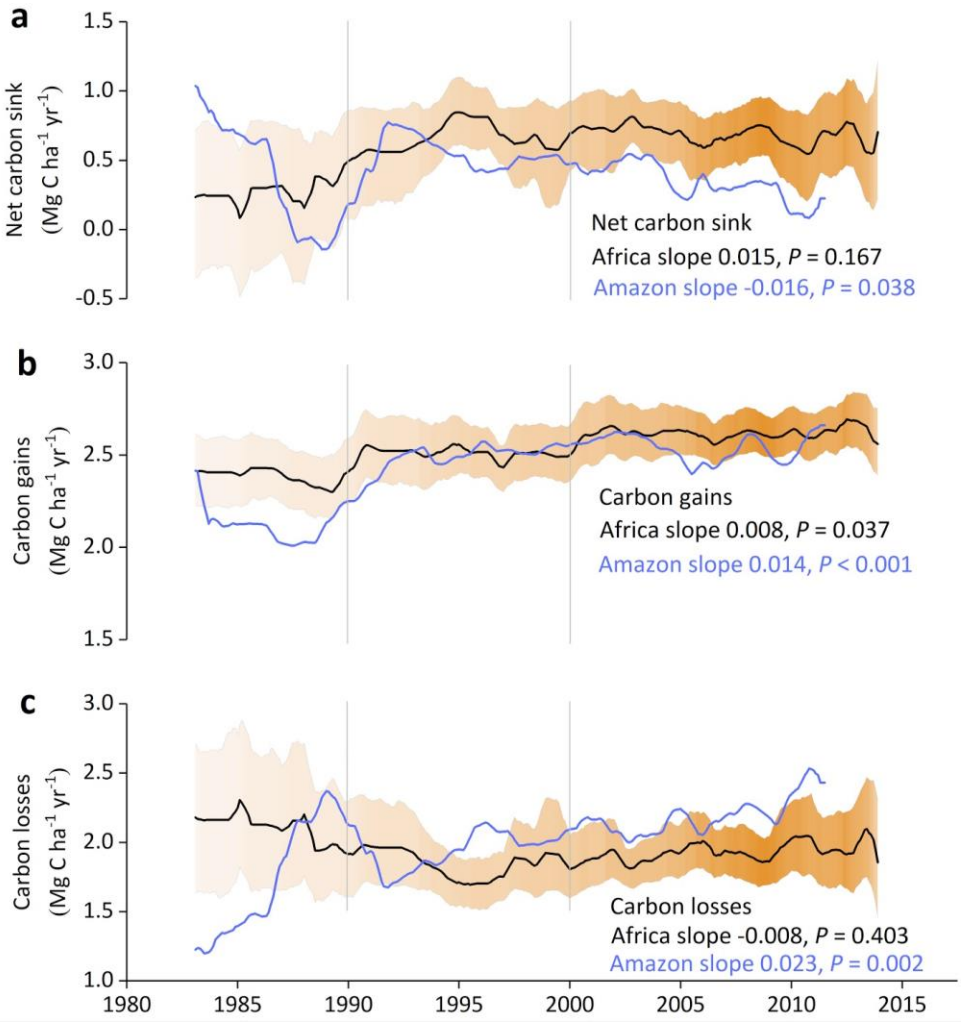

Figure 7. Time series of carbon dynamics from structurally-intact old-growth tropical forests in Africa and Amazonia from 1985 through 2015 (Data: Hubau et al., 2020).

While it is difficult to show the impact of climate extremes such as strong El Niños using in situ inventory data alone, bottom-up inventories of above ground biomass stocks compiled from microwave remote sensing observations provide a temporally denser record of such impacts. For example, contrary to Hubau et al. (2020), Wigneron et al. (2020) show that there was a strong legacy effect after the 2015-2016 El Niño event in both African and Amazon forest (0.9 and 0.5 Pg C loss in 2014-2017 respectively). For the overall tropics, Fan et al. (2019) use Vegetation Optical Depth (VOD) data from microwave sensors to show how changes in the above ground biomass of the forest of Tropical Africa and Tropical Asia contributed strongly to the interannual variability in CO_2 growth rates, while for semi-arid regions, those of Tropical America were the most important.

The net balance of tropical forest biomass remains the sum of the carbon gain from intact forest minus land use change, which is mostly deforestation. Estimates of deforestation in the Amazon fell from about 15000-20000 $km^2\ yr^{-1}$ in the 1990s to about 6000 $km^2 yr^{-1}$ in 2016-2017, but have recently peaked again (http://terrabrasilis.dpi.inpe.br/app/dashboard/deforestation/biomes/legal_amazon/rates) to around 10000 $km^2 yr^{-1}$. Preliminary analysis suggests that this increase would cause 12-14 teragrams of carbon (Tg C) to be released annually, compared to 8-10 Tg C over the period 2005-2015. The strong El Niño of 2015-2016 caused an estimated release of almost 19 Tg C, (https://www.globalfiredata.org/regional.html#amazonas) of which, 75% was due to forests.

Another possible cause of mortality could be a decrease in photosynthesis or GPP. Quantitative estimates of these quantities are now available from space-based observations of solar induced chlorophyll fluorescence (SIF). As plants absorb sunlight to perform

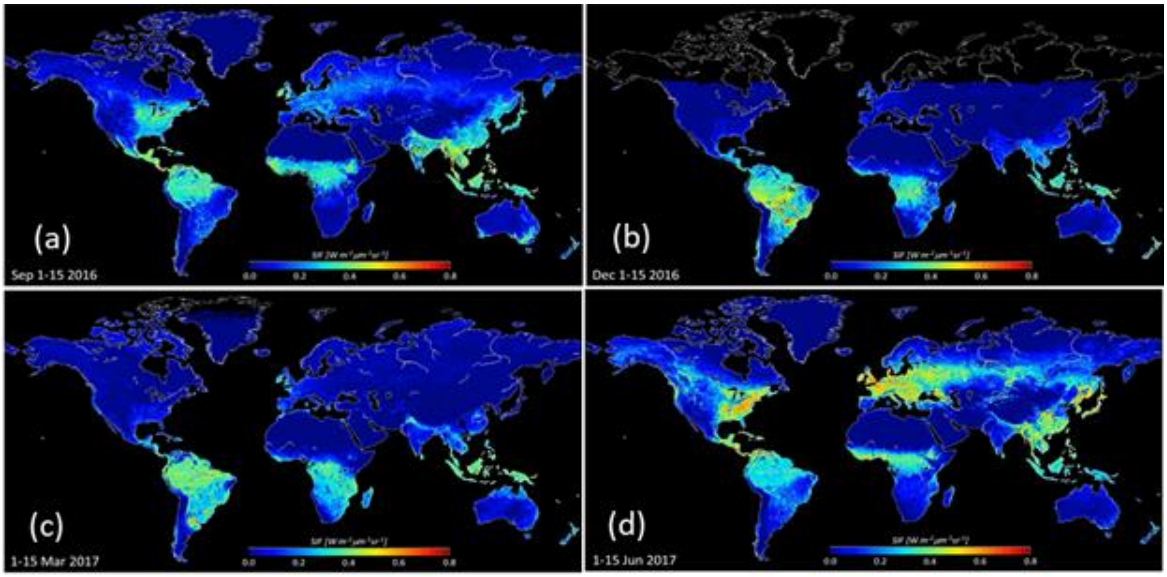

Figure 8. OCO-2 observations of SIF for (a) 1-15 September 2016; (b) 1-15 December 2016; (c) 1-15 March 2017, and 1-15 June 2017. Blue indicates low SIF and therefore low photosynthetic activity. The warmer colors indicate higher SIF and higher photosynthetic activity (Ying Sun, Personal communication,2018).

photosynthesis, a faction of that light (< 2%) is re-emitted at longer wavelengths (fluorescence), which can be detected in the cores of strong solar Fraunhofer lines by high resolution space-

based spectrometers (Frankenberg et al., 2014; Sun et al., 2018). SIF is a rapidly-responding indicator of light use efficiency that has been adopted as a functional proxy for GPP (Figure 8). Koren et al. (2018) find that SIF was strongly suppressed over areas with anomalously high temperatures and reduced availability of soil moisture. SIF fell below its climatological range starting from the end of the 2015 dry season (October), but returned to normal levels by February 2016 when atmospheric conditions returned to normal. Importantly, the impacts of the El Niño were not uniform across the Amazon basin.

The eastern part of the Amazon experienced a much larger (10–15%) reduction in SIF than the western part (2–5%). Koren et al. estimated the integrated loss of GPP across the Amazon basin relative to eight previous years to be 0.34 – 0.48 Pg C in the three-month period October-December 2015. Ciais et al. (2020) calculated a small sink of 0.06 Pg C yr^{-1} using a combination of top down and bottom up inventories for the whole of South America, albeit with a large uncertainty of 0.29 Pg C yr^{-1}. Thus, in contrast with the African sink, which shows no trend, the Amazon forest sink strength appears to be gradually declining, and that extreme events imposed on this trend cause additional losses.

5.3 Evidence for a Global Greening from Bottom-up Inventories

In a recent analysis of land use change over 1982-2016, Song et al. (2018) show that global tree cover has increased by 2.24 million km^2 (+7.1%) relative to the 1982 value. This overall net gain is the result of a net loss in the tropics being outweighed by a net gain in the extra tropics. Global bare ground cover has decreased by 1.16 million km^2 (−3.1%), most notably in agricultural regions of tropical and subtropical Asia. Of all land changes, 60% are associated with direct human activities and 40% with indirect drivers such as climate change.

Several factors are thought to impact vegetation greening, including rising atmospheric CO_2 concentrations, climate change, nitrogen deposition and land- use changes. Supporting the conclusions of Song et al., using long-term satellite records, Piao et al. (2020) find a significant global greening of vegetated areas since the 1980s, which they suggest has continued past 2010 (Figure 9). The most pronounced greening is observed in China and India and is due to afforestation and in particular agricultural intensification. They also analyzed a set of DGVMs that suggest CO_2 fertilization is the main driver of global vegetation greening. In addition, warming was the major cause of greening in boreal and Arctic biomes. However, in contrast to this result and in line with Hubau et al., they find that CO_2 fertilization had negative effects on greening in the tropics. Overall, they suggest that the greening contributed to mitigation of global warming through enhanced land carbon uptake and evaporative cooling, but could also lead to decreased albedo, which could potentially cause local warming.

847 Piao et al. (2020) find widespread greening occurred since the 1980's north of 50ºN.
848 Warming was considered the major cause of greening in boreal and Arctic biomes. However, a
849 small, but persistent browning was seen at 3% of the high latitudes between 1982 and 2014. Such
850 browning trends are caused by trends in disturbances such as fires, harvesting and insect

851 defoliation (Beck and Goetz, 2011). North American boreal forests exhibit browning areas nearly
852 20 times larger than the Eurasian boreal forests. Importantly, dramatic increases in fire

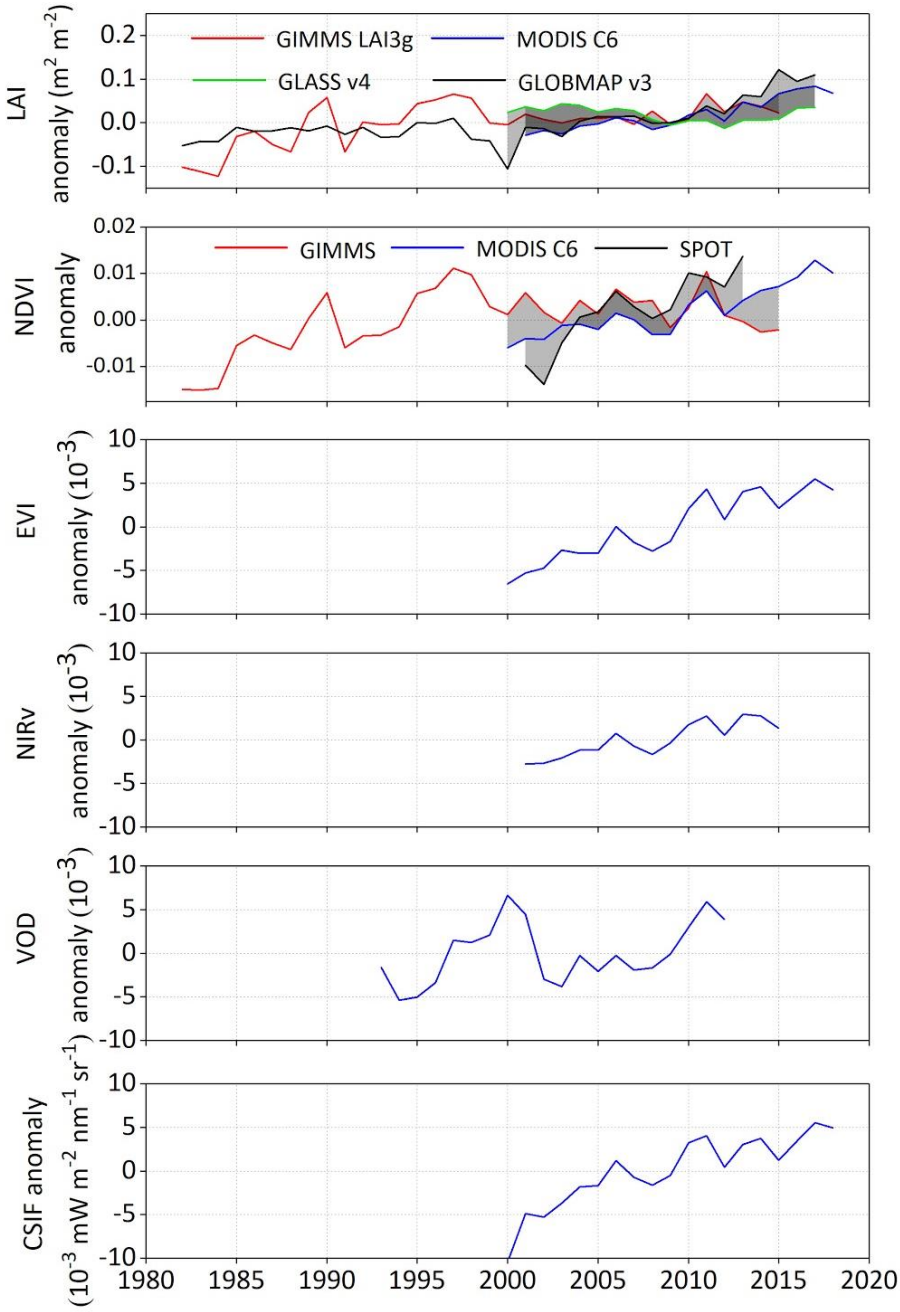

Figure 9. Changes in satellite- derived global vegetation indices, including anomalies in the normalized difference vegetation index (NDVI), Enhanced Vegetation Index (EVI), near-infrared reflectance of vegetation (NIRV), vegetation optical depth (VOD) and contiguous solar- induced fluorescence (CSIF) (Data: Piao et al., 2020.)

853 disturbances and insect infestation such as those from the bark beetle have also been seen in
854 browning areas, partially offsetting the decades long greening trend.

While the CO_2 emissions and uptake by agriculture and other land use practices are still highly uncertain, there is growing evidence that these activities are contributing to the global greening trend. Zeng et al. (2014) analyzed the impact of the Agricultural Green Revolution, which enhanced crop yields through hybridization, irrigation and fertilization, on the amplitude of the atmospheric CO_2 seasonal cycle. They use a DGVM to analyze CO_2 observations and atmospheric inversions for the 50-year period extending from 1961 to 2010. Between the decades 1961-1970 and 2001-2010, they attribute the observed the ~15% increase in the CO_2 seasonal amplitude to a peak growing season that now starts ~10 days earlier and lasts about two weeks longer, with the land biosphere absorbing ~0.5 Pg more carbon at its peak in July than it did at the beginning of the period. They find that the increased CO_2 seasonal amplitude originates primarily from two regions: the midlatitude cropland between 25º N and 60º N and the high-latitude natural vegetation between 50º N and 70º N. Zeng et al. note that the leading role of mid-latitude cropland in CO_2 uptake is reinforced by recent space-based observations of SIF, which show that at the peak of the growing season, cropland is substantially more productive than surrounding dense forests with similar climate conditions. These conclusions are reinforced by other studies of the relationship between SIF and crop productivity (Guan et al., 2016; 2017; He et al., 2020).

5.4 Current Status and Next Steps in Bottom-up Land Carbon Observations and Analysis

The overall picture that emerges from recent observations of aboveground biomass stocks is that the classical sinks in the tropical humid forests are slowly losing their sink strength, with these changes amplified by deforestation. In extra-tropical areas, greening has taken place due to afforestation and increased agriculture. At Arctic latitudes, browning, i.e. a loss of vegetation activity, is increasing. These trends provide the fragile background for a still slowly increasing land uptake. The underlying causes for these increases are complex and consist of interacting processes of CO_2 fertilization, nutrient and water availability compounded by climate variability. On top of this, the impact of human activities including deforestation and intensifying agriculture are additional complications.

This myriad of interacting processes complicates predictions of the future trajectory of the terrestrial sink. Until now, the sink has grown in harmony with the increase in fossil fuel emissions with the result that the atmospheric fraction has remained remarkably constant over the past 40 years or so. Theoretical and empirical evidence, such as that described here in this paper, suggest that this may stop at some point in the future. Theoretically it is unlikely that the global vegetation will continue to grow indefinitely. Water and nutrient shortages will impede increased growth (Wang et al., 2020). Similarly, the balance between GPP, as determined by plant photosynthetic properties, and the heterotrophic respiration is expected to shift. It has long been known that on short time scales, the efficiency of photosynthesis decreases beyond a critical temperature, while that of heterotrophic respiration continues to increase (Doughty et al., 2008; Mau et al., 2018). This behavior has recently been experimentally confirmed by Duffy et al. (2021) using FLUXNET data. How this works out at longer time scales, when heterotrophic carbon limitation on microbial decomposition may also start playing a role is virtually unknown (Soong et al., 2021). It is likely that the first signs of a deceleration of the terrestrial carbon sink, and a decoupling with the fossil fuel increase are already there, and that the atmospheric fraction will increase.

One factor that has impeded progress in the analysis of trends inferred from aboveground biomass stocks is they are not well represented in the current generation of DGVMs. For example, Sitch et al. (2015) use an ensemble of nine DGVMs to study global and regional processes and trends in the land sink for a period extending from 1990 - 2009. They conclude that for this period, the global land sink is increasing, led by CO_2 fertilization of plant production, with the largest increases seen in the natural ecosystems of the tropics. They find no significant trend in northern land regions. This is largely inconsistent with the observations presented above.

Another cause for concern is the recent finding that the effects of CO_2 fertilization appear to decline due to nutrient limitations and water availability (Wang et al., 2020). Like the results presented above, this conclusion is, largely based on satellite and ground-based data analysis of NDVI and SIF, and cannot be reproduced by the current generation of DGVMs. A decline in the effectiveness of CO_2 fertilization of the order as suggested by Wang et al. (2020) gives cause for concern of the efficiency of the terrestrial sink going forward. To date, both the land and ocean sink have increased steadily over time such that the airborne fraction has remained relatively stable since the 1960s (Raupach et al., 2014). If the land biospheric processes responsible for maintaining the airborne fraction are disrupted by human activities or climate variability and change, this could compromise our ability to predict the coupled evolution of the land carbon cycle and its interactions with an evolving climate.

Fortunately, advances in bottom-up observation capabilities and modeling tools are coming on line to facilitate more comprehensive and responsive monitoring and analysis of the land carbon cycle. Ground-based estimates of stocks and fluxes will continue to provide the most accurate and site-specific information. However, remote sensing observations from airborne and space-based active and passive sensors and modeling tools will play an increasingly important role for upscaling these results to yield useful constraints on regional to global scales.

Xiao et al. (2019) review the evolution of remote sensing observations of terrestrial carbon stocks over the past 50 years, spanning the electromagnetic spectrum from the visible, infrared, and microwave. They then review the methods being used to analyze the observations to yield quantitative estimates of carbon stocks and fluxes, including vegetation indices, SIF, light use efficiency models, DGVMs, as well as data driven (including machine learning) techniques. Xiao et al. discuss the use of these data and analysis techniques to quantify the impacts of disturbances and to quantify uncertainties in carbon stock estimates, noting advances achieved by integrating in situ and remote sensing observations into progressively more advanced, process-based carbon cycle models. Looking forward, they predict substantial improvements in our ability to track above ground biomass stocks, through the use of merged datasets, such as the NASA Harmonized LandSat and Sentinel 2 (HLS) products, ultra-high resolution imaging products from QuickBird, IKONOS, and UAVs, lidar measurements from GEDI, future active microwave products from NASA's NISAR (Rosen et al., 2016), TanDEM-L and BIOMASS missions (Quegan et al., 2019).

While in situ and space-based measurements of aboveground biomass play a critical role in efforts to monitor trends in managed and natural forest, they are not sufficient for monitoring the rapid turnover of carbon stocks in croplands and grasslands. Until recently, high resolution imaging observations and moderate resolution estimates of vegetation indices provided the primary tools for scaling up plot-based observations to national and continental scales. Recently, these capabilities have been augmented by space-based observations of SIF. SIF relates the

emission of excess radiative energy from the photosynthesis process of leaves at two wavelengths 685 nm and 740 nm to photosynthesis, or GPP. Estimates of SIF from GOME, GOME2, GOSAT, OCO-2 and TROPOMI are increasingly being used to monitor crop and grassland productivity and crop yield prediction (He et al., 2020; Peng et al., 2020; Parazoo et al., 2020; Qiu et al., 2020; Yin et al., 2020). Future SIF observations from the ESA FLuorescence EXplorer (FLEX), Japan's GOSAT-GW, NASA's GeoCarb, and the Copernicus CO2M missions promise substantial improvements in resolution.

To fully exploit these new measurements to describe long term trends in the terrestrial carbon cycle, the in situ and remote sensing measurements must be reconciled so that their climate data records can be combined to increase their spatial and temporal resolution and coverage. The protocol for cross-validating aboveground biomass products described by Duncanson et al. (2019) and the effort by the Forest Observation Initiative to develop a global in situ forest biomass databases for validating remote sensing observations (Schepaschenko et al., 2018) are positive steps in this direction. While the current generation of DGVMs and other terrestrial biosphere models are evolving rapidly and provided key insights into the processes driving the land carbon cycle, these modeling tools are still yielding widely diverging results the uptake of CO_2 by the land biosphere and its trends (i.e. Fisher et al., 2014; Sitch et al., 2015; Keenan and Williams, 2018; Parazoo et al., 2020). These limitations have raised concerns about their use in CO_2 emission inventory development activities (Grassi et al., 2018; Petrescu et al., 2020). Pioneering model intercomparison efforts such as the Carbon-Land Model Intercomparison Project (C-Lamp; Randerson et al., 2009) are being followed up by the International Land Model Benchmarking (ILAMB) project (see https://www.ilamb.org/) to address these concerns and accelerate the development of these critical tools.

6 The Atmospheric Carbon Cycle

Until recently, the concentrations of atmospheric CO_2 and other greenhouse gases were measured in situ by instruments deployed at surface stations, tall towers or on aircraft. Continuous measurements of atmospheric CO_2 were initiated in 1958 by Charles David Keeling of the Scripps Institution of Oceanography, when he established stations at Mauna Loa, Hawaii and the South Pole. These measurements are now being collected at a global network that includes the U.S. National Oceanic and Atmospheric Administration (NOAA) Global Greenhouse Gas Reference Network (GGGRN), the European Integrated Carbon Observation System (ICOS) network and other partners of the World Meteorological Organization Global Atmospheric Watch (WMO GAW) program. These in situ measurements provide the most

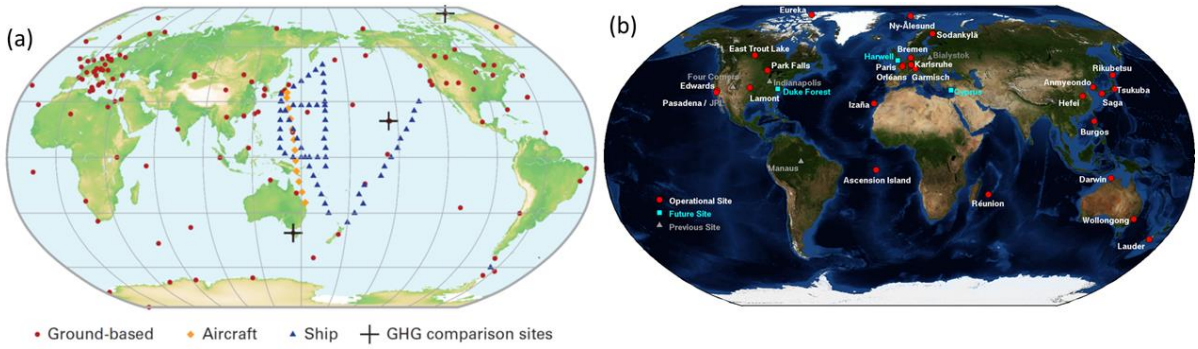

Figure 10: Spatial distribution of stations in the ground-based atmospheric CO_2 monitoring network. The vast majority of the stations are in North America and western Europe. (a) In situ CO_2 measurements are collected routinely at the WMO Global Atmospheric Watch Stations (from WMO Greenhouse Gas Bulletin, 25 Nov. 2019). (b) Solar-looking remote sensing observations of CO_2 are collected at Total Carbon Column Observing Network (TCCON) stations.

accurate estimates of the CO_2 concentrations and their trends on global scales. They also quantify chemical and isotopic tracers, such as carbon-14 (^{14}C), which help to discriminate fossil fuel from biogenic contributions to the observed CO_2 trends. Perhaps the most important asset of the ground based in situ measurements is the length of their climate data records, which now extend over 70 years. While the ground-based networks have grown over time, the spatial resolution and coverage of in situ measurements are still far too limited to identify and quantify the natural and anthropogenic emission sources emitting CO_2 into the atmosphere and the natural "sinks" absorbing it at the surface on spatial scales ranging large urban areas to nations. The coverage is particularly sparse in Arctic, boreal and tropical land regions and over most ocean basins (Figure 10).

Recent advances in space based remote sensing capabilities are providing new insights into the current state of the atmospheric carbon cycle as well as the primary processes controlling its interactions with the land and ocean carbon reservoirs. With the launch of Japan's Greenhouse gases Observing SATellite, GOSAT in 2009, and NASA's Orbiting Carbon Observatory in 2014, space-based remote sensing measurements are complementing the ground-based and airborne CO_2 measurements with much greater spatial resolution and coverage, yielding tens of thousands of observations over the sunlit hemisphere each day. These two satellites have recently been joined by their sister missions, GOSAT-2 and OCO-3, providing additional coverage and resolution. These space-based sensors collect high-resolution spectra of reflected sunlight within molecular oxygen (O_2) and CO_2 bands that can be analyzed to yield precise, spatially resolved estimates of the column-averaged CO_2 dry air mole fraction, XCO_2. The principal challenge of this technique is the need for unprecedented levels of precision and accuracy for a space-based atmospheric trace gas measurement. While intense local sources, such as large coal-fired power plants or large urban areas can increase the near surface CO_2 concentrations by more than 10%, these variations decay rapidly with altitude, such that they rarely yield XCO_2 variations larger than 1-2 ppm (0.25 to 0.5%) on the spatial scale of a satellite footprint (1 to 100 km^2). Natural sinks of CO_2, such as forests or ocean basins, produce even smaller changes in XCO_2.

In addition to XCO_2, these sensors collect simultaneous observations of SIF, providing additional constraints on the CO_2 uptake by the land biosphere. The primary challenge of this approach is the need for unprecedented precision and accuracy to resolve the small (< 0.25% or 1 ppm) XCO_2 variations associated with surface sources and sinks of CO_2. While these space-based measurements are not as accurate as those collected by ground-based and airborne systems, they complement those observations with improved coverage and spatial resolution.

Atmospheric CO_2 estimates collected by ground-based, airborne, and space-based sensors are now being assimilated into atmospheric inverse models, along with meteorological data and space based global measurements of the land biosphere to provide new insights into the carbon cycle. These models illustrate the spatial and temporal relationships between SIF and the seasonal CO_2 drawdown in the northern hemisphere spring (Eldering et al., 2017; Byrne et al., 2018; Yin et al., 2020; Qui et al., 2020). They have also been used to quantify the atmospheric signature of the land biosphere's response to the record-setting 2015-2016 El Niño (Chatterjee et al., 2017; Liu et al., 2017; Palmer et al., 2019). The high spatial and temporal resolution of these atmospheric CO_2 observations, combined with their global coverage, should facilitate the development of improved diagnostic models for studying processes operating in the present-day carbon cycle. This evolving land-ocean-atmosphere carbon monitoring system also fosters the

development of more comprehensive and reliable prognostic models for predicting the evolution of the carbon cycle as it responds to climate change.

From a carbon monitoring perspective, these atmospheric measurements are now providing quantitative constraints on CO_2 emission and uptake at policy relevant spatial and temporal scales. CO_2 estimates retrieved from GOSAT and OCO-2 measurements clearly show persistent positive anomalies associated with the anthropogenic emissions over East Asia, Western Europe and eastern North America (Hakkarainen et al., 2016; 2019; Wang et al., 2018). On smaller scales, space-based XCO_2 estimates are being used to quantify CO_2 emissions from large urban areas (Hedelius et al., 2018; Wu et al., 2018; Wu et al., 2020) and individual power plants (Nassar et al., 2017; Reuter et al., 2019). Estimates of CO_2 emissions and uptake derived from atmospheric measurements of XCO_2 are not as source specific as traditional bottom-up statistical methods, which infer CO_2 emissions from fuel use, power generation statistics, etc. However, they complement those methods by providing an integral constraint on the total amount of CO_2 added to or removed from the atmosphere by all natural and anthropogenic processes.

The availability of high spatial resolution atmospheric emissions products within a few weeks of acquisition could help to identify and track rapidly-evolving emission hotspots that are often missed in the bottom-up statistical inventories. As these tools are integrated into a more comprehensive carbon management system, they could also help carbon managers to assess the effectiveness of their carbon management strategies, and help to identify emerging emission reduction opportunities.

6.1 The Tropical Land Carbon Cycle Did Not Recover as Expected from 2015–2016 El Niño

As noted above, bottom-up inventories indicate that the strength of the tropical forest sink is gradually declining over time. This conclusion is reinforced by atmospheric CO_2 observations. Gatti et al. (2014), using in situ observations of atmospheric CO_2, determined that the Amazon basin lost 0.48 ± 0.18 Pg C yr^{-1} during a dry year (2010), but was carbon neutral (0.06 ±0.1 Pg C yr^{-1}) when measurements were taken during a wet year (2011). Correcting for carbon losses, they derived a basin net biome exchange that was carbon neutral during the dry year. During the wet year, vegetation was a net carbon sink of 0.25 ± 0.14 Pg C yr^{-1}. The latter value compares well with the bottom-up estimates by Hubau et al. (2020).

The availability of time-resolved global measurements of atmospheric CO_2 at high spatial resolution is providing a more comprehensive description of impacts of severe weather and climate on the exchange of carbon between land and ocean reservoirs and the atmosphere on regional scales. These emerging capabilities were recently demonstrated in studies of the record-setting 2015-2016 El Niño. GOSAT and OCO-2 measurements collected over the central and eastern tropical Pacific basin were combined to quantify 0.5 ppm XCO_2 decreases associated with reductions in outgassing in the tropical Pacific Ocean during March through July of 2015 (Chatterjee et al., 2017). These reduced CO_2 values were then replaced by 0.5 to 2 ppm increases in XCO_2 associated with reduced uptake and increased emissions of CO_2 by tropical forests in South America, Africa and tropical Asia (Liu et al., 2017; Heymann et al., 2017; Palmer et al., 2019; Crowell et al., 2019; Figure 11).

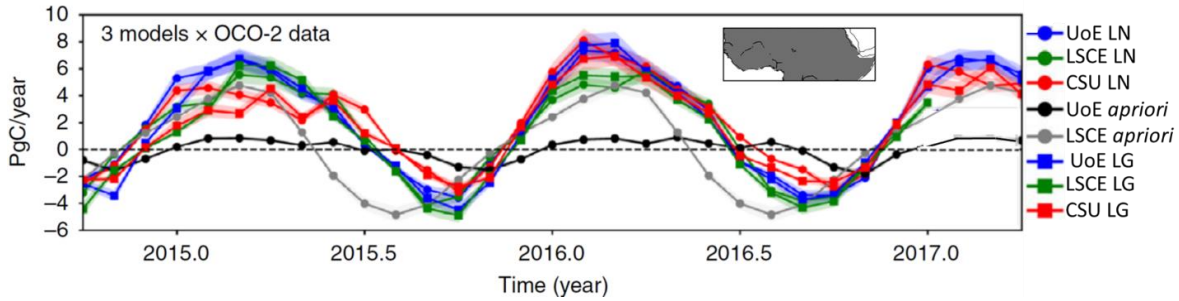

Figure 11. CO_2 fluxes from tropical northern Africa inferred from the University of Edinburgh (UoE), LSCE and Colorado State University (CSU) models constrained by in situ CO_2 measurements as well as XCO_2 data from GOSAT and OCO-2. Positive fluxes indicate CO_2 emissions from the land surface to the atmosphere. LN and LG denote OCO-2 XCO_2 measurements taken using nadir and glint observing modes, respectively. The geographical region is shown in the inset. Fluxes inferred from OCO-2 data have larger amplitudes and a larger seasonal cycle than those from in situ data. An extended mission will provide new opportunities to validate these results and track their changes (Adapted from Palmer et al., 2019).

Liu et al., (2017) find that the pan-tropical biosphere released an additional 2.36 ± 0.34 Pg C into the atmosphere, or about 78% of the global total. Emissions originated throughout the tropics with 0.91 ± 0.24, 0.85 ± 0.21, and 0.60 ± 0.31 Pg C from tropical South America, tropical Africa, and tropical Asia, respectively. Although the enhanced emissions from these three regions were comparable, *different* processes appeared to dominate in each region. Fire emissions dominated over tropical Asia. Both increased respiration and fires associated with historically high temperatures dominated over tropical Africa. Increased CO_2 over the Amazon was attributed to GPP reductions associated with drought. These results support the hypothesis that El Niño related increases in CO_2 growth rates are primarily due to tropical land carbon fluxes, but they show that specific mechanisms can differ from continent to continent.

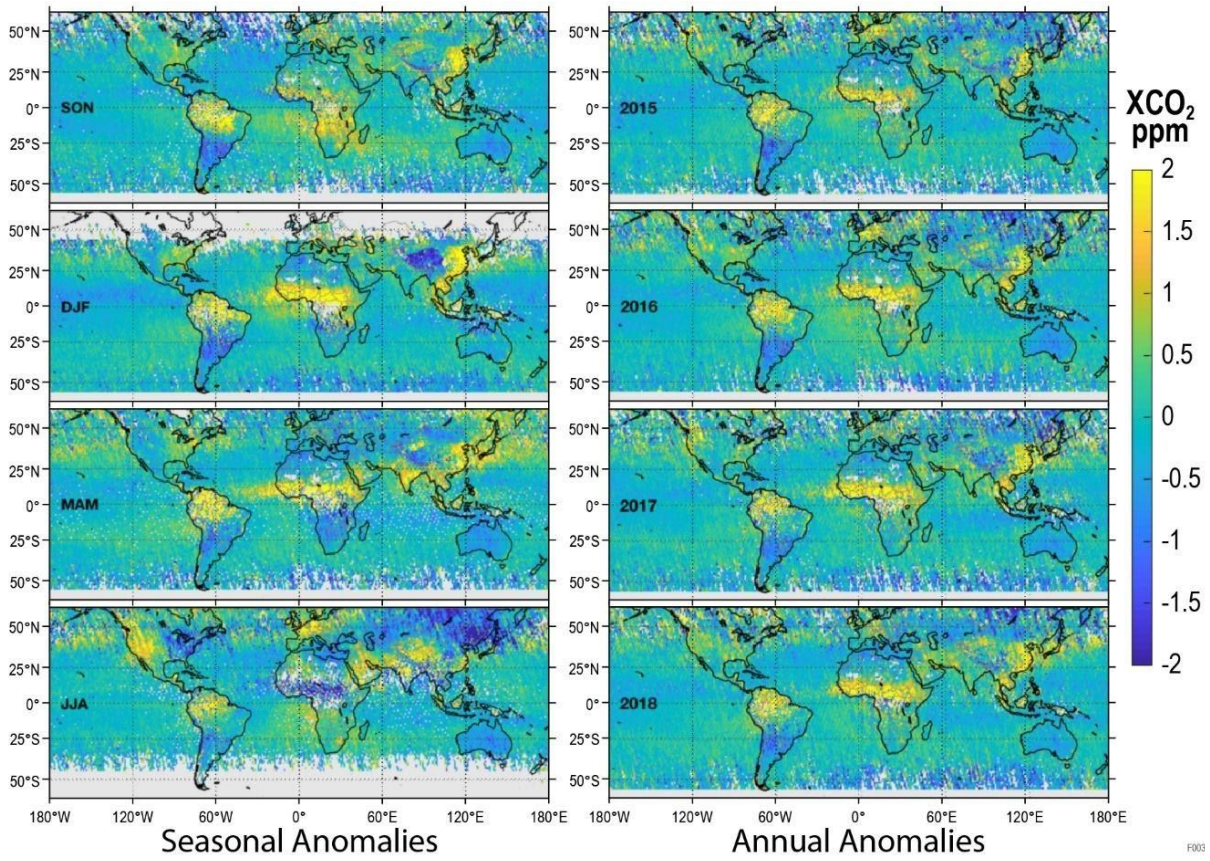

Figure 12. OCO-2 XCO_2 estimates indicate that some regions have persistently high (positive) or low (negative) spatial anomalies that persist from season to season (left, integrated over the four-year period) and from year to year (right). A longer data record is needed to determine whether the tropical anomalies reflect short-term climate variations or long-term climate trends. (Adapted from Hakkarainen et al., 2019).

Palmer et al., (2019) use three different models to analyze *in situ* CO_2 measurements along with XCO_2 and SIF observations from Japan's Greenhouse gases Observing SATellite (GOSAT) and OCO-2 (Figure 11). Like Liu et al., in 2015–2016, they find that the largest CO_2 emissions over western Ethiopia and western tropical Africa, where there are large soil organic carbon stores and substantial land use change. While the amplitude of the XCO_2 anomalies that

produced these sources may have been overestimated in the early OCO-2 XCO_2 products used in this investigation (version 7), they clearly reveal important components of the tropical carbon budget that is largely missing from in carbon flux inverse models constrained by *in situ* measurements alone.

As the 2015-2016 El Niño transitioned to a weak La Niña in 2017, and then to more neutral conditions in 2018, OCO-2 XCO_2 and SIF estimates indicate that tropical forests, once thought to be significant net sinks of CO_2 (Pan et al., 2011; Sellers et al., 2018) may now be persistent net sources (Hakkarainen et al., 2019; Palmer et al., 2019; Crowell et al., 2019). Hakkarainen et al. (2019) processed OCO-2 Version 9 (V9) XCO_2 data to remove the seasonal cycle and reveal spatially persistent anomalies. They find positive XCO_2 anomalies over tropical forests with amplitudes as high as 2 ppm above the background (Figure 12). The spatial extent of the Amazon anomaly was slightly greater during the 2015–2016 El Niño than in 2017, but the positive XCO_2 anomalies there have persisted from season to season and from year to year throughout the OCO-2 mission. The Amazon is now a persistent *source* of CO_2, rather than a sink. Positive anomalies over topical Africa and Southeast Asia are seen on annual time scales. However, in Figure 11, tropical African fluxes are negative during June-July-August (JJA), indicating that this region becomes a weak sink during that season (Palmer et al., 2019). These conclusions are supported by some satellite-based aboveground biomass studies (Baccini et al., 2017; Wigneron et al., 2020), but are inconsistent with plot-based studies (Pan et al., 2011; Hubau et al., 2020), which conclude that tropical forests are absorbing less CO_2, but are still a net sink of carbon.

Additional insight into the tropical land carbon cycle can be obtained by comparing XCO_2 anomalies to observations of SIF. Specifically, the largest positive CO_2 anomalies derived from the space-based XCO_2 estimates are seen in regions where SIF observations indicate the highest photosynthetic activity (Figure 8). This suggests that in spite of significant growth, tropical forests are now emitting more CO_2 than they absorb, when integrated over the annual cycle. This may have always been the case, but it may also be due to increased respiration, drought stress, fires, and other processes.

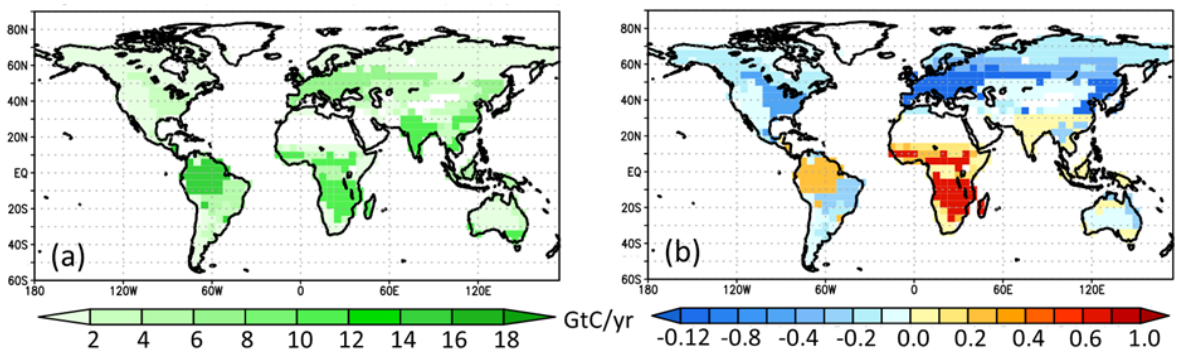

Figure 13. (a) GPP from OCO-2 SIF and (B) Net Biospheric Exchange (NBE) from XCO_2 and SIF, both expressed in gigatons of carbon per year (Pg C yr^{-1}) for 2015-2018. Negative NBE indicates sinks while positive values indicate sources. NBE is typically < 5% of the GPP, but is positive in the tropics where we see the highest GPP, in sharp contrast to existing models (Junjie Liu, Personal communication, 2019).

These conclusions are reinforced by experiments that assimilate XCO_2 and SIF results into atmospheric inverse models (Liu et al., 2017; 2020; Palmer et al., 2019; Chevallier et al., 2019; Crowell et al., 2019). Even in the Amazon and tropical Africa, where the GPP exceeds 10 Pg C yr^{-1} (Figure 13a), the net biospheric exchange (NBE) can still be positive (Figure 13b). This contradicts results from carbon flux inversion models constrained by in situ data, alone, which indicate that, at least until recently, these tropical forests were significant net sinks of CO_2 (Hubau et al., 2020).

6.2 New Insights into the Extratropical Land Biosphere from Space

Unlike for the tropics, the XCO_2 anomalies and retrieved CO_2 fluxes from northern temperate and boreal forests are generally more consistent with expectations. During the NH summer (JJA in Figure 12), we see negative XCO_2 anomalies. Annual average flux inversion experiments show moderately strong GPP and negative NBE (Figure 13). The OCO-2 XCO_2 and SIF measurement therefore indicate that these forests have continued to be significant net CO_2 sinks as the CO_2 seasonal cycle amplitude has grown in response to warming. While mid- and high-latitude CO_2 fluxes derived from inverse models constrained by OCO-2 XCO_2 and SIF estimates are generally consistent with those from earlier flux inversion experiments constrained by *in situ* CO_2 data alone (Lucht et al., 2002; Graven et al., 2013; Byrne et al., 2018), there are substantial differences in amplitude and phase in some regions (Reuter et al., 2017; Crowell et al., 2019; Palmer et al., 2019; Chevallier et al., 2019).

Space-based observations of XCO_2 and SIF provide unique opportunities to study the relationships between the land and atmospheric carbon cycles and the hydrological cycle. Yin et al. (2020) combine SIF with atmospheric CO_2 observations to quantify the effects of large-scale flooding on cropland carbon sequestration. Widespread flooding during spring and early summer of 2019 delayed crop planting across the U.S. Midwest. As a result, satellite observations of SIF from OCO-2 and the TROPOspheric Monitoring Instrument (TROPOMI) reveal a shift of 16 days in the seasonal cycle of photosynthetic activity relative to 2018, along with a 15% lower peak photosynthesis. Yin et al. find that the 2019 anomaly produced an estimated GPP reduction of -0.21 Pg C in June and July that was partially compensated in August and September with a +0.14 Pg C increase. The growing season integral corresponds to a 4% reduction in cropland GPP for the Midwest, but a 3% increase for areas where cropland occupies less than 10% of the land. Using an atmospheric transport model, they show that a decline of ~0.1 Pg C in the net carbon uptake in June and July is consistent with observed ~10 ppm CO_2 enhancements in the midday boundary layer from the Atmospheric Carbon and Transport - America (ACT-America) aircraft and the ~1 ppm increases in XCO_2 seen by OCO-2.

In another study, Gonsamo et al. (2019) combined OCO-2 SIF observations with soil moisture (SM) observations from NASA's Soil Moisture Active Passive (SMAP) mission to study the impact of environmental limiting factors on terrestrial ecosystem productivity of drylands and croplands. For drylands (dry sub-humid, semi-arid, and arid zones) and the majority of croplands, soil water content is typically low and topsoil moisture is critical for plant growth. As expected, SMAP SM retrievals show positive daily relationships with OCO-2 SIF for drylands and croplands of the tropics and Australia, where SM is limiting plant growth and concurrent data records are sufficient to make statistical inferences. Negative relationships between SIF and SM were observed in forested areas of mid-latitude dry sub humid zones with high average annual SM. In these regions, SIF showed a positive relationship with air

1149 temperature. They find strong evidence that the OCO-2 SIF is accurately capturing monthly
1150 SMAP SM dynamics, particularly for regions with distinct seasonality of rainfall such as Sub-
1151 Saharan North Africa, Indian subcontinent, and southern Africa.

1152 ### *6.3 Lessons Learned from Space-based XCO_2 Estimates over the Ocean*

1153 In general, XCO_2 anomalies over the ocean were expected to be much smaller than those
1154 over land, but they have still yielded some surprises in first-generation space-based observations
1155 of CO_2. For example, the earliest version of the OCO-2 product, version 7 (v7) revealed large (2-
1156 3 ppm) positive XCO_2 anomalies over the midlatitude ocean (20 – 50 S) in the southern
1157 hemisphere during the Austral winter. These anomalies were initially suspicious because they
1158 were not seen in the XCO_2 observations from the Total Carbon Column Observing Network
1159 (TCCON) stations at Lauder, New Zealand or Wollongong, or Reunion Island (Wunch et al.,
1160 2017). However, they could not be dismissed immediately because there are few CO_2
1161 measurements over the ocean at the latitudes where they had their largest amplitudes. Retrieval
1162 algorithm validation efforts subsequently traced these anomalies to a bias introduced by a thin
1163 layer of volcanic aerosol in the stratosphere that had been neglected in the retrieval algorithm
1164 (O'Dell et al., 2018). This bias was corrected in the version 8 (v8) and later versions of the OCO-
1165 2 products by explicitly retrieving the stratospheric aerosol optical depth.

1166 While the v8 and version 9 (v9) OCO-2 XCO_2 products were generally more reliable
1167 over the ocean at mid latitudes (O'Dell et al. 2018; Kiel et al., 2019), they included a new
1168 anomaly that compromised their acceptance by the ocean carbon cycle community. In contrast to
1169 existing carbon cycle models, which assume that ocean-atmospheric CO_2 fluxes are correlated
1170 with ocean surface pCO_2 values, Figure 12 shows persistent negative XCO_2 anomalies over the
1171 tropical Pacific and Indian Oceans, where surface ocean pCO_2 is high (Figure 3, top). The lowest
1172 persistent spatial anomalies in XCO_2 are seen in regions that receive the highest rainfall (1000 -
1173 3000 mm/year), suggesting a possible correlation. Comparisons of OCO-2 XCO_2 estimates with
1174 TCCON XCO_2 observations indicate that the OCO-2 estimates are systematically low over the
1175 topical Pacific and Indian Oceans (S. Kulawik personal communication, 2019), but this does not
1176 expain the apparent spatial correlation of the deepest anomalies with the rain bands. These
1177 spatial correlations are not entirely surprising. Atmospheric CO_2 dissolves in cloud and
1178 raindrops, reducing the pH of rain to values between 5 and 6 even for regions well away from
1179 anthropogenic nitrate and sulfate acid rain sources (Willey et al., 2000; Bogan et al., 2009; Liu et
1180 al., 2010). Liu et al. (2010) estimate that precipitation transports ~0.2 Pg C yr^{-1} (0.35 to 0.7 Pg
1181 CO_2) from the atmosphere to the ocean. This process is not seen in carbon cycle models because
1182 most assume that rain contains no inorganic carbon, and falls with a pH of 7.0. If these OCO-2
1183 XCO_2 anomalies can be validated, this assumption will have to be revisited.

1184 ### *6.4 The Continuing Need for in situ Measurements of CO_2 and other Greenhouse Gases*

1185 While this first generation of space-based measurements of CO_2 have provided new
1186 insights into land, ocean, and atmospheric carbon cycles, they have also revealed some key
1187 limitations of this approach, and the continuing need to maintain and expand the ground-based
1188 and airborne atmospheric greenhouse measurement networks. First, while CO_2 and CH_4 can now
1189 be measured from space with the accuracies need to quantify surface sources and sinks, other
1190 critical greenhouse gases including nitrous oxide (N_2O), chlorofluorocarbons (CFCs),
1191 hydrochlorofluorocarbons (HCFCs), hydrofluorocarbons (HFCs), perfluorocarbons (PFCs), and

sulfur hexafluoride (SF_6) cannot be measured to adequate accuracy. For these gases, as well as CO_2 and CH_4, in situ measurements continue to provide the most reliable means for tracking their concentrations on hemispheric to global scales. These measurements therefore continue to be a critical element of any global stocktake of these gases, like that mandated by the UNFCCC Paris Agreement. Other species that are useful for discriminating fossil fuel from biospheric CO_2 emissions, such as carbon-14 (^{14}C) can also only be measured in situ (Miller et al., 2012; 2020).

While spatial coverage is a critical asset of space-based atmospheric CO_2 measurements, there are situations where in situ measurements complement the coverage provided by these data. For example, remote sensing observations of near-surface CO_2 can only be collected in regions that are sufficiently free of clouds and aerosols. In situ measurements are therefore essential in persistently cloudy regions like those occupied by the intertropical convergence zone (ITCZ), and the Asian summer monsoon. In situ measurements are also needed at high latitudes during the winter, where clouds, low sun angles, and the low reflectivity of snow and ice covered surfaces at shortwave infrared wavelengths reduce the number and quality of remote sensing observations of CO_2. In addition, in situ data from instruments on airborne platforms complement the vertically-integrated remote sensing results with information about the vertical profile of CO_2, which can provide critical insight into net flux of CO_2 into the atmosphere. Finally, because the air-sea flux of CO_2 is determined mainly by the pCO_2 gradient between the ocean surface layer and the atmospheric surface boundary layer, in situ observations of near-surface atmospheric CO_2 concentrations are critical over the ocean.

Finally, because both surface in situ and remote sensing observations are more accurate than space-based remote sensing measurements, these data are critical for validating the remote sensing measurements. Currently, space-based XCO_2 estimates are validated against ground-based remote sensing observations collected by the Total Carbon Column Observing Network (TCCON), which, in turn, are validated against airborne in situ measurements, to provide a transfer standard to the WMO atmospheric greenhouse gas standard (Wunch et al., 2017). This validation approach has yielded valuable information about surface and atmospheric properties that introduce bias and scatter in the space-based remote sensing measurements. However, while this network now includes 27 stations in 14 countries, it still provides little coverage of the tropics and high latitudes, some of the most dramatic features are seen in the space-based remote sensing data.

While the number of ground-based and airborne in situ and remote sensing reference stations have grown slowly over the past decade, new measurement capabilities are coming on line that promise substantial increases in coverage. The up-looking remote sensing measurements being collected by the TCCON spectrometers are being complemented by measurements from smaller, less costly, and more portable Bruker EM27/SUN systems. These spectrometers are now being deployed as networks in urban settings (Hedelius et al., 2018) and in remote locations (Frey et al., 2019). In situ vertical profiles of CO_2, CH_4 and other gases are now being collected at altitudes as high as 25 km by AirCore instruments deployed on low-cost weather balloons (Karion et al., 2010). Additional in situ profiles and upper tropospheric measurements are now being made by commercial aircraft in Japan's Comprehensive Observation Network for Trace gases by Airliner (CONTRAIL) and Europe's In-service Aircraft for a Global Observing System (IAGOS).

7 Discussion

When integrated over the industrial age, the land sink has roughly balanced the land use source. The ocean has therefore been the only *de facto* cumulative net sink of fossil carbon from the atmosphere (Friedlingstein et al., 2019; 2020). However, since 1958, when continuous atmospheric CO_2 measurements have been available, CO_2 emissions from fossil fuel combustion have increased by about a factor of four, from less than 2.5 Pg C yr^{-1} to almost 10 Pg C yr^{-1} in 2019. During this period, the land sink has taken up an increasing fraction of anthropogenic emissions. Together, sinks in ocean and on land have absorbed enough anthropogenic CO_2 to limit the fraction that has remained in the atmosphere to a remarkably constant value around 45% (Raupach et al., 2014). This implies that, to first order, the uptake capacity of the ocean and land sinks has increased in step with the emissions (Friedlingstein et al., 2020). There has been debate as to whether increases in the atmospheric fraction, i.e. declines in sink efficiency, are already observable (Canadell et al., 2007; Knorr 2009; Raupach et al., 2014). Even if an increasing atmospheric fraction is not yet detectable, process-level understanding and regional trends indicate that the atmospheric fraction should increase as climate change progresses. While the exact timing and magnitude of changes in the land and ocean sinks remains unclear, the likelihood is high that substantial climate-carbon feedbacks will occur during this century. Any upward change in the atmospheric fraction, or reduction in sink capacity, will decrease the allowable fossil carbon that can still be burned without violating the temperature targets specified in the Paris agreement.

For the ocean, despite remaining uncertainties and missing closure terms, distinct methodologies for quantifying the ocean sink agree that the sink has increased over the industrial era, including in recent decades. Since the uptake of atmospheric CO_2 on annual to decadal time scales is primarily controlled by the pCO_2 gradient at its surface, the carbon sink is expected to grow steadily as long as near-exponential growth of atmospheric pCO_2 continues. However, if anthropogenic emissions are reduced, atmospheric pCO_2 will grow more slowly, and thus there will be a reduced ocean carbon sink even if the ocean circulation and chemical buffer capacity do not change. To understand these likely changes, it is essential that ocean carbon studies start to focus more attention on the near-term response to emission mitigation scenarios (Hausfather and Peters, 2020). If emissions are not mitigated, current climate models suggest that by the middle to late 21st century, a slowing ocean overturning rate and reduced chemical capacity in the ocean will reduce the rate of growth in the ocean sink.

To develop an integrated ocean carbon observing system that can track the evolution of the ocean sink on the annual to interannual timescales most relevant to climate change policy, we need to sustain existing and continue to develop improved observation systems for the surface and interior ocean. Ocean carbon instruments deployed on autonomous platforms are revolutionizing ocean carbon measurement spatial and temporal resolution and coverage, but reduced uncertainties in the carbonate constants are needed to fully exploit these data. High-quality shipboard observations will continue to be required. We also need improved ocean hindcast models and better understanding of uncertainties in observation-based data products derived through statistical extrapolation of sparse surface ocean pCO_2 data.

For the land carbon cycle, the picture is more complicated and appears to already be changing. Classical sinks in the tropical humid forests are slowly losing their strength and these changes are amplified by the losses associated with deforestation, forest degradation and extreme climate events. In the extra tropics, bottom-up measurements show evidence for a mid-latitude

greening associated with afforestation and increased agriculture, accompanied by increased browning in some parts of the Arctic. Overall, these trends provide the fragile background for a slowly increasing land uptake of CO_2. Over the next century, carbon-climate feedback is expected to play a larger role in the Arctic, although the magnitude and timing of those changes is subject to considerable debate (Schuur et al., 2015).

Space-based remote sensing observations are helping to revolutionize our ability to monitor the land and atmospheric carbon cycles to anthropogenic forcing and a changing climate. From a bottom-up perspective, microwave and lidar measurements are providing higher spatial and temporal resolution estimates of above ground biomass stocks. SIF measurements are providing a more responsive estimate of light use efficiency and CO_2 uptake by plants. From a top-down perspective, space-based remote sensing estimates of XCO_2 are complementing ground-based and aircraft in situ measurements with much greater spatial and temporal resolution and coverage. These space-based measurements sometimes reinforce, amplify or contradict the results inferred from ground-based in situ measurements, painting a somewhat controversial picture of the evolution of the land carbon cycle. For example, in the tropics, both space-based microwave estimates of above ground biomass (Wigneron et al., 2020) and top-down atmospheric inverse models constrained by space-based estimates of XCO_2 (Liu et al., 2017; 2020; Palmer et al., 2019; Crowell et al., 2019) indicate that the humid tropical forests never fully recovered from the 2015-2016 El Niño, and have transitioned from net sinks to net sources of CO_2. Meanwhile, at mid- and high latitudes, bottom-up and top-down models constrained by space-based remote sensing measurements largely reinforce the in situ results, showing a long term increase in the amplitude of the seasonal cycle (Graven et al., 2013; Byrne et al., 2018; 2020; Liu et al., 2020) and that mid-latitude and boreal forests are strong net sinks of CO_2 when averaged over the seasonal cycle. More generally, the space based measurements are also providing more information about rapid changes in the land carbon cycle associated with severe weather, such as droughts (Gonsamo et al., 2019; Castro et al., 2020) and floods (Yin et al., 2020). They are also beginning to provide estimates of CO_2 emissions from fossil fuel combustion and other human activities (Hakkarainen et al., 2016; 2019; Wang et al., 2018; Hedelius et al., 2018; Wu et al., 2018; 2020; Reuter et al., 2019).

In spite of these advances, the reliability of the space-based remote sensing results are still a subject of substantial debate within the land carbon cycle community. This is especially true for the tropics, where CO_2 fluxes derived from the space-based XCO_2 estimates differ in both sign and magnitude from the results of earlier flux inversion experiments constrained by bottom-up stock or flux estimates or ground-based in situ measurements of atmospheric CO_2. This apparent inconsistency suggests one of three possibilities. First, the space-based XCO_2 estimates might still include biases that compromise the accuracy of the top-down flux estimates. Recent efforts to validate the space-based XCO_2 estimates using measurements from TCCON and other standards (Wunch et al., 2017) indicate biases with amplitudes less than one third as large as the observed tropical XCO_2 anomalies. However, there are few TCCON stations or other validation capabilities in the tropics. Second, fluxes constrained by surface in situ measurements, alone, may tell an incomplete story of the land carbon cycle in sparsely sampled regions. The spatial resolution and coverage provided by surface in situ measurements of carbon stocks, fluxes, or atmospheric CO_2 are still very limited, especially in the tropics and boreal regions, where the largest flux differences are seen. Both top-down and bottom-up methods may yield unreliable results where there are few measurements. Third, flux estimates based on the much denser space-based XCO_2 measurements may be tracking changes in the natural carbon

cycle on time and space scales too short to be resolved by the in situ measurements of stocks or CO_2 concentrations. There is increasing evidence from atmospheric CO_2 measurements and modeling studies and other carbon cycle observations, that the tropical land carbon cycle is evolving rapidly in response to human activities (deforestation and degradation, biomass burning, land use change) and climate change (drought, heat stress, flooding). Satellite observations of aboveground biomass (Baccini et al., 2017) also support this conclusion.

All three of these possibilities may be valid to some extent. To address these questions and improve our understanding of the land carbon cycle in the tropics and at high latitudes, we need additional ground-based and aircraft validation measurements in these areas, advances in the space-based measurement calibration, retrieval algorithms, and validation techniques to further reduce regional scale biases and a longer, continuous space-based data record that clearly resolves the carbon cycle impacts of short-term climate anomalies from long-term secular climate trends.

8 Conclusions

Our understanding of the carbon cycle and its response to natural and anthropogenic forcing has grown steadily over the past two decades as more advanced carbon cycle measurement systems have been deployed and their results have been analyzed with more sophisticated diagnostic and prognostic carbon cycle models. These results reveal a strongly coupled, dynamic system that responds on daily, to seasonal, to interannual time scales across spatial scales spanning individual fields, forest plots or coal-fired power plants on land or individual eddies in the ocean to entire continents or ocean basins. While surface or ocean interior in situ measurements still provide the most precise and accurate results, these data are now being complemented by a broad range of ground and ocean-based, airborne and space based remote sensing observations that extend their spatial resolution and coverage. The growing international collaborations between the top-down and bottom-up carbon cycle measurement and modeling communities, with their continued focus on a rigorous peer review process is contributing to the transparency of the carbon emission inventory process, an increasingly urgent requirement of any carbon management system.

While these observations and models have provided new insights into this system, they have also revealed measurement gaps and modeling limitations that must be addressed to develop a true global carbon monitoring system that can track changes in both natural and anthropogenic sources and sinks of CO_2 on policy relevant time and space scales. For example, space-based remote sensing observations of atmospheric CO_2 and land and ocean surface properties can expand the coverage and resolution of surface-based in situ measurements. However, passive remote sensing observations are largely precluded in persistently cloudy regions such as tropical rain forests, or mid- and high-latitude forests during the fall, winter and spring. These regions are often centers of action in the carbon cycle, but are also among the most challenging to observe systematically with surface-based in situ measurement systems. Remote sensing observations provide little insight into the carbon budget of the interior ocean, but here networks of autonomous in situ sensors are providing new tools for gathering data. Like remote sensing observations, their data typically has larger uncertainties and biases than conventional shipboard in situ measurements. Thus, a robust ocean carbon observing system will require continued shipboard observations for calibration and validation.

Top-down atmospheric CO_2 inventories are now complementing bottom-up statistical inventory methods by providing an integral constraint on total CO_2 emitted into the atmosphere and absorbed at the surface on scales ranging from large urban areas to nations. However, the inventory community has been slow to adopt top-down methods because they are much less source specific, and thus provide less direct, actionable information to policy makers than the bottom-up inventories. Optimal methods for combining top-down and bottom up emissions estimates are essential to both improve the accuracy and ensure the transparency urban to national scale inventories should be a high priority in any carbon management system. An effort to integrate top-down and bottom-up methods could also yield significant scientific benefits by fostering the development of more reliable models for diagnosing the current state of the carbon cycle, and for more accurately predicting the carbon cycle response to a changing climate.

The world's space agencies are actively working to coordinate ambitious plans for an expanded space-based remote sensing capability that supports atmospheric CO_2 measurements, high resolution maps of land surface type and biomass and ocean biological productivity. These efforts are being led by the Committee on Earth Observation Satellites (CEOS) and Coordination Group on Meteorological Satellites (CGMS) through their Joint Working Group on Climate (WGClimate) Greenhouse Gas Task team. In parallel, national agencies such as the U.S. NOAA and Japan's National Institute for Environmental Studies (NIES) and European organizations, such ICOS and IAGOS, are working with international organizations including WMO GAW and the Global Climate Observing System and the Global Ocean Observing System (GCOS, GOOS) to coordinate the deployment of ground-based, ocean and airborne in situ sensors. These programs are receiving less attention and much less resources than the space-based measurement systems, but are equally critical to a global carbon monitoring system. The modeling systems needed to ingest and analyze the data collected by these expanding measurement systems are also advancing, but efforts to organize carbon cycle modeling efforts are also receiving less attention from the carbon cycle science community and their stakeholders. Ambitious efforts to track changes in the emission and uptake of CO_2 associated with human activities and the carbon cycle's response to climate change, such as the global stocktakes mandated by the UNFCCC Paris agreement, will require both expanded capabilities and much more coordination among all of these groups.

9 Open Research

This is a review of other published work. No new data has been created or archived specifically for this manuscript. Original data are available through the citations listed here. Figures have been redrawn to avoid copyright conflicts.

10 Acknowledgments

Some of the work presented here was performed at the Jet Propulsion Laboratory, California Institute of Technology under contract to the National Aeronautics and Space Administration (NASA). Government sponsorship acknowledged. We thank Amanda Fay for assistance with Figures 3 and 4. Figure 2 was designed by GAM and Natalie Renier, WHOI Creative, with funding from Ocean Carbon & Biogeochemistry (OCB) Project Office that has support from the US National Science Foundation (NSF) and NSF, NASA. GAM acknowledges support from NSF OCE-1948624 and US National Oceanic and Atmospheric Administration (NA20OAR4310340). HD was supported by the European Commission, Horizon 2020

Framework Programme (VERIFY, grant no. 776810) and the Netherlands Earth System Science Centre (NESSC), financially supported by the Ministry of Education, Culture and Science (OCW) (grant 024.002.001). JH acknowledges funding from the Initiative and Networking Fund of the Helmholtz Association (Helmholtz Young Investigator Group Marine Carbon and Ecosystem Feedbacks in the Earth System, MarESys), Grant Number: VH- NG-1301. TT acknowledges support from the EU H2020 framework program (EuroSea, grant no. 862626) The writing of this paper was initiated at the GCOS joint panel meeting in Marrakech, 18-22 March, 2019.

11 References

Ajani, J. I., Keith, H., Blakers, M., Mackey, B. G. and King, H. P. (2013). Comprehensive carbon stock and flow accounting: A national framework to support climate change mitigation policy. *Ecological Economics*, **89**, 61-72. doi:10.1016/j.ecolecon.2013.01.010

Álvarez, M., Fajar, N. M., Carter, B. R., Guallart, E. F., Pérez, F. F., Woosley, R. J. and Murata, A. (2020). Global Ocean Spectrophotometric pH Assessment: Consistent Inconsistencies. *Environ. Sci. Technol.*, **54**, 10977-10988. doi:10.1021/acs.est.9b06932

Anav, A., Friedlingstein, P., Beer, C., Ciais, P., Harper, A., Jones, C., Murray-Tortarolo, G., Papale, D., Parazoo, N. C., Peylin, P., Piao, S., Sitch, S., Viovy, N., Wiltshire, A. and Zhao, M. (2015). Spatiotemporal patterns of terrestrial gross primary production: A review. *Rev. Geophys.*, **53**, 785–818. doi:10.1002/2015RG000483

Andrew, R. M. (2020). A comparison of estimates of global carbon dioxide emissions from fossil carbon sources. *Earth Syst. Sci. Data*, **12**, 1437–1465. doi:10.5194/essd-12-1437-2020

Aumont, O., Orr, J.C., Monfray, P., Ludwig, W., Amiotte-Suchet, P. and Probst, J.-L. (2001). Riverine-driven interhemispheric transport of carbon. *Global Biogeochemical Cycles.* **15**, 393–405. doi:10.1029/1999GB001238

Aumont, O., Ethé, C., Tagliabue, A., Bopp, L. and Gehlen, M. (2015). PISCES-v2: An ocean biogeochemical model for carbon and ecosystem studies. *Geosci. Model Dev.*, **8**, 2465–2513. doi:10.5194/gmd-8-2465-2015

Ayers, J.M. and Strutton, P.G. (2013). Nutrient variability in Subantarctic Mode Waters forced by the Southern Annular Mode and ENSO: Subantarctic mode water nutrients. *Geophysical Research Letters*, **40**, 3419–3423. doi:10.1002/grl.50638

Baccini, A., Walker, W., Carvalho, L., Farini, M., Sulla-Menashe, D. and Houghton, R. A. (2017). Tropical forests are a net carbon source based on aboveground measurements of gain and loss. *Science.* **358**, 230–234. doi:10.1126/science.aam5962

Bakker, D. C. E., Pfeil, B., Smith, K., Hankin, S., Olsen, A., Alin, S. R., Cosca, C., Harasawa, S., Kozyr, A., Nojiri, Y., O'Brien, K. M., Schuster, U., Telszewski, M., Tilbrook, B., Wada, C., Akl, J., Barbero, L., Bates, N. R., Boutin, J., Bozec, Y., Cai, W.-J., Castle, R. D., Chavez, F. P., Chen, L., Chierici, M., Currie, K., de Baar, H. J. W., Evans, W., Feely, R. A., Fransson, A., Gao, Z., Hales, B., Hardman-Mountford, N. J., Hoppema, M., Huang, W.-J., Hunt, C. W., Huss, B., Ichikawa, T., Johannessen, T., Jones, E. M., Jones, S. D., Jutterström, S., Kitidis, V., Körtzinger, A., Landschützer, P., Lauvset, S. K., Lefévre, N., Manke, A. B., Mathis, J. T., Merlivat, L., Metzl, N., Murata, A., Newberger, T., Omar, A. M., Ono, T., Park, G.-H., Paterson, K., Pierrot, D., Ríos, A. F., Sabine, C. L., Saito, S.,

Salisbury, J., Sarma, V. V. S. S., Schlitzer, R., Sieger, R., Skjelvan, I., Steinhoff, T., Sullivan, K. F., Sun, H., Sutton, A. J., Suzuki, T., Sweeney, C., Takahashi, T., Tjiputra, J., Tsurushima, N., van Heuven, S. M. A. C., Vandemark, D., Vlahos, P., Wallace, D. W. R., Wanninkhof, R. and Watson, A. J. (2014). An update to the Surface Ocean CO_2 Atlas (SOCAT version 2). *Earth Syst. Sci. Data*, **6**, 69-90. doi:10.5194/essd-6-69-2014

Bakker, D. C. E., Pfeil, B., Landa, C. S., Metzl, N., O'Brien, K. M., Olsen, A., Smith, K., Cosca, C., Harasawa, S., Jones, S. D., Nakaoka, S. I., Nojiri, Y., Schuster, U., Steinhoff, T., Sweeney, C., Takahashi, T., Tilbrook, B., Wada, C., Wanninkhof, R., Alin, S. R., Balestrini, C. F., Barbero, L., Bates, N. R., Bianchi, A. A., Bonou, F., Boutin, J., Bozec, Y., Burger, E. F., Cai, W. J., Castle, R. D., Chen, L., Chierici, M., Currie, K., Evans, W., Featherstone, C., Feely, R. A., Fransson, A., Goyet, C., Greenwood, N., Gregor, L., Hankin, S., Hardman-Mountford, N. J., Harlay, J., Hauck, J., Hoppema, M., Humphreys, M. P., Hunt, C. W., Huss, B., Ibanhez, J. S. P., Johannessen, T., Keeling, R., Kitidis, V., Kortzinger, A., Kozyr, A., Krasakopoulou, E., Kuwata, A., Landschutzer, P., Lauvset, S. K., Lefevre, N., Lo Monaco, C., Manke, A., Mathis, J. T., Merlivat, L., Millero, F. J., Monteiro, P. M. S., Munro, D. R., Murata, A., Newberger, T., Omar, A. M., Ono, T., Paterson, K., Pearce, D., Pierrot, D., Robbins, L. L., Saito, S., Salisbury, J., Schlitzer, R., Schneider, B., Schweitzer, R., Sieger, R., Skjelvan, I., Sullivan, K. F., Sutherland, S. C., Sutton, A. J., Tadokoro, K., Telszewski, M., Tuma, M., van Heuven, S. M. A. C., Vandemark, D., Ward, B., Watson, A. J. and Xu, S. (2016). A multi-decade record of high-quality fCO_2 data in version 3 of the Surface Ocean CO_2 Atlas (SOCAT). *Earth Syst. Sci. Data*, 8, 383-413. doi:10.5194/essd-8-383-2016

Bakker, D. C. E., Alin, S. R., Bates, N., Becker, M., Castaño-Primo, R., Cosca, C. E., Cronin, M., Kadono, K., Kozyr, A., Lauvset, S. K., Metzl, N., Munro, D. R., Nakaoka, S., O'Brien, K. M., Ólafsson, J., Olsen, A., Pfeil, B., Pierrot, D., Smith, K., Sutton, A. J., Takahashi, T., Tilbrook, B., Wanninkhof, R., Andersson, A., Atamanchuk, D., Benoit-Cattin, A., Bott, R., Burger, E. F., Cai, W.-J., Cantoni, C., Collins, A., Corredor, J. E., Cronin, M. F., Cross, J. N, Currie, K. I., De Carlo, E. H., DeGrandpre, M. D., Dietrich, C., Emerson, S., Enright, M. P., Evans, W., Feely, R. A., García-Ibáñez, M. I., Gkritzalis, T., Glockzin, M., Hales, B., Hartman, S. E., Hashida, G., Herndon, J., Howden, S. D., Humphreys, M. P., Hunt, C. W., Jones, S. D., Kim, S., Kitidis, V., Landa, C. S, Landschützer, P., Lebon, G. T., Lefèvre, N., Lo Monaco, C., Luchetta, A., Maenner Jones, S., Manke, A. B., Manzello, D., Mears, P., Mickett, J., Monacci, N. M., Morell, J. M., Musielewicz, S., Newberger, T., Newton, J., Noakes, S., Noh, J.-H., Nojiri, Y., Ohman, M., Ólafsdóttir, S., Omar, A. M., Ono, T., Osborne, J., Plueddemann, A. J., Rehder, G., Sabine, C. L, Salisbury, J. E., Schlitzer, R., Send, U., Skjelvan, I., Sparnocchia, S., Steinhoff, T., Sullivan, K. F., Sutherland, S. C., Sweeney, C., Tadokoro, K., Tanhua, T., Telszewski, M., Tomlinson, M., Tribollet, A., Trull, T., Vandemark, D., Wada, C., Wallace, D. W. R., Weller, R. A., and Woosley, R. J. (2020). Surface Ocean CO_2 Atlas Database Version 2020 (SOCATv2020) (NCEI Accession 0210711), NOAA National Centers for Environmental Information. doi:10.25921/4xkx-ss49

Baldocchi, D., Falge, E., Gu, L., Olson, R., Hollinger, D., Running, S. W., Anthoni, P., Bernhofer, C., Davis, K. J., Evans, R., Fuentes, J., Goldstein, A., Katul, G., Law, B., Lee, X., Malhi, Y., Meyers, T., Munger, W., Oechel, W., Paw, U. K. T., Pilegaard, K., Schmid, H. P., Valentini, R., Verma, S., Vesala, T., Wilson, K. and Wofsy, S. (2001).

FLUXNET: A new tool to study the temporal and spatial variability of ecosystem-scale carbon dioxide, water vapor, and energy flux densities. *Bull. Amer. Meteor. Soc.*, **82**, 2415–2434. doi:10.1175/1520-0477

Baldocchi D. D. (2003). Assessing the eddy covariance technique for evaluating carbon dioxide exchange rates of ecosystems: past, present and future. *Global Change Biology*, **9**, 479–492. doi:10.1046/j.1365-2486.2003.00629.x

Ballantyne, A. P., Alden, C. B., Miller, J. B., Tans, P. P. and White, J. W. C. (2012). Increase in observed net carbon dioxide uptake by land and oceans during the past 50 years. *Nature*, **488**, 70–72. doi:10.1038/nature11299

Beck, S. A. and Goetz, S. J. (2011). Satellite observations of high northern latitude vegetation productivity changes between 1982 and 2008: ecological variability and regional differences. *Environ. Res. Lett*., **6**, 045501. doi:10.1088/1748-9326/6/4/045501

Beer, C., Reichstein, M., Tomelleri, E., Ciais, P., Jung, M., Carvalhais, N., Rödenbeck, C., Arain, M. A., Baldocchi, D., Bonan, G., B., Bondeau, A., Cescatti, A., Lasslop,G., Lindroth, A., Lomas, M., Luyssaert, S., Margolis, H., Oleson, K. W., Roupsard, O., Veenendaal, E., Viovy, N., Williams, C., Woodward, F., I. and Papale, D. (2010). Terrestrial gross carbon dioxide uptake: global distribution and covariation with climate. *Science*, **329**, 834–838. doi:10.1126/science.1184984

Bennedsen, M., Hildebrand, E. and Koopman, S. (2019). Trend analysis of the airborne fraction and sink rate of anthropogenically released CO_2. *Biogeosciences*, **16**, 3651–3663. doi:10.5194/bg-16-3651-2019

Boden T. A., Marland G. and Andres R. J. (2017). Global, Regional, and National Fossil-Fuel CO_2 Emissions. Carbon Dioxide Information Analysis Center, Oak Ridge National Laboratory, U.S. Department of Energy, Oak Ridge, Tenn., U.S.A. doi:10.3334/CDIAC/00001_V2017

Bogan, R. A. J., Ohde, S., Arakaki, T., Mori, I. and McLeod, C. W. (2009). Changes in rainwater pH associated with atmospheric carbon dioxide after the Industrial Revolution. *Water, Air, and Soil Pollution*, **196**, 263-271. doi:10.1007/s11270-008-9774-0

Bolin, B., Björkström, A., Holmén, K. and Moore, B. (1983). The simultaneous use of tracers for ocean circulation studies. *Tellus B*, **35B**, 206–236. doi:10.1111/j.1600-0889.1983.tb00025.x

BP Statistical Review of World Energy 2020. available at https://www.bp.com/en/global/corporate/energy-economics/statistical-review-of-world-energy/co2-emissions.html, last access 1 February 2021.

Brienen, R. J.W., Phillips, O. L., Feldpausch, T. R., Gloor, E., Baker, T. R., Lloyd, J., Lopez-Gonzalez, G., Monteagudo-Mendoza, A., Malhi, Y., Lewis, S. L., Vásquez Martinez, R., Alexiades, M., Álvarez Dávila, E., Alvarez-Loayza, P., Andrade, A., Aragão, L. E. O. C., Araujo-Murakami, A., Arets, E. J. M. M., Arroyo, L., Aymard, C. A. G., Bánki, O.S., Baraloto, C., Barroso, J., Bonal, D., Boot, R. G. A. , Camargo, J. L. C., Castilho, C. V., Chama, V., Chao, K. J., Chave, J., Comiskey, J. A., Cornejo Valverde, F., da Costa, L., de Oliveira, E. A., Di Fiore, A., Erwin, T. L., Fauset, S., Forsthofer, M., Galbraith, D. R., Grahame, E. S., Groot, N., Hérault, B., Higuchi, N., Honorio Coronado, E. N., Keeling,

H., Killeen, T. J., Laurance, W. F., Laurance, S., Licona, J., Magnussen, W. E., Marimon, B. S., Marimon-Junior, B. H., Mendoza, C., Neill, D. A., Nogueira, E. M., Núñez, P., Pallqui Camacho, N. C., Parada, A., Pardo-Molina, G., Peacock, J., Peña-Claros, M., Pickavance, G. C., Pitman, N. C. A., Poorter, L., Prieto, A., Quesada C. A., Ramírez, F., Ramírez-Angulo, H., Restrepo, Z., Roopsind, A., Rudas, A., Salomão, R. P., Schwarz, M., Silva, N., Silva-Espejo, J. E., Silveira, M., Stropp, J., Talbot, J., ter Steege, H., Teran-Aguilar, J., Terborgh, J., Thomas-Caesar, R., Toledo, M., Torello-Raventos, M., Umetsu, R. K., van der Heijden, G. M. F., van der Hout, P., Guimarães, Vieira I. C., Vieira, S. A., Vilanova, E., Vos ,V. A. and Zagt, R. J. (2015). Long-term decline of the Amazon carbon sink. *Nature*, **519**(7543), 344-348. doi:10.1038/nature14283

Bronselaer,B., and Zanna, L. (2020), Heat and carbon coupling reveals ocean warming due to circulation changes. *Nature*, **584**, 227–233. doi:10.1038/s41586-020-2573-5

Bushinsky, S. M., Landschützer, P., Rödenbeck, C., Gray, A. R., Baker, D., Mazloff, M. R., Resplandy, L., Johnson, K. S., and Sarmiento, J. L. (2019). Reassessing Southern Ocean air-sea CO_2 flux estimates with the addition of biogeochemical float observations. *Global Biogeochemical Cycles*, **33**(11), 1370-1388, doi:10.1029/2019GB006176

Byrne, B., Wunch, D., Jones, D. B. A., Strong, K., Deng, F., Baker, I., Köhler, P., Frankenberg, C., Joiner, J., Arora, V. K., Badawy, B., Harper, A. B., Warneke, T., Petri, C., Kivi, R. and Roehl, C. M. (2018). Evaluating GPP and respiration estimates over northern midlatitude ecosystems using solar-induced fluorescence and atmospheric CO_2 measurements. *Journal of Geophysical Research: Biogeosciences*, **123**(9), 2976–2997. doi:10.1029/2018JG004472

Byrne, B., Liu, J., Lee, M., Baker, I., Bowman, K. W., Deutscher, N. M., Feist, D. G., Griffith D. W. T., Iraci, L. T., Kiel, M., Kimball, J. S., Miller, C. E., Morino, I., Parazoo, N. C., Petri, C., Roehl, C. M., Sha, M. K., Strong, K., Velazco, V. A., Wennberg, P. O. and Wunch, D. (2020). Improved constraints on northern extratropical CO2 fluxes obtained by combining surface-based and space-based atmospheric CO_2 measurements. *Journal of Geophysical Research: Atmospheres*, **125**, e2019JD032029. doi:10.1029/2019JD032029

Canadell, J. G., Le Quéré, C., Raupach, M. R., Field, C. B. , Buitenhuis, E., Ciais, P., Conway, T. J., Gilett, N. P., Houghton, J. T. and Marland, G. (2007). Contributions to accelerating atmospheric CO_2 growth from economic activity, carbon intensity, and efficiency of natural sinks. *Proceedings of the National Academy of Sciences*, **104**, 18,866 – 18,870. doi:10.1073/ pnas.0702737104

Carroll, D., Menemenlis, D., Adkins, J. F., Bowman, K. W., Brix, H., Dutkiewicz, S., Fenty, I., Gierach, M. M., Hill, C., Jahn, O., Landschützer, P., Lauderdale, J. M., Liu, J., Manizza, M., Naviaux, J. D., Rodenbeck, C., Schimel, D. S., Van der Stocken, T. and Zhang, H. (2020). The ECCO-Darwin data-assimilative global ocean biogeochemistry model: Estimates of seasonal to multi-decadal surface ocean pCO_2 and air-sea CO_2 flux. *J. Adv. Model. Earth Syst.*, **12**, e2019MS001888. doi:10.1029/2019MS001888

Carvalhais, N., Forkel, M., Khomik, M., Bellarby, J., Jung, M., Migliavacca, M. Mu, M., Saatchi, S., Santoro, M., Thurner, M., Weber, U., Ahrens, B., Beer, C., Cescatti, A., Randerson, J. T. and Reichstein, M. (2014). Global covariation of carbon turnover times with climate in terrestrial ecosystems. *Nature*, **514**(7521) 213-7. doi:10.1038/nature13731

1584 Castro, A. O., Chen, J., Zang, C. S., Shekhar, A., Jimenez, J. C., Bhattacharjee, S., Kindu, M.,
1585 Morales, V. H. and Ramming, A. (2020). OCO-2 Solar-Induced Chlorophyll
1586 Fluorescence Variability across Ecoregions of the Amazon Basin and the Extreme
1587 Drought Effects of El Nino (2015-2016), *Remote Sensing*, **12**(7), 1202.
1588 doi:10.3390/rs12071202

1589 Chatterjee, A., Gierach, M. M., Sutton, A. J., Feely, R. A., Crisp, D., Eldering, A., Gunson, M.
1590 R., O'Dell, C. W., Stephens, B. B. and Schimel, D. S. (2017). Influence of El Niño on
1591 atmospheric CO_2 over the tropical Pacific Ocean: Findings from NASA's OCO-2
1592 mission. *Science*, **358**, eaam5776. doi:10.1126/science.aam5776

1593 Chevallier, F., Ciais, P., Conway, T. J., Aalto, T., Anderson, B. E., Bousquet, P., Brunke, E. G.,
1594 Ciattaglia, L., Esaki, Y., Frohlich, M., Gomez, A. J., Gomez-Pelaez, A. J., Haszpra, L.,
1595 Krummel, P., Langenfelds, R., Leuenberger, M., Machida, T., Maignan, F., Matsueda,
1596 H., Morgui, J. A., Mukai, H., Nakazawa, T., Peylin, P., Ramonet, M., Rivier, L., Sawa,
1597 Y., Schmidt, M., Steele, P., Vay, S. A., Vermeulen, A. T., Wofsy, S. and Worthy, D.
1598 (2010). CO_2 surface fluxes at grid point scale estimated from a global 21-year reanalysis
1599 of atmospheric measurements. *Journal of Geophysical Research: Atmospheres*, **115**,
1600 D21307. doi:10.1029/2010JD013887

1601 Chevallier, F., Remaud, M. O'Dell, C. W., Baker, D., Peylin, P. and Cozic, A. (2019). Objective
1602 evaluation of surface and satellite driven CO_2 atmospheric inversion. *Atmospheric*
1603 *Chemistry and Physics*, **19**, 14233–14251. doi:10.5194/acp-19-14233-2019

1604 Ciais, P., Dolman, A. J., Bombelli, A., Duren, R., Peregon, A., Rayner, P. J., Miller, C., Gobron,
1605 N., Kinderman, G., Marland, G., Gruber, N., Chevallier, F., Andres, R. J., Balsamo, G.,
1606 Bopp, L., Bréon, F.-M., Broquet, G., Dargaville, R., Battin, T. J., Borges, A.,
1607 Bovensmann, H., Buchwitz, M., Butler, J., Canadell, J. G., Cook, R. B., DeFries, R.,
1608 Engelen, R., Gurney, K. R., Heinze, C., Heimann, M., Held, A., Henry, M., Law, B.,
1609 Luyssaert, S., Miller, J., Moriyama, T., Moulin, C., Myneni, R. B., Nussli, C.,
1610 Obersteiner, M., Ojima, D., Pan, Y., Paris, J.-D., Piao, S. L., Poulter, B., Plummer, S.,
1611 Quegan, S., Raymond, P., Reichstein, M., Rivier, L., Sabine, C., Schimel, D., Tarasova,
1612 O., Valentini, R., Wang, R., van der Werf, G., Wickland, D., Williams, M. and Zehner,
1613 C. (2014). Current systematic carbon-cycle observations and the need for implementing a
1614 policy-relevant carbon observing system, *Biogeosciences*, **11**, 3547–3602.
1615 doi:10.5194/bg-11-3547-2014

1616 Ciais, P., Yao, Y., Gasser, T., Baccini, A., Wang, Y., Lauerwald, R., Peng, S., Bastos, A., Li, W.,
1617 Raymnd, P. A., Canadell, J. G., Peters, G. P., Andres, R. J., Chang, J., Yue, C., Dolman,
1618 A. J., Haverd, V., Hartman, J., Laruelle, G., Konings, A. G., King, A. W., Liu, Y.,
1619 Luyssaert, S., Maignan, F., Patra, P. K., Peregon, A., Regnier, P., Pongratz, J., Poulter,
1620 B., Shvidenko, A., Valentini, R., Wang, R., Broquet, G., Yin, Y., Zscheischler, J.,
1621 Guenet, B., Goll, D., S., Ballantyne, A.-P., Yang, H., Qiu, C. and Zhu, D. (2020).
1622 Empirical estimates of regional carbon budgets imply reduced global soil heterotrophic
1623 respiration. *National Science Review*, **0**, nwaa145,1-14. doi:10.1093/nsr/nwaa145

1624 Clement, D., and Gruber, N. (2018). The eMLR(C*) Method to determine decadal changes in the
1625 global ocean storage of anthropogenic CO_2. *Global Biogeochemical Cycles*, **32**, 654-679.
1626 doi:10.1002/2017gb005819

1627 Claustre, H., Johnson, K. S., and Takeshita, Y. (2020). Observing the global ocean with
1628 Biogeochemical-Argo, *Annual Review of Marine Science*, **12**, 23-48.
1629 doi:10.1146/annurev-marine-010419-010956

1630 Crowell, S., Baker, D., Schuh, A., Basu, S., Jacobson, A., Chevallier, F., Liu, J., Deng, F., Feng,
1631 L., McKain, K., Chatterjee, A., Miller, J., Stephens, B., Eldering, A., Crisp, D., Schimel,
1632 D., Nassar, R., O'Dell. C., Oda, T., Sweeney, C., Palmer, P., and Jones, D. (2019). The
1633 2015-2016 carbon cycle as seen from OCO-2 and the global in situ network. *Atmospheric*
1634 *Chemistry and Physics*, **19**, 7347–7376. doi:10.5194/acp-19-7347-2019

1635 Denman, K.L., G. Brasseur, A. Chidthaisong, P. Ciais, P.M. Cox, R.E. Dickinson, D.
1636 Hauglustaine, C. Heinze, E. Holland, D. Jacob, U. Lohmann, S Ramachandran, P.L. da
1637 Silva Dias, S.C. Wofsy and X. Zhang, (2007). Couplings between changes in the climate
1638 system and biogeochemistry. In: Climate Change 2007: The Physical Science Basis.
1639 Contribution of Working Group I to the Fourth Assessment Report of the
1640 Intergovernmental Panel on Climate Change [Solomon, S., Qin ,D., Manning, M., Chen,
1641 Z., Marquis, M., Avery, K. B., Tignor, M. and Miller, H. L. (eds.)]. Cambridge
1642 University Press, Cambridge, United Kingdom and New York, NY, USA.

1643 Denvil-Sommer, A., M. Gehlen, M. Vrac, and C. Mejia (2019). LSCE-FFNN-v1: A two-step
1644 neural network model for the reconstruction of surface ocean pCO_2 over the global ocean.
1645 *Geosci. Model Dev.*, **12**(5), 2091–2105. doi:10.5194/gmd-12-2091-2019

1646 DeVries, T. (2014). The oceanic anthropogenic CO_2 sink: Storage, air-sea fluxes, and transports
1647 over the industrial era, *Global Biogeochemical Cycles*, **28**(7), 631–647.
1648 doi:10.1002/2013GB004739

1649 DeVries, T., Holzer, M. and Primeau, F. (2017). Recent increase in oceanic carbon uptake driven
1650 by weaker upper-ocean overturning. *Nature,* **542**, 215–218. doi:10.1038/nature21068

1651 DeVries, T., Le Quéré, C., Andrews, O., Berthet, S., Hauck, J., Ilyina, T., Landschützer, P.,
1652 Lenton, A., Lima, I. D., Nowicki, M., Schwinger, J., Séférian, R. (2019). Decadal trends
1653 in the ocean carbon sink. *Proceedings of the National Academy of Sciences,* 201900371.
1654 doi:10.1073/pnas.1900371116

1655 Dlugokencky, E. J., Hall, B.D., Montzka, S.A., Dutton, G., Muhle, J. and Elkins, J.W. (2018).
1656 Long-lived greenhouse gases [in "State of the Climate in 2017"]. *Bulletin of the American*
1657 *Meteorological Society*, **99**(8), S46-S48. doi:10.1175/2018BAMSStateoftheClimate.1

1658 Doney S.C., Lindsay, K., Caldeira, K., Campin, J.-M., Drange, H., Dutay, J. C., Follows, M.,
1659 Gao, Y., Gnanadesikan, A., Gruber, N., Ishida, A., Joos, F., Madec, G., Maier-Reimer,
1660 E., Marshall, J. C., Matear, R. J., Monfray, P., Mouchet, A., Najjar, R., Orr, J. C.,
1661 Plattner, G.-K., Sarmiento, J., Schlitzer, R., Slater, R., Totterdell, I. J., Weirig, M. F.,
1662 Yamanaka, Y. and Yool, A. (2004). Evaluating global ocean carbon models: The
1663 importance of realistic physics. *Global Biogeochemical Cycles,* **18** (3), GB3017.
1664 doi:10.1029/2003GB002150

1665 Doughty, C. E. and Goulden, M. L. (2008). Are tropical forests near a high temperature
1666 threshold? *Journal of Geophysical Research: Biogeosciences,* **113**, G00B07.
1667 doi:10.1029/2007JG000632

Duffy, K., A., Schwalm, C. R., Arcus, V. L., Koch, G. W., Liang, L. L. and Schipper, L. A. (2021). How close are we to the temperature tipping point of the terrestrial biosphere? *Science Advances*, **7**, eaay1052.

Duncanson, L., Armston, J., Disney, M., Avitabile, V., Barbier, N., Calders, K., Carter, S., Chave, J., Herold, M., Crowther, T. W., Falkowski, M., Kellner, J. R., Labrière, N., Lucas, R., MacBean, N., McRoberts, R. E., Meyer, V., Naesset, E., Nickeson, J. E., Paul, K. I., Phillips, O. L., Réjou-Méchain, M., Román, M., Roxburgh, S., Saatchi, S., Schepaschenko, D., Scipal, K., Siqueira, P. R., Whitehurst, A. and Williams, M. (2019). The importance of consistent global forest aboveground biomass product Validation. *Surveys in Geophysics volume*, **40**, 979–999. doi:10.1007/s10712-019-09538-8

Eddebbar, Y. A., Rodgers, K. B., Long, M. C., Subramanian, A. C., Xie S.-P. and Keeling, R. F. (2019). El Niño-like physical and biogeochemical ocean response to tropical eruptions. *Journal of Climate*, **32**(9), JCLI–D–18–0458.1, doi:10.1175/JCLI-D-18-0458.1

Eldering, A.,Wennberg, P. O., Crisp, D., Schimel, D., Gunson, M. R., Chatterjee, A., Liu J., Schwandner, Y. Sun, C.W. O'Dell, C. Frankenberg, T. Taylor, B. Fisher, G.B. Osterman, D. Wunch, F., Hakkarainen, J. and Tamminen, J. **(**2017). The Orbiting Carbon Observatory-2 early science investigations of regional carbon dioxide fluxes. *Science* , **358**, eaam5745. doi:10.1126/science.aam5745

Enting, I.G., Trudinger, C.M. and Francey, R.J. (1995). A synthesis inversion of the concentration and $\delta^{13}C$ atmospheric CO_2. *Tellus*, **47B**, 35-52. doi:10.1034/j.1600-0889.47.issue1.5.x

Fan, L., Wigneron, J.-P., Ciais, P., Chave, J., Brandt, M., Fensholt, R., Saatchi, S. S. Bastos, A., Al-Yaari, A., Hufkens, K., Qin, Y., Xiao, X., Chen, C., Myneni, R. B., Rernandez-Moran, R., Mialon, A., Rodriguez-Fernandez, N. J., Kerr, Y., Tian, F. and Peñuelas, J. (2019). Satellite-observed pantropical carbon dynamics. *Nature Plants*, **5**, 944–951. doi:10.1038/s41477-019-0478-9

Fay, A. R., McKinley, G. A. (2013). Global trends in surface ocean pCO_2 from in situ data. *Global Biogeochemical Cycles*, **27**, 541–557. doi:10.1002/gbc.20051

Fay, A.R., Gregor, L., Landschützer, P. McKinley, G.A., Gruber, N., Gehlen, M., Iida, Y., Laruelle, G. G., Rödenbeck, C. and Zeng J. (2021). Harmonization of global surface ocean pCO_2 mapped products and their flux calculations; an improved estimate of the ocean carbon sink. *Earth Syst. Sci. Data*, submitted 2020.

Fay, A. R., Lovenduski, N. S., McKinley, G. A., Munro, D. R., Sweeney, C., Gray, A. R., Landschützer, P., Stephens, B. B., Takahashi ,T. and Williams, N. (2018). Utilizing the Drake Passage Time-series to understand variability and change in subpolar Southern Ocean pCO_2. *Biogeosciences*, **15**(12), 3841–3855. doi:10.5194/bg-15-3841-2018

Fisher, J. B., Huntzinger, D. N., Schwalm, C. R. and Sitch, S. (2014). Modeling the terrestrial biosphere. *Annual Review of Environment and Resources*, **39**, 91–123. doi:10.1146/annurev-environ-012913-093456

Fong, M. B. and Dickson, A. G. (2019). Insights from GO-SHIP hydrography data into the thermodynamic consistency of CO_2 system measurements in seawater. *Marine Chemistry*, **211**, 52-63. doi:10.1016/j.marchem.2019.03.006

Frankenberg, C., O'Dell, C., Berry, J., Guanter, L., Joiner, J., Köhler, P., Pollock, R. and Taylor, T. E. (2014). Prospects for chlorophyll fluorescence remote sensing from the orbiting carbon observatory-2. *Remote Sensing of Environment*, **147**, 1–12. doi:10.1016/j.rse.2014.02.007. ISSN 0034–4257

Frey, M., Sha, M. K., Hase, F., Kiel, M., Blumenstock, T., Harig, R., Surawicz, G., Deutscher, N. M., Shiomi, K., Franklin, J. E., Bösch, H., Chen, J., Grutter, M., Ohyama, H., Sun, Y., Butz, A., Mengistu Tsidu, G., Ene, D., Wunch, D., Cao, Z., Garcia, O., Ramonet, M., Vogel, F. and Orphal, J. (2019). Building the COllaborative Carbon Column Observing Network (COCCON): long-term stability and ensemble performance of the EM27/SUN Fourier transform spectrometer. *Atmospheric Measurement Technologies*, **12**, 1513–1530. doi:10.5194/amt-12-1513-2019

Friedlingstein, P., Jones, M. W., O'Sullivan, M., Andrew, R. M., Hauck, J., Peters, G. P., Peters, W., Pongratz, J., Sitch, S., Le Quéré, C., Bakker, D. C. E., Canadell, J. G., Ciais, P., Jackson, R. B., Anthoni, P., Barbero, L., Bastos, A., Bastrikov, V., Becker, M., Bopp, L., Buitenhuis, E., Chandra, N., Chevallier, F., Chini, L. P., Currie, K. I., Feely, R. A., Gehlen, M., Gilfillan, D., Gkritzalis, T., Goll, D. S., Gruber, N., Gutekunst, S., Harris, I., Haverd, V., Houghton, R. A., Hurtt, G., Ilyina, T., Jain, A. K., Joetzjer, E., Kaplan, J. O., Kato, E., Klein Goldewijk, K., Korsbakken, J. I., Landschützer, P., Lauvset, S. K., Lefèvre, N., Lenton, A., Lienert, S., Lombardozzi, D., Marland, G., McGuire, P. C., Melton, J. R., Metzl, N., Munro, D. R., Nabel, J. E. M. S., Nakaoka, S.-I., Neill, C., Omar, A. M., Ono, T., Peregon, A., Pierrot, D., Poulter, B., Rehder, G., Resplandy, L., Robertson, E., Rödenbeck, C., Séférian, R., Schwinger, J., Smith, N., Tans, P. P., Tian, H., Tilbrook, B., Tubiello, F. N., van der Werf, G. R., Wiltshire, A. J. and Zaehle, S. (2019). Global Carbon Budget 2019. *Earth Syst. Sci. Data*, **11**, 1783–1838. doi:10.5194/essd-11-1783-2019

Friedlingstein, P., O'Sullivan, M., Jones, M. W., Andrew, R. M., Hauck, J., Olsen, A., Peters, G. P., Peters, W., Pongratz, J., Sitch, S., Le Quéré, C., Canadell, J. G., Ciais, P., Jackson, R. B., Alin, S., Aragão, L. E. O. C., Arneth, A., Arora, V., Bates, N. R., Becker, M., Benoit-Cattin, A., Bittig, H. C., Bopp, L., Bultan, S., Chandra, N., Chevallier, F., Chini, L. P., Evans, W., Florentie, L., Forster, P. M., Gasser, T., Gehlen, M., Gilfillan, D., Gkritzalis, T., Gregor, L., Gruber, N., Harris, I., Hartung, K., Haverd, V., Houghton, R. A., Ilyina, T., Jain, A. K., Joetzjer, E., Kadono, K., Kato, E., Kitidis, V., Korsbakken, J. I., Landschützer, P., Lefèvre, N., Lenton, A., Lienert, S., Liu, Z., Lombardozzi, D., Marland, G., Metzl, N., Munro, D. R., Nabel, J. E. M. S., Nakaoka, S.-I., Niwa, Y., O'Brien, K., Ono, T., Palmer, P. I., Pierrot, D., Poulter, B., Resplandy, L., Robertson, E., Rödenbeck, C., Schwinger, J., Séférian, R., Skjelvan, I., Smith, A. J. P., Sutton, A. J., Tanhua, T., Tans, P. P., Tian, H., Tilbrook, B., van der Werf, G., Vuichard, N., Walker, A. P., Wanninkhof, R., Watson, A. J., Willis, D., Wiltshire, A. J., Yuan, W., Yue, X. and Zaehle, S. (2020). Global Carbon Budget 2020. *Earth Syst. Sci. Data*, **12**, 3269–3340. doi:10.5194/essd-12-3269-2020

1751 Friis, K., Körtzinger, A., Pätsch, J. and Wallace, D. W. R. (2005). On the temporal increase of
1752 anthropogenic CO_2 in the subpolar North Atlantic. *Deep-Sea Research.* **52**, 681-698.
1753 doi:10.1016/j.dsr.2004.11.017

1754 Frölicher, T. L., Joos, F., Raible, C. C. and Sarmiento, J. L. (2013). Atmospheric CO_2 response
1755 to volcanic eruptions: The role of ENSO, season, and variability. *Global Biogeochemical*
1756 *Cycles*, **27**, 239-251. doi:10.1002/gbc.20028

1757 Frölicher, T.L., Rodgers, K. B., Stock, C. A., Cheung, W. W. L. (2016). Sources of uncertainties
1758 in 21st century projections of potential ocean ecosystem stressors: Uncertainties in
1759 stressor projections. *Global Biogeochemical Cycles*, **30**, 1224–1243.
1760 doi:10.1002/2015GB005338

1761 Galbraith, E. D., and Skinner, L. C. (2020). The biological pump during the last glacial
1762 maximum. *Annual Reviews of Marine Science* **12**, 559–586. doi:10.1146/annurev-marine-
1763 010419-010906

1764 Gatti L.V., Gloor M., Miller J. B., Doughty C. E., Malhi Y., Domingues L. G., Basso L. S.,
1765 Martinewski A., Correia C. S., Borges V. F., Freitas S., Braz R., Anderson L. O., Rocha
1766 H., Grace J., Phillips O. L., and Lloyd J. (2014). Drought sensitivity of Amazonian
1767 carbon balance revealed by atmospheric measurements. *Nature*, **506**, 76-80.
1768 doi:10.1038/nature12957

1769 Gloege, L., McKinley, G. A., Landschützer, P., Fay, A., Frölicher, T., Fyfe, J. C., Illyina ,T.,
1770 Jones, S.D., Lovenduski, N. S., Rödenbeck ,C., Rodgers K. B., Schlunegger, S. and
1771 Takano, Y. (2020). Quantifying errors in observationally-based estimates of ocean carbon
1772 sink variability. *Global Biogeochemical Cycles*, in review.
1773 doi:10.1002/essoar.10502036.1

1774 Gonsamo, A., Chen, J. M., He, L., Sun, Y., Rogers, C. and Liu, J. (2019). Exploring SMAP and
1775 OCO-2 observations to monitor soil moisture control on photosynthetic activity of global
1776 drylands and croplands, *Remote Sensing of Environment*, **232**, 111314.
1777 doi:10.1016/j.rse.2019.111314

1778 Goris, N., Tjiputra, J. F., Olsen, A., Schwinger, J., Lauvset S. K. and Jeansson E. (2018).
1779 Constraining projection-based estimates of the future North Atlantic carbon uptake.
1780 *Journal of Climate*, **31**(10), 3959–3978, doi:10.1175/JCLI-D-17-0564.1

1781 Grassi, G., House, J., Kurz, W. A., Cescatti, A., Houghton, R. A., Peters, G. P., Sanz, M. J.,
1782 Viñas, R. A., Alkama, R., Arneth, A., Bondeau, A., Dentener, F., Fader, M., Federici, S.,
1783 Friedlingstein, P., Jain, A. K., Kato, E., Koven, C. D., Lee, D., Nabel, J. E. M. S.,
1784 Nassikas, A. A., Perugini, L., Rossi, S., Sitch, S., Viovy, N., Wiltshire, A. and Zaehle, S.
1785 (2018). Reconciling global-model estimates and country reporting of anthropogenic
1786 forest CO_2 sinks. *Nature Climate Change*, **8**, 914–920. doi.org/10.1038/s41558-018-
1787 0283-x

1788 Graven, H. D., Keeling, R. F., Piper, S. C., Patra, P. K., Stephens, B. B., Wofsy, S. C., Welp, L.
1789 R., Sweeney, C. and Tans, P. P. (2013). Enhanced seasonal exchange of CO_2 by northern
1790 ecosystems since 1960, *Science*, **341**(6150): 1085–1089. doi:10.1126/science.1239207

1791 Gregor, L., Lebehot, A. D. Kok, S. and Scheel Monteiro, P. M. (2019). A comparative
1792 assessment of the uncertainties of global surface-ocean CO_2 estimates using a machine

learning ensemble (CSIR-ML6 version 2019a); have we hit the wall? *Geosci. Model Dev.*, **12**, 5113–5136. doi:10.5194/gmd-12-5113-2019

Gruber, N., Clement, D., Carter, B.R., Feely, R.A., Van Heuven, S., Hoppema, M., Ishii, M., Key, R.M., Kozyr, A., Lauvset, S.K., Lo Monaco, C., Mathis, J.T., Murata, A., Olsen, A., Perez, F.F., Sabine, C.L., Tanhua, T., and Wanninkhof, R. (2019a). The oceanic sink for anthropogenic CO_2 from 1994 to 2007. *Science* **363**, 1193-1199. doi:10.1126/science.aau5153

Gruber, N., Landschützer, P., and Lovendusk, N. S. (2019b). The variable Southern Ocean carbon sink. *Annual Reviews of Marine Sci*ence, **11**, 159–186. doi:10.1146/annurev-marine-121916-063407

Guan, K., Berry, J. A., Zhang, Y., Joiner, J., Guanter, L., Badgley, G. and Lobell, D. B. (2016). Improving the monitoring of crop productivity using spaceborne solar-induced fluorescence. *Global Change Biology*, **22**(2), 716–726. doi:10.1111/gcb.13136

Guan, K., Wu, J., Kimball, J. S., Anderson, M. C., Frolking, S., Li, B., Hain, C. R. and Lobell, D. B. (2017). The shared and unique values of optical, fluorescence, thermal and microwave satellite data for estimating large-scale crop yields. *Remote Sensing of Environment*, **199**, 333–349. doi:10.1016/j.rse.2017.06.043

Gurney, K. R., Liang, J., O'Keeffe, D., Patarasuk, R., Hutchins, M., Huang, J., Rao, P. and Song, Y. (2019). Comparison of global downscaled versus bottom-up fossil fuel CO_2 emissions at the urban scale in four U.S. urban areas. *Journal of Geophysical Research: Atmospheres*, **124**(5), 2823--2840. doi:10.1029/2018JD028859

Hakkarainen, J., Ialongo, I. and Tamminen, J. (2016). Direct space-based observations of anthropogenic CO_2 emission areas from OCO-2. *Geophysical Research Letters*, **43**, 11,400–11,406. doi:10.1002/2016GL070885

Hakkarainen, J., Ialongo, I., Maksyutov, S., and Crisp, D. (2019). Analysis of Four Years of Global XCO_2 Anomalies as Seen by Orbiting Carbon Observatory-2, *Remote Sensing*, **11**, 850. doi:10.3390/rs11070850

Hansis, E., Davis, S. J. and Pongratz, J. (2015). Relevance of methodological choices for accounting of land use change carbon fluxes. *Global Biogeochemical Cycles*, **29**, 1230–1246. doi:10.1002/2014GB004997

Hauck, J., Völker, C., Wang, T., Hoppema, M., Losch, M. and Wolf-Gladrow, D.A. (2013). Seasonally different carbon flux changes in the Southern Ocean in response to the southern annular mode. *Global Biogeochemical Cycles*, **27**, 1236–1245. doi:10.1002/2013GB004600

Hauck, J., Völker, C., Wolf-Gladrow, D. A., Laufkötter, C., Vogt, M., Aumont, O., Bopp, L., Buitenhuis, E. T., Doney, S. C., Dunne, J., Gruber, N., Hashioka, T., John, J., Le Quéré, C., Lima, I. D., Nakano, H., Séférian, R. and Totterdell, I. (2015). On the Southern Ocean CO_2 uptake and the role of the biological carbon pump in the 21st century. *Global Biogeochemical Cycles*, **29**, 1451–1470. doi:10.1002/2015GB005140

Hauck, J., Zeising, M., Le Quéré, C., Gruber, N., Bakker, D. C. E., Bopp, L., Chau, T. T. T., Gürses, Ö., Ilyina, T., Landschützer, P., Lenton, A., Resplandy, L., Rödenbeck, C., Schwinger, J. and Séférian, R. (2020). Consistency and challenges in the ocean carbon

sink estimate for the Global Carbon Budget. *Frontiers in Marine Science*, **7**, 571720. doi:10.3389/fmars.2020.571720

Hausfather, Z. and Peters, G. P. (2020). Emissions - the "business as usual" story is misleading. *Nature*, **577**(7792), 618–620, doi:10.1038/d41586-020-00177-3

He, L., Magney, T., Dutta, D., Yin, Y., Köhler, P., Grossmann, K., Stutz, J., Dold, C., Hatfield, J., Guan, K., Peng, B. and Frankenberg, C. (2020). From the ground to space: Using solar-induced chlorophyll fluorescence to estimate crop productivity. *Geophysical Research Letters*, **47**, e2020GL087474. doi:10.1029/2020GL087474

Hedelius, J. K., Liu, J., Oda, T., Maksyutov, S., Roehl, C. M., Iraci, L., Podolske, J., Hillyard, P., Liang, J., Gurney, K., Wunch, D. and Wennberg P. (2018). Southern California megacity CO_2, CH_4, and CO flux estimates using ground- and space-based remote sensing and a Lagrangian model, *Atmospheric Chemistry and Physics*, **18**, 16271-16291. doi:10.5194/acp-18-16271-2018

Henson, S. A., Beaulieu, C. and Lampitt, R. (2016). Observing climate change trends in ocean biogeochemistry: when and where. *Global Change Biology*, **22**, 1561–1571. doi:10.1111/gcb.13152

Heymann, J., Reuter, M., Buchwitx, M., Schneising, O., Bovensmann, H., Burrows, J. P., Massart, S., Kaiser, J. W., and Crisp, D. (2017). CO_2 emission of Indonesian fires in 2015 estimated from satellite-derived atmospheric CO_2 concentrations. *Geophysical Research Lett*ers, 44, 1537-1544. doi: 10.1002/2016GL072042

Hoppema, M., Bakker, K., van Heuven, S. M. A. C., van Ooijen, J. C. and de Baar, H. J. W. (2015). Distributions, trends and inter-annual variability of nutrients along a repeat section through the Weddell Sea (1996–2011). *Marine Chemistry*, **177**, 545–553. doi:10.1016/j.marchem.2015.08.007

Houghton, R. A. (2003). Revised estimates of the annual net flux of carbon to the atmosphere from changes in land use and land management 1850–2000. *Tellus*, **55B**, 378–390. doi:10.1034/j.1600-0889.2003.01450.x

Houghton, R. A. and Nassikas, A. A. (2017). Global and regional fluxes of carbon from land use and land cover change 1850–2015. *Global Biogeochemical Cycles*, **31**, 456–472. doi:10.1002/2016GB005546

Hubau, W., Lewis, S. L., Phillips O. L., Affum-Baffoe, Beeckman, K. H., Cuni-Sanchez, A., Ewango, C. E. N., Fauset, S., Sheil, D., Sonké, B., Sullivan, M. J. P., Sunderland,T., Thomas, S. C., Abernethy, K. A., Adu-Bredu, S., Amani C. A., Baker, T. R., Banin, L. F., Baya, F., Begne, S. K., Bennett, A. C., Benedet, F., Bitariho, R., Bocko, Y. E., Boeckx, P., Boundja, P., Brienen, R. J. W., Brncic, T., Chezeaux, E., Chuyong, G. B., Clark, C. J., Collins, M., Comiskey, J. A., Coomes, D. A., Dargie, G. C., de Haulleville, T., Kamdem, M. N. D., Doucet, J. L., Esquivel-Muelbert, A., Feldpausch, T. R., Fofanah, A., Foli, E. G., Gilpin, M., Gloor, E., Gonmadje, C., Gourlet-Fleury, S., Hall, J. S., Hamilton, A. C., Harris, D. J., Hart, T. B., Hockemba, M. B. N., Hladik, A., Ifo, S. F., Jeffery, K. J., Jucker, T., Yakusu, E. K., Kearsley, E., Kenfack, D., Koch, A., Leal, M. E., Levesley, A., Lindsell, J. A., Lisingo, J., Lopez-Gonzalez, G., Lovett, J. C., Makana, J. R., Malhi, Y., Marshall, A. R., Martin, J., Martin, E. H., Mbayu, F. M., Medjibe ,V. P., Mitchard, E. T. A., Moore, S., Munishi, P. K. T., Bengone, N. N., Ojo, L., Ondo, F. E., Peh, K. S.,

Pickavance, G. C., Poulsen, A. D., Poulsen, J. R., Qie, L., Reitsma, J., Rovero, F., Swaine, M. D., Talbot, J., Taplin J., Taylor, D. D., Thomas, D. W., Toirambe, B., Mukendi, J. T., Tuagben, D., Umunay, P. M., van der Heijden, G. M. F., Verbeeck, H., Vleminckx, J., Willcock, S., Wöll, H., Woods, J. T. and Zemagho, L. (2020). Asynchronous carbon sink saturation in African and Amazonian tropical forests. *Nature*, **579**, 80–87. doi:10.1038/s41586-020-2035-0

Huber, M. B. and Zanna, L. (2017). Drivers of uncertainty in simulated ocean circulation and heat uptake. *Geophysical Research Letters*, **44**(3), 1402-1413. doi:10.1002/2016GL071587

Hurtt, G. C., Chini, L., Sahajpal, R., Frolking, S., Bodirsky, B. L., Calvin, K., Doelman, J. C., Fisk, J., Fujimori, S., Klein Goldewijk, K., Hasegawa, T., Havlik, P., Heinimann, A., Humpenöder, F., Jungclaus, J., Kaplan, J. O., Kennedy, J., Krisztin, T., Lawrence, D., Lawrence, P., Ma, L., Mertz, O., Pongratz, J., Popp, A., Poulter, B., Riahi, K., Shevliakova, E., Stehfest, E., Thornton, P., Tubiello, F. N., van Vuuren, D. P. and Zhang, X. (2020). Harmonization of global land use change and management for the period 850–2100 (LUH2) for CMIP6. *Geosci. Model Dev.*, **13**, 5425–5464. doi:10.5194/gmd-135425-2020

Iida, T., Odate, T., Fukuchi, M. (2013). Long-Term Trends of Nutrients and Apparent Oxygen Utilization South of the Polar Front in Southern Ocean Intermediate Water from 1965 to 2008. *PLoS ONE*, **8**, e71766. doi:10.1371/journal.pone.0071766

IEA World Energy Balances, 2020 Edition. Available from https://www.iea.org/subscribe-to-data-services/world-energy-balances-and-statistics, last viewed on 2 February 2021.

IPCC 2006, 2006 IPCC Guidelines for National Greenhouse Gas Inventories, Prepared by the National Greenhouse Gas Inventories Programme, Eggleston H.S., Buendia L., Miwa K., Ngara T. and Tanabe K. (eds). Published: IGES, Japan.

IPCC 2019, 2019 Refinement to the 2006 IPCC Guidelines for National Greenhouse Gas Inventories, Calvo Buendia, E., Tanabe, K., Kranjc, A., Baasansuren, J., Fukuda, M., Ngarize S., Osako, A., Pyrozhenko, Y., Shermanau, P. and Federici, S. (eds). Published: IPCC, Switzerland.

Ito, A. (2020). Constraining size-dependence of vegetation respiration rates, *Scientific Reports*, **10**, 4304. doi:10.1038/s41598-020-61239-0

Iudicone, D., Rodgers, K. B., Plancherel, Y., Aumont, O., Ito, T., Key, R. M., Madec, G. and Ishii, M. (2016). The formation of the ocean's anthropogenic carbon reservoir. *Scientific Reports*, **6**, 35473. doi:10.1038/srep35473

Jacobson, A. R., Mikaloff Fletcher, S. E., Gruber, N., Sarmiento, J. L. and Gloor, M. (2007). A joint atmosphere-ocean inversion for surface fluxes of carbon dioxide: 1. Methods and global-scale fluxes. *Global Biogeochemical Cycles*, **21**(1), 273. doi:10.1029/1999GL900363

Janssens-Maenhout, G., Crippa, M., Guizzardi, D., Muntean, M., Schaaf, E., Dentener, F., Bergamaschi, P., Pagliari, V., Olivier, J. G. J., Peters, J. A. H. W., van Aardenne, J. A., Monni, S., Doering, U., Petrescu, A. M. R., Solazzo, E. and Oreggioni, G. D. (2019).

EDGAR v4.3.2 Global Atlas of the three major greenhouse gas emissions for the period 1970–2012. *Earth Syst. Sci. Data*, **11**, 959-1002. doi:10.5194/essd-11-959-2019

Janssens-Maenhout, G., Pinty, B., Dowell, M., Zunker, H., Andersson, E., Balsamo, G., Bézy, J. L., Brunhes, T., Bösch, H., Bojkov, B., Brunner, D., Buchwitz, M., Crisp, D., Ciais, P., Counet, P., Dee, D., Denier van der Gon, H., Dolman, H., Drinkwater, M., Dubovnik O., Engelen, R., Fehr, T., Fernandez, V., Heimann, M., Holmlund, K., Houweling, S., Husband, R., Juvyns, O., Kentarchos, A., Landgraf, J., Lang, R., Löscher, A., Marshall, J., Meijer, Y., Nakajima, M., Palmer, P. I., Peylin, P., Rayner, P., Scholze, M., Sierk, B., Tamminen, J., Veefkind, P. (2020). Toward an operational anthropogenic CO_2 emissions monitoring and verification support capacity. *Bulletin of the American Meteorological Society*, **101**(8), E1439-E1451. doi:10.1175/BAMS-D-19-0017.1

Jian, J., Vargas, R., Anderson-Teixeira, K., Stell, E., Herrmann, V., Horn, M., Kholod, N., Manzon, J., Marchesi, R., Paredes, D. and Bond-Lamberty, B. (2020). A restructured and updated global soil respiration database (SRDB-V5). *Earth Syst. Sci. Data Discuss.* [preprint], doi:10.5194/essd-2020-136, in review.

Johnson, K. S., Jannasch, H. W., Coletti, L. J., Elrod, V. A., Martz, T. R., Takeshita, Y., Carlson, R. J. and Connery, J. G. (2016). Deep-Sea DuraFET: A pressure tolerant pH sensor designed for global sensor networks. *Analytical Chemistry*, **88**, 3249-3256. doi:10.1021/acs.analchem.5b04653

Jones, C. D. and P. M. Cox (2005). On the significance of atmospheric CO_2 growth rate anomalies in 2002– 2003. *Geophysical Research Letters*, **32**, L14816. doi:10.1029/2005GL023027

Joos, F., Bruno, M., Fink, R., Siegenthaler, U., Stocker, T. F., Le Quéré, C. and Sarmiento, J. L. (1996). An efficient and accurate representation of complex oceanic and biospheric models of anthropogenic carbon uptake. *Tellus B*, **48**, 397. doi:10.1034/j.1600-0889.1996.t01-2-00006.x

Jung, M., Reichstein, M. and Bondeau, A. (2009). Towards global empirical upscaling of FLUXNET eddy covariance observations: validation of a model tree ensemble approach using a biosphere model. *Biogeosciences*, **6**, 2001–2013. doi:10.5194/bg-6-2001-2009

Jung, M., Schwalm, C. Migliavacca, M., Walther, S., Camps-Valls, G., Koirala, S., Anthoni, P., Besnard, S., Bodesheim, P., Carvalhais, N., Chevallier, F., Gans, F., Goll, D. S., Haverd, V., Koehler, P., Ichii, K., Jain, A. K., Liu, J., Lombardozzi, D., Nabel, J. E. M. S., Nelson, J. A., O'Sullivan, M., Pallandt, M., Papale, D., Peters, W., Pongratz, J., Roedenbeck, C., Sitch, S., Tramontana, G., Walker, A., Weber, U. and Reichstein, M. (2020). Scaling carbon fluxes from eddy covariance sites to globe: synthesis and evaluation of the FLUXCOM approach. *Biogeosciences*, **17**, 1343–1365. doi: 10.5194/bg-17-1343-2020

Karion, A., Sweeney, C., Tans, P. P. and Newberger, T. (2010). AirCore: An innovative atmospheric sampling system. *Journal of Atmospheric and Oceanic Technology*, **27**, 1839–1853. doi:10.1175/2010JTECHA1448.1

Keenan, T. F., and Williams, C. A. (2018). The terrestrial carbon sink. *Annual Review of Environment and Resources*. **43**, 219-243. doi:10.1146/annurev-environ- 102017-030204

Keppler, L., Landschützer, P. (2019). Regional wind variability modulates the Southern Ocean carbon sink. *Scientific Reports*, **9**, 7384. doi:10.1038/s41598-019-43826-y

Key, R. M., Kozyr, A., Sabine, C. L., Lee, K., Wanninkhof, R., Bullister, J. L., Feely, R. A., Millero, F. J., Mordy, C. and Peng, T. H. (2004). A global ocean carbon climatology: Results from Global Data Analysis Project (GLODAP). *Global Biogeochemical Cycles*, **18**(4), GB4031. doi:10.1029/2004GB002247

Khatiwala, S., Primeau, F. and Hall, T. (2009). Reconstruction of the history of anthropogenic CO_2 concentrations in the ocean. *Nature*, **462,** 346–349. doi:10.1038/nature08526

Khatiwala, S., Tanhua, T., Mikaloff Fletcher, S., Gerber, M., Doney, C. S., Graven, H. D., Gruber, N., Mckinley, G. A., Murata, A. and Sabine, C. (2013). Global storage of anthropogenic carbon. *Biogeosciences*, **10**, 2169-2191, 2013. doi: 10.519/bg-10-2169-2013

Kiel, M., O'Dell, C. W., Fisher, B., Eldering, A., Nassar, R., MacDonald, C. G. and Wennberg, P. O. (2019). How bias correction goes wrong: measurement of XCO_2 affected by erroneous surface pressure estimates. *Atmospheric Measurement Techniques*, **12**, 2241-2259. doi: 10.5194/amt-12-2241-2019

Knorr, W. (2009). Is the airborne fraction of anthropogenic CO_2 emissions increasing? *Geophysical Research Letters*, **36**, L21710. doi:10.1029/2009GL040613

Koren, G., van Schaik, E., Araujo, A. C., Boersma, K. F., Gartner, A., Killaars, L., Kooreman, M. L., Kruijt, B., van der Laan-Luijkx, I. T., von Randow, C., Smith, N. E., and Peters, W. (2018). Widespread reduction in sun-induced fluorescence from the Amazon during the 2015/2016 El Nino. *Philosophical Transactions of the Royal Society of London. Series B: Biological Sciences*, **373**(1760), 20170408. doi:10.1098/rstb.2017.0408

Lacroix, F., T. Ilyina, and J. Hartmann (2020). Oceanic CO_2 outgassing and biological production hotspots induced by pre-industrial river loads of nutrients and carbon in a global modeling approach. *Biogeosciences*, **17**(1), 55–88. doi:10.5194/bg-17-55-2020

Landschützer, P., Gruber, N., Bakker, D. C. E., Schuster, U., Nakaoka, S., Payne, M. R., Sasse, T. P. and Zeng, J. (2013). A neural network-based estimate of the seasonal to inter-annual variability of the Atlantic Ocean carbon sink. *Biogeosciences*, **10**, 7793–7815. doi:10.5194/bg-10-7793-2013

Landschützer, P., Gruber, N., Bakker, D. C. E. and Schuster, U. (2014). Recent variability of the global ocean carbon sink. *Global Biogeochemical Cycles*, **28**, 927–949. doi:10.1002/2014GB004853

Landschützer, P., Gruber, N., Haumann, F. A., Rödenbeck, C., Bakker, D. C. E., van Heuven, S., Hoppema, M., Metzl, N., Sweeney, C., Takahashi, T., Tilbrook, B. and Wanninkhof, R. (2015). The reinvigoration of the Southern Ocean carbon sink. *Science* **349**, 1221–1224. doi:10.1126/science.aab2620

Landschützer, P., Laruelle, G. G. , Roobaert, A. and Regnier, P. (2020). A uniform pCO_2 climatology combining open and coastal oceans. *Earth Syst. Sci. Data*, **12**, 2537–2553. doi:10.5194/essd-2020-90

Langlais, C. E., Lenton, A., Matear, R., Monselesan, D., Legresy, B., Cougnon, E. and Rintoul, S. (2017). Stationary Rossby waves dominate subduction of anthropogenic carbon in the Southern Ocean. *Scientific Reports*, **7**, 17076. doi:10.1038/s41598-017-17292-3

Laufkötter, C., Vogt, M., Gruber, N., Aita-Noguchi, M., Aumont, O., Bopp, L., Buitenhuis, E., Doney, S. C., Dunne, J., Hashioka, T., Hauck, J., Hirata, T., John, J., Le Quéré, C., Lima, I.D., Nakano, H., Seferian, R., Totterdell, I., Vichi, M. and Völker, C. (2015). Drivers and uncertainties of future global marine primary production in marine ecosystem models. *Biogeosciences*, **12**, 6955–6984. doi:10.5194/bg-12-6955-2015

Laufkötter, C., Vogt, M., Gruber, N., Aumont, O., Bopp, L., Doney, S.C., Dunne, J.P., Hauck, J., John, J.G., Lima, I.D., Seferian, R. and Völker, C. (2016). Projected decreases in future marine export production: the role of the carbon flux through the upper ocean ecosystem. *Biogeosciences*, **13**, 4023–4047. doi:10.5194/bg-13-4023-2016

Lenton, A. and Matear, R. J. (2007). Role of the Southern Annular Mode (SAM) in Southern Ocean CO_2 uptake. *Global Biogeochemical Cycles*, **21**, GB2016. doi:10.1029/2006GB002714

Le Quéré, C., Rödenbeck, C., Buitenhuis, E. T., Conway, T. J., Langenfelds, R., Gomez, A., Labuschagne, C., Ramonet, M., Nakazawa, T., Metzl, N., Gillett, N. and Heimann, M. (2007). Saturation of the Southern Ocean CO_2 Sink Due to Recent Climate Change. *Science*, **316**, 1735–1738. doi:10.1126/science.1136188

Le Quéré, C., Raupach, M. R., Canadell, J. G., Marland, G., Bopp, L., Ciais, P., Conway, T. J., Doney, S. C., Feely, R. A., Foster, P., Friedlingstein, P., Gurney, K., Houghton, R. A., House, J. I., Huntingford, C., Levy, P. E., Lomas, M. R., Majkut, J., Metzl, N., Ometto, J. P., Peters, G. P., Prentice, I. C., Randerson, J. T., Running, S. W., Sarmiento, J. L., Schuster, U., Sitch, S., Takahashi, T., Viovy, N., van der Werf, G. R. and Woodward, F. I. (2009). Trends in the sources and sinks of carbon dioxide. *Nature Geosciences*, **2**, 831–836. doi:10.1038/ngeo689

Le Quéré, C., Takahashi, T., Buitenhuis, E. T., Rödenbeck, C. and Sutherland, S. C. (2010). Impact of climate change and variability on the global oceanic sink of CO_2. *Global Biogeochemical Cycles*, **24**(4), GB4007. doi:10.1029/2009GB003599

Le Quéré, C., Andres, R. J., Boden, T., Conway, T., Houghton, R. A., House, J. I., Marland, G., Peters, G. P., van der Werf, G. R., Ahlström, A., Andrew, R. M., Bopp, L., Canadell, J. G., Ciais, P., Doney, S. C., Enright, C., Friedlingstein, P., Huntingford, C., Jain, A. K., Jourdain, C., Kato, E., Keeling, R. F., Klein Goldewijk, K., Levis, S., Levy, P., Lomas, M., Poulter, B., Raupach, M. R., Schwinger, J., Sitch, S., Stocker, B. D., Viovy, N., Zaehle and S. and Zeng, N. (2013). The global carbon budget 1959–2011. *Earth Syst. Sci. Data*, **5**, 165–185. doi:10.5194/essd-5-165-2013

Le Quéré, C., Peters, G. P., Andres, R. J., Andrew, R. M., Boden, T. A., Ciais, P., Friedlingstein, P., Houghton, R. A., Marland, G., Moriarty, R., Sitch, S., Tans, P., Arneth, A., Arvanitis, A., Bakker, D. C. E., Bopp, L., Canadell, J. G., Chini, L. P., Doney, S. C., Harper, A., Harris, I., House, J. I., Jain, A. K., Jones, S. D., Kato, E., Keeling, R. F., Klein Goldewijk, K., Körtzinger, A., Koven, C., Lefèvre, N., Maignan, F., Omar, A., Ono, T., Park, G.-H., Pfeil, B., Poulter, B., Raupach, M.R., Regnier, P., Rödenbeck, C., Saito, S., Schwinger, J., Segschneider, J., Stocker, B.D., Takahashi, T., Tilbrook, B., van Heuven,

S., Viovy, N., Wanninkhof, R., Wiltshire, A. and Zaehle, S. (2014). Global carbon budget 2013. *Earth Syst. Sci. Data*, **6**, 235–263. doi:10.5194/essd-6-235-2014

Le Quéré, C., Moriarty, R., Andrew, R. M., Peters, G. P., Ciais, P., Friedlingstein, P., Jones, S. D., Sitch, S., Tans, P., Arneth, A., Boden, T. A., Bopp, L., Bozec, Y., Canadell, J. G., Chini, L. P., Chevallier, F., Cosca, C. E., Harris, I., Hoppema, M., Houghton, R. A., House, J. I., Jain, A. K., Johannessen, T., Kato, E., Keeling, R. F., Kitidis, V., Klein Goldewijk, K., Koven, C., Landa, C. S., Landschützer, P., Lenton, A., Lima, I. D., Marland, G., Mathis, J. T., Metzl, N., Nojiri, Y., Olsen, A., Ono, T., Peng, S., Peters, W., Pfeil, B., Poulter, B., Raupach, M. R., Regnier, P., Rödenbeck, C., Saito, S., Salisbury, J. E., Schuster, U., Schwinger, J., Séférian, R., Segschneider, J., Steinhoff, T., Stocker, B. D., Sutton, A. J., Takahashi, T., Tilbrook, B., van der Werf, G. R., Viovy, N., Wang, Y.-P., Wanninkhof, R., Wiltshire, A. and Zeng, N. (2015). Global carbon budget 2014. *Earth Syst. Sci. Data*, **7**, 47–85. doi:10.5194/essd-7-47-2015

Le Quéré, C., Moriarty, R., Andrew, R. M., Canadell, J. G., Sitch, S., Korsbakken, J. I., Friedlingstein, P., Peters, G. P., Andres, R.J., Boden, T. A., Houghton, R. A., House, J. I., Keeling, R. F., Tans, P., Arneth, A., Bakker, D. C .E., Barbero, L., Bopp, L., Chang, J., Chevallier, F., Chini, L. P., Ciais, P., Fader, M., Feely, R. A., Gkritzalis, T., Harris, I., Hauck, J., Ilyina, T., Jain, A. K., Kato, E., Kitidis, V., Klein Goldewijk, K., Koven, C., Landschützer, P., Lauvset, S. K., Lefèvre, N., Lenton, A., Lima, I. D., Metzl, N., Millero, F., Munro, D. R., Murata, A., Nabel, J. E. M. S., Nakaoka, S., Nojiri, Y., O'Brien, K., Olsen, A., Ono, T., Pérez, F. F., Pfeil, B., Pierrot, D., Poulter, B., Rehder, G., Rödenbeck, C., Saito, S., Schuster, U., Schwinger, J., Séférian, R., Steinhoff, T., Stocker, B. D., Sutton, A. J., Takahashi, T., Tilbrook, B., van der Laan-Luijkx, I. T., van der Werf, G. R., van Heuven, S., Vandemark, D., Viovy, N., Wiltshire, A., Zaehle, S. and Zeng, N. (2015). Global Carbon Budget 2015. *Earth Syst. Sci. Data*, **7**, 349–396. doi:10.5194/essd-7-349-2015

Le Quéré, C., Andrew, R. M., Canadell, J. G., Sitch, S., Korsbakken, J. I., Peters, G. P., Manning, A. C., Boden, T. A., Tans, P. P., Houghton, R. A., Keeling, R. F., Alin, S., Andrews, O. D., Anthoni, P., Barbero, L., Bopp, L., Chevallier, F., Chini, L. P., Ciais, P., Currie, K., Delire, C., Doney, S. C., Friedlingstein, P., Gkritzalis, T., Harris, I., Hauck, J., Haverd, V., Hoppema, M., Klein Goldewijk, K., Jain, A. K., Kato, E., Körtzinger, A., Landschützer, P., Lefèvre, N., Lenton, A., Lienert, S., Lombardozzi, D., Melton, J. R., Metzl, N., Millero, F., Monteiro, P. M. S., Munro, D. R., Nabel, J. E. M. S., Nakaoka, S., O'Brien, K., Olsen, A., Omar, A. M., Ono, T., Pierrot, D., Poulter, B., Rödenbeck, C., Salisbury, J., Schuster, U., Schwinger, J., Séférian, R., Skjelvan, I., Stocker, B. D., Sutton, A. J., Takahashi, T., Tian, H., Tilbrook, B., van der Laan-Luijkx, I. T., van der Werf, G. R., Viovy, N., Walker, A. P., Wiltshire, A. J. and Zaehle, S. (2016). Global Carbon Budget 2016. *Earth Syst. Sci. Data*, **8**, 605–649. doi:10.5194/essd-8-605-2016

Le Quéré, C., Andrew, R. M., Friedlingstein, P., Sitch, S., Hauck, J., Pongratz, J., Pickers, P. A., Korsbakken, J .I., Peters, G. P., Canadell, J. G., Arneth, A., Arora, V. K., Barbero, L., Bastos, A., Bopp, L., Chevallier, F., Chini, L.P., Ciais, P., Doney, S. C., Gkritzalis, T., Goll, D. S., Harris, I., Haverd, V., Hoffman, F. M., Hoppema, M., Houghton, R. A., Hurtt, G., Ilyina, T., Jain, A.K., Johannessen, T., Jones, C. D., Kato, E., Keeling, R. F., Goldewijk, K. K., Landschützer, P., Lefèvre, N., Lienert, S., Liu, Z., Lombardozzi, D., Metzl, N., Munro, D. R., Nabel, J. E. M. S., Nakaoka, S., Neill, C., Olsen, A., Ono, T.,

Patra, P., Peregon, A., Peters, W., Peylin, P., Pfeil, B., Pierrot, D., Poulter, B., Rehder, G., Resplandy, L., Robertson, E., Rocher, M., Rödenbeck, C., Schuster, U., Schwinger, J., Séférian, R., Skjelvan, I., Steinhoff, T., Sutton, A., Tans, P. P., Tian, H., Tilbrook, B., Tubiello, F. N., van der Laan-Luijkx, I. T., van der Werf, G. R., Viovy, N., Walker, A. P., Wiltshire, A. J., Wright, R., Zaehle, S. and Zheng, B. (2018a). Global Carbon Budget 2018. *Earth Syst. Sci. Data,* **10**, 2141–2194. doi:10.5194/essd-10-2141-2018

Le Quéré, C., Andrew, R. M., Friedlingstein, P., Sitch, S., Pongratz, J., Manning, A. C., Korsbakken, J. I., Peters, G. P., Canadell, J. G., Jackson, R. B., Boden, T. A., Tans, P. P., Andrews, O. D., Arora, V. K., Bakker, D. C. E., Barbero, L., Becker, M., Betts, R. A., Bopp, L., Chevallier, F., Chini, L. P., Ciais, P., Cosca, C .E., Cross, J., Currie, K., Gasser, T., Harris, I., Hauck, J., Haverd, V., Houghton, R. A., Hunt, C. W., Hurtt, G., Ilyina, T., Jain, A. K., Kato, E., Kautz, M., Keeling, R. F., Klein Goldewijk, K., Körtzinger, A., Landschützer, P., Lefèvre, N., Lenton, A., Lienert, S., Lima, I., Lombardozzi, D., Metzl, N., Millero, F., Monteiro, P. M. S., Munro, D. R., Nabel, J. E. M. S., Nakaoka, S., Nojiri, Y., Padin, X. A., Peregon, A., Pfeil, B., Pierrot, D., Poulter, B., Rehder, G., Reimer, J., Rödenbeck, C., Schwinger, J., Séférian, R., Skjelvan, I., Stocker, B. D., Tian, H., Tilbrook, B., Tubiello, F. N., van der Laan-Luijkx, I. T., van der Werf, G. R., van Heuven, S., Viovy, N., Vuichard, N., Walker, A. P., Watson, A. J., Wiltshire, A. J., Zaehle, S. and Zhu, D. (2018b). Global Carbon Budget 2017. *Earth Syst. Sci. Data,* **10**, 405–448. doi:10.5194/essd-10-405-2018

Liu, J., Bowman, K., Schimel, D., Parazoo, N., Jiang, Z., Lee, M., Bloom, A., Wunch, D., Gurney, K., Menemenlis, D., Gierach, M., Crisp, D. and Eldering A. (2017). Contrasting carbon cycle responses of the tropical continents to the 2015–2016 El Niño. *Science,* **358**, eaam5690. doi: 10.1126/science.aam5690

Liu, J., Wennberg, P. O., Parazoo, N. C., Yin, Y. and Frankenberg, C. (2020). Observational constraints on the response of high-latitude northern forests to warming. *AGU Advances,* **2**, e2020AV000228. doi:10.1029/2020AV000228

Liu, Z., Dreybrodt, W. and Wang, H. (2010). A new direction in effective accounting for the atmospheric CO_2 budget: Considering the combined action of carbonate dissolution, the global water cycle and photosynthetic uptake of DIC by aquatic organisms. *Earth Science Reviews,* **99**, 169-172. doi:10.1016/j.earscirev.2010.03.001

Long, M. C., Lindsay, K., Peacock, S., Moore, J. K., and Doney, S. C. (2013). Twentieth-century oceanic carbon uptake and storage in CESM1(BGC). *Journal of Climate*, **26**, 6775–6800. doi:10.1175/JCLI-D-12-00184.1

Lovenduski, N. S., Gruber, N. and Doney, S.C. (2008). Toward a mechanistic understanding of the decadal trends in the Southern Ocean carbon sink: Southern Ocean CO_2 flux trends. *Global Biogeochemical Cycles,* **22**(3), GB3016. doi:10.1029/2007GB003139

Lovenduski, N. S., Gruber, N., Doney, S. C. and Lima, I. D. (2007). Enhanced CO_2 outgassing in the Southern Ocean from a positive phase of the Southern Annular Mode. *Global Biogeochemical Cycles,* **21**(2), GB2026. doi:10.1029/2006GB002900

Lucht, W., Prentice, C., Myneni, R. B., Sitch, S., Friedlingstein, P., Cramer, W., Bousquet, P., Buermann, W. and Smith, B. (2002). Climatic control of the high-latitude vegetation

greening trend and Pinatubo effect. *Science*, **296**(5573), 1687–1689. doi:10.1126/science.1071828

MacDougall, A. H., Frölicher, T. L., Jones, C. D., Rogelj, J., Matthews, H. D., Zickfeld, K., Arora, V. K., Barrett, N. J., Brovkin, V., Burger, F. A., Eby, M., Eliseev, A. V., Hajima, T., Holden, P. B., Jeltsch-Thömmes, A., Koven, C., Mengis, N., Menviel, L., Michou, M., Mokhov, I. I., Oka, A., Schwinger, J., Séférian, R., Shaffer, G., Sokolov, A., Tachiiri, K., Tjiputra , J., Wiltshire, A. and Ziehn, T. (2020). Is there warming in the pipeline? A multi-model analysis of the zero emissions commitment from CO_2. *Biogeosciences*, **17**, 2987–3016. doi:10.5194/bg-17-2987-2020

Maier-Reimer, E. (1993). Geochemical cycles in an ocean general circulation model. Preindustrial tracer distributions. *Global Biogeochemical Cycles*, **7**, 645–677, 1993. doi:10.1029/93GB01355

Marsay, C.M., Sanders, R. J., Henson, S. A., Pabortsava, K., Achterberg, E. P. and Lampitt, R. S. (2015). Attenuation of sinking particulate organic carbon flux through the mesopelagic ocean. *Proceedings of the National Academy of Sciences*, **112**, 1089. doi:10.1073/pnas.1415311112

Mau, A. C., Reed, S. C., Wood, T. E. and Cavaleri, M. A. (2018). Temperate and tropical forest canopies are already functioning beyond their thermal thresholds for photosynthesis. *Forests*, **9**, 47. doi:10.3390/f9010047

McKinley, G., Follows, M., and Marshall, J. (2004). Mechanisms of air-sea CO_2 flux variability in the equatorial Pacific and the North Atlantic. *Global Biogeochemical Cycles*, **18**(2), GB2011. doi:10.1029/2003GB002179

McKinley, G. A., Fay, A. R., Takahashi, T. and Metzl, N. (2011). Convergence of atmospheric and North Atlantic carbon dioxide trends on multidecadal timescales. *Nature Geosci*, **4**, 606–610. doi:10.1038/ngeo1193

McKinley, G. A., Pilcher, D. J., Fay, A. R., Lindsay, K., Long, M. C. and Lovenduski, N. S. (2016). Timescales for detection of trends in the ocean carbon sink. *Nature*, **530**(7591), 469–472. doi:10.1038/nature16958

McKinley, G. A., Fay, A. R., Lovenduski ,N. S. and Pilcher, D. J. (2017). Natural variability and anthropogenic trends in the ocean carbon sink. *Annual Review of Marine Science*, **9**(1), 125–150, doi:10.1146/annurev-marine-010816-060529

McKinley, G. A., Fay, A. R., Eddebbar, Y. A., Gloege L. and Lovenduski, N. S. (2020). External forcing explains recent decadal variability of the ocean carbon sink. *AGU Advances*, **1**(2), 1, e2019AV000149. doi:10.1029/2019AV000149

Mikaloff Fletcher, S. E., Gruber, N., Jabobson, A. R., Doney, S., C., Sutkiewicz, S., Gerber, M., Follows, M., Joos, F., Lindsay, K., Menemenlis, D., Mouchet, A., Müller, S., A. and Sarmiento, J. L. (2006). Inverse estimates of anthropogenic CO_2 uptake, transport, and storage by the ocean, *Global Biogeochemical Cycles*, **20**, GB2002. doi:10.1029/2005GB002530

Miller, J. B., Lehman, S. J., Montzka, S. A., Sweeney, C., Miller, B. R., Karion, A., Wolak, C., Dlugokencky, E. J., Southon, J., Turnbull, J. C. and Tans, P. P. (2012). Linking emissions

of fossil fuel CO_2 and other anthropogenic trace gases using atmospheric $^{14}CO_2$. *Journal of Geophysical Research: Atmospheres*, **117**, D08302. doi:10.1029/2011JD017048

Miller, J. B., Lehman, S. J., Verhulst, K. R., Miler, C., E., Duren, R. M., Yadav, V., Newman, S. and Sloop, C. D. (2020). Large and seasonally varying biospheric CO_2 fluxes in the Los Angeles megacity revealed by atmospheric radiocarbon. *Proceedings of the National Academy of Sciences*, **117**, 26681-26687. doi:10.1073/pnas.2005253117

Mongwe, N. P., Vichi, M. and Monteiro, P. M. S. (2018). The seasonal cycle of pCO_2 and CO_2 fluxes in the Southern Ocean: diagnosing anomalies in CMIP5 Earth system models. *Biogeosciences*, **15**, 2851–2872. doi:10.5194/bg-15-2851-2018

Moore, J. K., Fu, W., Primeau, F., Britten, G. L., Lindsay, K., Long, M., Doney, S. C., Mahowald, N., Hoffman, F. and Randerson, J. T. (2018). Sustained climate warming drives declining marine biological productivity. *Science*, 359, 1139–1143. doi:10.1126/science.aao6379

Nassar, R., Hill, T. G., McLinden, C. A., Wunch, D., Jones, D. B.A. and Crisp D. (2017). Quantifying CO_2 emissions from individual power plants from space. *Geophysical Research Letters*, **44**(19), 10045-10053. doi:10.1002/2017GL074702

Oda, T., Maksyutov, S. and Andres, S. J. (2018). The Open-source Data Inventory for Anthropogenic Carbon dioxide (CO_2), version 2016 (ODIAC2016): A global, monthly fossil-fuel CO_2 gridded emission data product for tracer transport simulations and surface flux inversions. *Earth Syst. Sci. Data*, **10**, 87-107. doi:10.5194/essd-10-87-2018

O'Dell, C. W., Eldering, A., Wennberg, P. O., Crisp, D., Gunson, M. R., Fisher, B., Frankenberg, C., Kiel, M., Lindqvist, H., Mandrake, L., Merrelli, A., Natraj, V., Nelson, R. R., Osterman, G. B., Payne, V. H., Taylor, T. E., Wunch, D., Drouin, B. J., Oyafuso, F., Chang, A., McDuffie, J., Smyth, M., Baker, D. F., Basu, S., Chevallier, F., Crowell, S. M. R., Feng, L., Palmer, P. I., Dubey, M., García, O. E., Griffith, D. W. T., Hase, F., Iraci, L. T., Kivi, R., Morino, I., Notholt, J., Ohyama, H., Petri, C., Roehl, C. M., Sha, M. K., Strong, K., Sussmann, R., Te, Y., Uchino, O. and Velazco, V. A. (2018). Improved retrievals of carbon dioxide from Orbiting Carbon Observatory-2 with the version 8 ACOS algorithm, *Atmospheric Measurement Techniques*, **11**(12): 6539–6576. doi:10.5194/amt-11-6539-2018

Olsen, A., Lange, N., Key, R. M., Tanhua, T., Bittig, H. C., Kozyr, A., Àlvarez, M., Azetsu-Scott, K., Becker, S., Brown, P. J., Carter, B. R., Cotrim da Cunha, L., Feely, R. A., van Heuven, S., Hoppema, M., Ishii, M., Jeansson, E., Jutterström, S., Landa, C. S., Lauvset, S. K., Michaelis, P., Murata, A., Pérez, F. F., Pfeil, B., Schirnick, C., Steinfeldt, R., Suzuki, T., Tilbrook, B., Velo, A., Wanninkhof, R., and Woosley, R. J. (2021). GLODAPv2.2020 – the second update of GLODAPv2. *Earth Syst. Sci. Data Discuss.* doi:10.5194/essd-2020-165, in review, 2020.

Palmer, P. I., Feng, L., Baker, D., Chevallier, F., Bösch, H. and Somkuti, P. (2019). Net carbon emissions from African biosphere dominate pan-tropical atmospheric CO_2 signal, *Nature Communications*, **10**, 3344. doi:10.1038/s41467-019-11097-w

Pan, Y., Birdsey, R. A., Fang, J., Houghton, R., Kauppi, P. E., Kurz, W. A., Phillips, O. L., Shvidenko, A., Lewis, S. L., Canadell, J. G., Ciais, P., Jackson, R. B., Pacala, S. W., McGuire, A. S., Piao, S., Rautiainen, A., Sitch, S. and Hayes, D. (2011). A large and

2214 persistent carbon sink in the world's forests. Science, 333, 988-993.
2215 doi:10.1126/science.1201609

2216 Panassa, E., Santana-Casiano, J. M., González-Dávila, M., Hoppema, M., van Heuven, S. M. A.
2217 C., Völker, C., Wolf-Gladrow, D. and Hauck, J. (2018). Variability of nutrients and
2218 carbon dioxide in the Antarctic Intermediate Water between 1990 and 2014. *Ocean*
2219 *Dynamics*, **68**, 295–308. doi:10.1007/s10236-018-1131-2

2220 Parazoo, N. C., Magney, T., Norton, A., Raczka, B., Bacour, C., Maignan, F., Baker, I., Zhang,
2221 Y., Qiu, B., Shi, M., MacBean, N., Bowling, D. R., Burns, S., Blanken, P. D., Stutz, J.,
2222 Grossmann, K. and Frankenberg, C. (2020). Wide discrepancies in the magnitude and
2223 direction of modeled solar-induced chlorophyll fluorescence in response to light
2224 conditions. *Biogeosciences*, **17**, 3733–3755. doi:10.5194/bg-17-3733-2020

2225 Pardo, P. C., Tilbrook, B., Langlais, C., Trull, T.W. and Rintoul, S. R. (2017). Carbon uptake
2226 and biogeochemical change in the Southern Ocean, south of Tasmania. *Biogeosciences*,
2227 **14**, 5217–5237. doi:10.5194/bg-14-5217-2017

2228 Pearson, T. R. H., Brown, S., Murray, L. and Sidman, G. (2017). Greenhouse gas emissions from
2229 tropical forest degradation: an underestimated source. *Carbon Balance and Management*,
2230 **12**, 3. doi:10.1186/s13021-017-0072-2

2231 Peng, B., Guan, K. Y., Zhou, W. , Jiang, C. Y., Frankenberg, C., Sun, Y., He, L. Y. and Kohler,
2232 P. (2020). Assessing the benefit of satellite-based Solar-Induced Chlorophyll
2233 Fluorescence in crop yield prediction. *International Journal of Applied Earth*
2234 *Observation and Geoinformation*, **90**, 102126. doi:10.1016/j.jag.2020.102126

2235 Petrescu, A. M. R., Peters, G. P., Janssens-Maenhout, G., Ciais, P., Tubiello, F. N., Grassi, G.,
2236 Nabuurs, G.-J., Leip, A., Carmona-Garcia, G., Winiwarter, W., Höglund-Isaksson, L.,
2237 Günther, D., Solazzo, E., Kiesow, A., Bastos, A., Pongratz, J., Nabel, J. E. M. S.,
2238 Conchedda, G., Pilli, R., Andrew, R. M., Schelhaas, M.-J. and Dolman, A. J. (2020).
2239 European anthropogenic AFOLU greenhouse gas emissions: a review and benchmark
2240 data. *Earth Syst. Sci. Data*, **12**, 961–1001, doi:10.5194/essd-12-961-2020

2241 Pfeil, B., Olsen, A., Bakker, D. C. E., Hankin, S., Koyuk, H., Kozyr, A., Malczyk, J., Manke, A.,
2242 Metzl, N., Sabine, C. L., Akl, J., Alin, S. R., Bates, N., Bellerby, R. G. J., Borges, A.,
2243 Boutin, J., Brown, P. J., Cai, W.-J., Chavez, F. P., Chen, A., Cosca, C., Fassbender, A. J.,
2244 Feely, R. A., González-Dávila, M., Goyet, C., Hales, B., Hardman-Mountford, N.,
2245 Heinze, C., Hood, M., Hoppema, M., Hunt, C. W., Hydes, D., Ishii, M., Johannessen, T.,
2246 Jones, S. D., Key, R. M., Körtzinger, A., Landschützer, P., Lauvset, S. K., Lefèvre, N.,
2247 Lenton, A., Lourantou, A., Merlivat, L., Midorikawa, T., Mintrop, L., Miyazaki, C.,
2248 Murata, A., Nakadate, A., Nakano, Y., Nakaoka, S., Nojiri, Y., Omar, A. M., Padin, X.
2249 A., Park, G.-H., Paterson, K., Perez, F. F., Pierrot, D., Poisson, A., Ríos, A. F., Santana-
2250 Casiano, J. M., Salisbury, J., Sarma, V. V. S. S., Schlitzer, R., Schneider, B., Schuster,
2251 U., Sieger, R., Skjelvan, I., Steinhoff, T., Suzuki, T., Takahashi, T., Tedesco, K.,
2252 Telszewski, M., Thomas, H., Tilbrook, B., Tjiputra, J., Vandemark, D., Veness, T.,
2253 Wanninkhof, R., Watson, A. J., Weiss, R., Wong, C. S. and Yoshikawa-Inoue, H. (2013).
2254 A uniform, quality controlled Surface Ocean CO_2 Atlas (SOCAT). *Earth Syst. Sci. Data*,
2255 **5**, 125–143. doi:10.5194/essd-5-125-2013

Piao, S., Wang, X., Park, T., Chen, C., Lian, X., He, Y. Bjerke, J. W., Chen, A., Ciais, P., Tommervik, H., Nemani, R. R. and Myneni, R. B. (2020). Characteristics, drivers and feedbacks of global greening. *Nat. Rev. Earth Environ.*, **1**, 14–27. doi:10.1038/s43017-019-0001-x

Quegan, S., Toan, L. T., Chave, J., Dall, J., Exbrayat, J. F., Minh, D. H. T., Lomas, M., D'Alessandro, M. M., Paillou, P., Papathanassiou, K., Rocca, F., Saatchi, S., Scipal, K., Shugart, H., Smallman, T. L., Soja, M. J., Tebaldini, S., Ulander, L., Villard, L. and Williams, M. (2019). The European Space Agency BIOMASS mission: measuring forest above-ground biomass from space. *Remote Sens. Environ.*, **227**, 44–60. doi:10.1016/j.rse.2019.03.032

Qiu, B., Ge, J., Guo, W. D., Pittman, A. J. and Mu, M. Y. (2020). Responses of Australian dryland vegetation to the 2019 heat wave at a sub daily scale. *Geophysical Research Letters*, **47**, e2019GL086569. doi:10.1029/2019GL086569

Ramankutty N., Gibbs, H. K., Achard, F., Defries, R., Foley, J. A. and Houghton, R. A. (2007). Challenges to estimating carbon emissions from tropical deforestation. *Global Change Biology*, **13**, 51–66. doi: 10.1111/j.1365-2486.2006.01272.x

Randerson, J. T., Hoffman, F. M., Thornton, P. E., Mahowald, N. M., Lindsay, K., Lee, Y. H., Nevison, C. D. Doney, S. C., Bonan, G., Stöckli, R., Covey, C., Running, S. W. and Fung, I. Y. (2009). Systematic assessment of terrestrial biogeochemistry in coupled climate–carbon models. *Global Change Biology*, **15**(10), 2462-2484. doi: 10.1111/j.1365-2486.2009.01912.x

Randerson, J. T., Lindsay, K., Munoz, E., Fu, W., Moore, J. K., Hoffman, F. M., Mahowald, N. M. and Doney, S. C. (2015). Multi-century changes in ocean and land contributions to the climate-carbon feedback. *Global Biogeochemical Cycles*, **29**, 744-759. doi:10.1002/2014GB005079

Raupach, M. R., Canadell, J. G. and Le Quéré, C. (2008). Anthropogenic and biophysical contributions to increasing atmospheric CO_2 growth rate and airborne fraction. *Biogeosciences*, **5**, 1601–1613. doi:10.5194/bg-5-1601-2008

Raupach, M. R., Gloor, M., Sarmiento, J. L., Canadell, J. G., Frölicher, T. L., Gasser, T., Houghton, R. A., Le Quéré, C. and Trudinger, C. M. (2014). The declining uptake rate of atmospheric CO_2 by land and ocean sinks. *Biogeosciences*, **11**(13), 3453–3475. doi:10.1007/s10584-009-9596-0

Regnier, P., Friedlingstein, P., Ciais, P., Mackenzie, F. T., Gruber, N., Janssens, I. A., Laruelle, G. G., Lauerwald, R., Luyssaert, S., Andersson, A. J., Arndt, S., Arnosti, C., Borges, A. V., Dale, A. W., Gallego-Sala, A., Goddéris, Y., Goossens, N., Hartmann, J., Heinze, C., Ilyina, T., Joos, F., LaRowe, D. E., Leifeld, J., Meysman, F. J. R., Munhoven, G., Raymond, P. A., Spahni, R., Suntharalingam, P. and Thullner, M. (2013). Anthropogenic perturbation of the carbon fluxes from land to ocean. *Nature Geosciences*, **6**, 597–607. doi:10.1038/ngeo1830

Resplandy, L., Keeling, R. F., Rodenbeck, C.,. Stephens, B. B, Khatiwala, S., Rodgers, K. B., Long, M. C., Bopp, L. and. Tans, P. P. (2018). Revision of global carbon fluxes based on a reassessment of oceanic and riverine carbon transport. *Nature Geoscience*, **11**, 504–509. doi:10.1038/s41561-018-0151-3

Reuter, M., Buchwitz, M., Schneising, O., Noël, S., Bovensmann, H. and Burrows, J. P. (2017). A fast atmospheric trace gas retrieval for hyperspectral instruments approximating multiple scattering—Part 2: Application to XCO_2 retrievals from OCO-2. *Remote Sensing*, **9**, 1102. doi: 10.3390/rs9111102

Reuter, M., Buchwitz., M., Schneising, O., Krautwurst, S., O'Dell, C. W., Richter, A., Bovensmann, H. and Burrows, J. P. (2019). Towards monitoring localized CO_2 emissions from space: Co-located regional CO_2 and NO_2 enhancements observed by the OCO-2 and S5P satellites. *Atmospheric Chemistry and Physics*, **19**, 9371–9383. doi:10.5194/acp-19-9371-2019

Ridge, S. M. and McKinley, G. A. (2020a). Advective controls on the North Atlantic anthropogenic carbon sink. *Global Biogeochemical Cycles*, **34**(7), 1138. doi:10.1029/2019GB006457

Ridge, S. M. and G. A. McKinley (2020b). Ocean carbon uptake under aggressive emission mitigation. *Biogeosciences Discussions* doi:10.5194/bg-2020-254, in review, 2020.

Rödenbeck, C., Bakker, D. C. E., Metzl, N., Olsen, A., Sabine, C., Cassar N., Reum, F., Keeling, R. F and Heimann, M. (2014). Interannual sea-air CO_2 flux variability from an observation-driven ocean mixed-layer scheme. *Biogeosciences*, **11**(1), 4599–4613. doi:10.5194/bg-11-4599-2014

Rödenbeck, C., Bakker, D. C. E., Gruber, N., Iida, Y., Jacobson, A. R., Jones, S., Landschützer, P., Metzl, N., Nakaoka, S., Olsen, A., Park, G.-H., Peylin, P., Rodgers, K. B., Sasse, T. P., Schuster, U., Shutler, J. D., Valsala, V., Wanninkhof, R. and Zeng, J. (2015). Data-based estimates of the ocean carbon sink variability – first results of the Surface Ocean pCO_2 Mapping intercomparison (SOCOM). *Biogeosciences*, **12**, 7251–7278. doi:10.5194/bg-12-7251-2015

Rodgers, K. B., Schlunegger, S., Slater, R. D., Ishii, M., Frolicher, T. L., Toyama, K., Plancherel, Y., Aumont, O. and Fassbender, A. J. (2020). Reemergence of anthropogenic carbon into the ocean's mixed layer strongly amplifies transient climate sensitivity. *Geophysics Research Letters*, **47**(18), 130. doi:10.1002/2017GL073758

Rosen, P., Hensley, S., Shaffer, S., Edelstein, W., Kim, Y., Kumar, R., Misra, T., Bhan, R., Satish, R. and Sagi, R. (2016). An update on the NASA-ISRO dual-frequency dbf SAR (NISAR) mission. *2016 IEEE International Geoscience and Remote Sensing Symposium*. IEEE, New York, pp. 2106–2108. doi:10.1109/IGARSS.2016.7729543

Rudnick, D. L. (2016). Ocean Research Enabled by Underwater Gliders. *Annual Review of Marine Science*, **8**, 519-541. doi:10.1146/annurev-marine-122414-033913

Saatchi, S. S., Harris, N. L., Brown, S., Lefsky, M., Mitchard, E. T. A., Salas, W., Zutta, B. R., Buermann, W., Lewis, S. L., Hagen, S., Petrova, S., White, L., Silman, M. and Morel, A. (2011). Benchmark map of forest carbon stocks in tropical regions across three continents. *Proceedings of the National Academy of Sciences*, **108**, 9899-9904. doi: 10.1073/pnas.1019576108

Sabine, C. L., Feely, R. A., Gruber, N., Key, R. M., Lee, K., Bullister, K. L., Wanninkhof, R. Wong, C. S., Wallace, D. W. R. Wallace, Tilbrook, B., Millero, F. J., Peng, T.-H., Kozyr,

A., Ono, T. and Rois, A. F. (2004). The oceanic sink for anthropogenic CO_2. *Science*, **305**, 367–371. doi:10.1126/science.1097403

Sabine, C. L. and Tanhua, T. (2010). Estimation of anthropogenic CO_2 inventories in the ocean. *Annual Reviews of Marine Sciences*, **2**, 175-198. doi:10.1146/annurev-marine-120308-080947

Sabine, C., Sutton, A., McCabe, K., Lawrence-Slavas, N., Alin, S., Feely, R., Jenkins, R., Maenner, S., Meinig, C., Thomas, J., van Ooijen, E., Passmore, A. and Tilbrook, B. (2020). Evaluation of a new carbon dioxide system for autonomous surface vehicles. *J. Atmos. Ocean. Technol.*, **37**, 1305-1317. doi:10.1175/JTECH-D-20-0010.1

Sarmiento, J. L., and Sundquist E. T. (1992). Revised budget for the oceanic uptake of anthropogenic carbon dioxide, *Nature*, **356**, 589–593. doi:10.1038/356589a0

Sarmiento, J. L. and Gruber, N. (2006). Ocean Biogeochemical Dynamics. Princeton University Press. ISBN: 0-691-01707-7. doi:10.1017/S0016756807003755

Scharlemann, J. P. W., Tanner, E. V. J., Hiederer, R. and Kapos, V. (2014). Global soil carbon: understanding and managing the largest terrestrial carbon pool. *Carbon Management*, **5**, 81-91. doi:10.4155/cmt.13.77

Schepaschenko, D., Moltchanova, E., Shvidenko, A., Blyshchyk, V., Dmitriev, E., Martynenko, O., See, L. and Kraxner F. (2018). Improved estimates of biomass expansion factors for russian forests. *Forests*, **9**, 312. doi:10.3390/f9060 312

Schourup-Kristensen, V., Sidorenko, D., Wolf-Gladrow, D. A. and Völker, C. (2014). A skill assessment of the biogeochemical model REcoM2 coupled to the Finite Element Sea Ice–Ocean Model (FESOM 1.3). *Geosci. Model Dev.*, **7**, 2769–2802. doi:10.5194/gmd-7-2769-2014

Schuur, E. A. G., McGuire, A. D., Schädel, C., Grosse, G., Harden, J. W., Hayes, D. J., Hugelius, G., Koven, C. D., Kuhry, P., Lawrence, D. M., Natali, S. M., Olefeldt, D., Romonovsky, V. E. Schaefer, K., Truetsky, M. R., Treat, C. C. and Vonk, J. E. (2015). Climate change and the permafrost carbon feedback. *Nature*, **520**, 171-179. doi:10.1038/nature14338

Schwinger, J., Tjiputra, J. F., Heinze, C., Bopp, L., Christian, J. R., Gehlen, M., Ilyina, T., Jones, C. D., Salas-Mélia, D., Segschneider, J., Séférian, R. and Totterdell, I. (2014). Nonlinearity of ocean carbon cycle feedbacks in CMIP5 Earth system models. *Journal of Climate*, **27**, 3869–3888. doi:10.1175/JCLI-D-13-00452.1

Schwinger, J., Goris, N., Tjiputra, J. F., Kriest, I., Bentsen, M., Bethke, I., Ilicak, M., Assmann, K. M. and Heinze, C. (2016). Evaluation of NorESM-OC (versions 1 and 1.2), the ocean carbon-cycle stand-alone configuration of the Norwegian Earth System Model (NorESM1). *Geosci. Model Dev.*, **9**, 2589–2622. doi:10.5194/gmd-9-2589-2016

Schwinger, J. and Tjiputra, J. (2018). Ocean carbon cycle feedbacks under negative emissions. *Geophysical Research Letters*, **26**(3), 5289. doi:10.1088/1748-9326/11/5/055006

Seelmann, K., Aßmann, S. and Körtzinger, A. (2019). Characterization of a novel autonomous analyzer for seawater total alkalinity: Results from laboratory and field tests. *Limnology and Oceanography: Methods*, **17**, 515-532. doi:10.1002/lom3.10329

2381 Sellers, P. J., Schimel, D. S., Moore III, B., Liu, J. and Eldering, A. (2018). Observing Carbon
2382 Cycle-Climate Feedbacks from Space, *Proceedings of the National Academy of Sciences*,
2383 **115**(31), 7860-7868. doi:10.1073/pnas.1716613115

2384 Sigman, D. M., Hain, M. P. and Haug, G. H. (2010). The polar ocean and glacial cycles in
2385 atmospheric CO_2 concentration. *Nature*, **466**, 47–55. doi:10.1038/nature09149

2386 Sitch, S., Friedlingstein, P., Gruber, N., Jones, S. D., Murray-Tortarolo, G., Ahlström, A.,
2387 Doney, S. C., Graven, H., Heinze, C., Huntingford, C., Levis, S., Levy, P. E., Lomas, M.,
2388 Poulter, B., Viovy, N., Zaehle, S., Zeng, N., Arneth, A., Bonan, G., Bopp, L., Canadell, J.
2389 G., Chevallier, F., Ciais, P., Ellis, R., Gloor, M., Peylin, P., Piao, S. L., Le Quéré, C.,
2390 Smith, B., Zhu, Z. and Myneni, R. (2015). Recent trends and drivers of regional sources
2391 and sinks of carbon dioxide. *Biogeosciences*, **12**, 653–679. doi:10.5194/bg-12-653-2015

2392 Smith P., Bustamante, M., Ahammad, H., Clark, H., Dong, H., Elsiddig, E. A., Haberl, H.,
2393 Harper, R., House, J., Jafari M., Masera, O., Mbow, C., Ravindranath N. H., Rice C. W.,
2394 Robledo Abad, C., Romanovskaya, A., Sperling, F. and Tubiello F. (2014) Agriculture,
2395 Forestry and Other Land Use (AFOLU). In: Climate Change 2014: Mitigation of Climate
2396 Change. Contribution of Working Group III to the Fifth Assessment Report of the
2397 Intergovernmental Panel on Climate Change [Edenhofer, O., R. Pichs-Madruga, Y.
2398 Sokona, E. Farahani, S. Kadner, K. Seyboth, A. Adler, I. Baum, S. Brunner, P.
2399 Eickemeier, B. Kriemann, J. Savolainen, S. Schlömer, C. von Stechow, T. Zwickel and
2400 J.C. Minx (eds.)]. Cambridge University Press, Cambridge, United Kingdom and New
2401 York, NY, USA.

2402 Song, X.-P., Hansen, M. C., Stehman, S. V., Potapov, P. V., Tyukavina, A., Vermote, E. F. and
2403 Townshend, J. R. (2018). Global land change from 1982 to 2016. *Nature*, **560**., 639-343.
2404 doi:10.1038/s41586-018-0411-9

2405 Soong, J. L., Fuchslueger, L., Marañon-Jimenez, S., Torn, M. S., Janssens, I. A., Penuelas, J.,
2406 and Richter, A. (2019). Microbial carbon limitation, 2021. The need for integrating
2407 microorganisms into our understanding of ecosystem carbon cycling. *Global Change*
2408 *Biology*, **26**, 1953–1961. doi:10.1111/gcb.14962

2409 Spawn, S. A., Sullivan, C. C., Lark, T. J. and Gibbs, H. K. (2020). Harmonized global maps of
2410 above and belowground biomass carbon density in the year 2010. *Scientific Data*, **7,** 112.
2411 doi:10.1038/s41597-020-0444-4

2412 Stamell, J., Rustagi, R. R., Gloege, L. and McKinley, G. A. (2021). Strengths and weaknesses of
2413 three Machine Learning methods for pCO_2 interpolation. *Geosci. Model Dev. Discuss.*
2414 [preprint], https://doi.org/10.5194/gmd-2020-311, in review, 2020.

2415 Stock, C. A., Dunne, J. P., Fan, S., Ginoux, P., John, J., Krasting, J. P., Laufkötter, C., Paulot, F.
2416 and Zadeh, N. (2020). Ocean biogeochemistry in GFDL's Earth System Model 4.1 and its
2417 response to increasing atmospheric CO_2. *J. Adv. Model. Earth Syst.*, **12**,
2418 e2019MS002043. doi:10.1029/2019MS002043

2419 Sun, Y., Frankenberg, C., Jung, J., Joiner, J., Guanter, L., Köhler, P. and Magney, T. (2018).
2420 Overview of solar-Induced chlorophyll fluorescence (SIF) from the Orbiting Carbon
2421 Observatory-2: Retrieval, cross-mission comparison, and global monitoring for GPP.
2422 *Remote Sensing of Environment*, **209**, 808-823. doi:10.1016/j.rse.2018.02.016

Sundquist, E.T., (1993). The global carbon dioxide budget. *Science*, **259**, 934–941. doi:10.1126/science.259.5097.934

Sutton, A. J., Sabine, C. L., Maenner-Jones, S., Lawrence-Slavas, N., Meinig, C., Feely, R. A., Mathis, J. T., Musielewicz, S., Bott, R., McLain, P. D., Fought, H. J. and Kozyr, A. (2014). A high-frequency atmospheric and seawater pCO_2 data set from 14 open-ocean sites using a moored autonomous system. *Earth Syst. Sci. Data*, **6**, 353-366. doi:10.5194/essd-6-353-2014

Takahashi, T., Sutherland, S. C., Sweeney, C., Poisson, A., Metzl, N., Tilbrook, B., Bates, N., Wanninkhof, R., Feely, R. A., Sabine, C., Olafsson, J., Nojiri, Y. (2002). Global sea–air CO_2 flux based on climatological surface ocean pCO_2, and seasonal biological and temperature effects. *Deep Sea Research Part II: Topical Studies in Oceanography*, **49**, 9–10, 1601-1622. doi:10.1016/S0967-0645(02)00003-6

Takahashi, T., Sutherland, S. C., Wanninkhof, R., Sweeney, C., Feely, R. A., Chipman, D. W., Hales, B., Friederich, G., Chavez, F., Sabine, C., Watson, A., Bakker, D. C. E., Schuster, U., Metzl, N., Yoshikawa-Inoue, H., Ishii, M., Midorikawa, T., Nojiri, Y., Körtzinger, A., Steinhoff, T., Hoppema, M., Olafsson, J., Arnarson, T.S., Tilbrook, B., Johannessen, T., Olsen, A., Bellerby, R., Wong, C. S., Delille, B., Bates, N. R. and de Baar, H. J. W. (2009). Climatological mean and decadal change in surface ocean pCO_2, and net sea–air CO_2 flux over the global oceans. *Deep Sea Research Part II: Topical Studies in Oceanography*, **56**, 554–577. doi:10.1016/j.dsr2.2008.12.009

Takeshita, Y., Johnson, K. S., Coletti, L. J., Jannasch, H. W., Walz, P. M. and Warren, J. K. (2020). Assessment of pH dependent errors in spectrophotometric pH measurements of seawater. *Marine Chemistry*, **223**, 103801. doi:10.1016/j.marchem.2020.103801

Takeshita, Y., Johnson, K. S., Martz, T. R., Plant, J. N. and Sarmiento, J. L. (2018). Assessment of autonomous pH measurements for determining surface seawater partial pressure of CO_2. *Journal of Geophysical Research: Oceans*, **123**, 4003-4013. doi:10.1029/2017jc013387

Tanhua, T., van Heuven, S., Key, R. M., Velo, A., Olsen, A. and Schirnick, C. (2010). Quality control procedures and methods of the CARINA database. *Earth Syst. Sci. Data* **2**, 35–49. doi:10.5194/essd-2-35-2010

Tanhua, T. and Keeling, R. F. (2012). Changes in column inventories of carbon and oxygen in the Atlantic Ocean. *Biogeosciences*, **9**, 4819-4833. doi:10.5194/bg-9-4819-2012

van der Werf, G. R., Randerson, J. T., Giglio, L., van Leeuwen, T. T., Chen, Y., Rogers, B. M., Mu, M., van Marle, M. J. E., Morton, D. C., Collatz, G. J., Yokelson, R. J. and Kasibhatla, P. S. (2017). Global fire emissions estimates during 1997–2016. *Earth Syst. Sci. Data*, **9**, 697–720. doi:10.5194/essd-9-697-2017

Verdy, A. Mazloff, M. R. (2017). A data assimilating model for estimating Southern Ocean biogeochemistry. *Journal of Geophysical Research: Oceans*, **122**, 6968–6988. doi:10.1002/2016JC012650

Wang, S., Zhang, Y., Hakkarainen, J., Ju, W., Liu, Y., Jiang, F. and He, W. (2018). Distinguishing anthropogenic CO_2 emissions from different energy intensive industrial

sources using OCO-2 observations: A case study in northern China. *Journal of Geophysical Research: Atmospheres*, **123**, 9462–9473. doi:10.1029/2018JD029005

Wang, S., Zhang, Y., Ju, W., Chen, J. M., Ciais, P., Cescatti, A., Sardans, J., Janssens, I. A., Wu, M., Berry, J. A., Campbell, E., Fernandez-Martinez, M., Alkama, R., Sitch, S., Friedlingstein, P., Smith, W. K., Yuan, W., He, W., Lombardozzi, D., Kautz, M., Zhu, D., Lienert, S., Kato, E., Poulter, B., Sanders, T. G. M., Kruger, I., Wang, R., Zeng, N., Tian, H., Vulchard, N., Jian, A., K., Wiltshire, A., Haverd, V., Goll, D. S. and Penuelas, J. (2020). Recent global decline of CO_2 fertilization effects on vegetation photosynthesis. *Science*, **370**, 1295–1300. doi: 10.1126/science.abb7772

Watson, A. J., Schuster, U., Shutler, J. D., Holding, T., Ashton, I. G. C.,Landschützer, P. , Woolf, D. K. and Goddijn-Murphy, L. (2020). Revised estimates of ocean-atmosphere CO_2 flux are consistent with ocean carbon inventory. *Nature Communications*, **11**, 4422. doi:10.1038/s41467-020-18203-3

Waugh, D. W., Hall, T. M., McNeil, B. I., Key, R. and Matear, R. J. (2006). Anthropogenic CO_2 in the oceans estimated using transit-time distributions. *Tellus*, **58B**, 376-389. doi:10.1111/j.1600-0889.2006.00222.x

Welp, L., Keeling, R. and Meijer, H. A. J. (2011). Interannual variability in the oxygen isotopes of atmospheric CO_2 driven by El Niño. *Nature*, **477**, 579–582. doi:10.1038/nature10421

Wigneron, J.-P., Fan, L., Ciais, P., Bastos, A., Brandt, M., Chave, J., Saatchi, S., Baccini, A. and Fensholt, R. (2020). Tropical forests did not recover from the strong 2015–2016 El Niño event. *Science Advances*, **6**, eaay4603. doi:10.1126/sciadv.aay4603

Williams, N. L., Juranek, L. W., Feely, R. A., Johnson, K. S., Sarmiento, J. L., Talley, L. D., Dickson, A. G., Gray, A. R., Wanninkhof, R., Russell, J. L., Riser, S. C. and Takeshita, Y. (2017). Calculating surface ocean pCO_2 from biogeochemical Argo floats equipped with pH: An uncertainty analysis. *Global Biogeochemical Cycles*, **31**, 591-604. doi:10.1002/2016GB005541

Willey, J. D., Kieber, R. J., Eyman, M. S. and Avery Jr., G. B. (2000). Rainwater dissolved organic carbon: Concentrations and global flux. *Global Biogeochemical Cycles*, **14**, 139-148. doi: 10.1007/s11270-008-9774-0

Woolf, D. K., Shutler, J. D., Goddijn-Murphy, L., Watson, A. J., Chapron, B., Nightingale, P. D., Donlon, C. J., Piskozub, J., Yelland, M. J., Ashton, I., Holding, T., Schuster, U., Girard-Ardhuin, F., Grouazel, A., Piolle, J.-F., Warren, M., Wrobel-Niedzwiecka, I., Land, P. E., Torres, R., Prytherch, J., Moat, B., Hanafin, J., Ardhuin, F. and Paul, F. (2019). Key uncertainties in the recent air-sea flux of CO_2. *Global Biogeochemical Cycles*, **33**, 1548-1563. doi:10.1029/2018GB006041

Wu, D., Lin, J. C., Fasoli, B., Oda, T., Ye, X., Lauvaux, T., Yang, E. G. and Kort, E. A. (2018). A Lagrangian approach towards extracting signals of urban CO_2 emissions from satellite observations of atmospheric column CO_2 (XCO_2): X-Stochastic Time-Inverted Lagrangian Transport model ("X-STILT v1"). *Geoscientific Model Development*, **11**(12): 4843–4871. doi:10.5194/gmd-11-4843-2018

Wu, D. E., Lin, J. C., Oda, T. and Kort, E. A. (2020). Space-based quantification of per capita CO2 emissions from cities, *Environmental Research Letters*, **15**, 035004. doi:10.1088/1748-9326/ab68eb

Wunch, D., Wennberg, P. O., Osterman, G., Fisher, B., Naylor, B., Roehl, C. M., O'Dell, C., Mandrake, L., Viatte, C., Griffith, D. W., Deutscher, N. M., Velazco, V. A., Notholt, J., Warneke, T., Petri, C., De Maziere, M., Sha, M. K., Sussmann, R., Rettinger, M., Pollard, D., Robinson, J., Morino, I., Uchino, O., Hase, F., Blumenstock, T., Kiel, M., Feist, D. G., Arnold, S. G., Strong, K., Mendonca, J., Kivi, R., Heikkinen, P., Iraci, L., Podolske, J., Hillyard, P. W., Kawakami, S., Dubey, M. K., Parker, H. A., Sepulveda, E., Rodriguez, O. E. G., Te, Y., Jeseck, P., Gunson, M. R., Crisp, D. and Eldering, A. (2017). Comparisons of the Orbiting Carbon Observatory-2 (OCO-2) XCO_2 measurements with TCCON, *Atmospheric Measurement Tech*niques, **10**, 2209–2238. doi:10.5194/amt-10-2209-2017

Xiao, J., J. Chen, Davis, K. J. and Reichstein, M. (2012). Advances in upscaling of eddy covariance measurements of carbon and water fluxes. *Journal Geophysical Research: Biogeosciences*, **117**, G00J01. doi:10.1029/2011JG001889

Xiao, J., Chevallier, F., Gomez, C., Guanter, L., Hicke, J. A., Huete, A. R., Ichii, K., Ni, W., Pang, Y., Rahman, A. F. Sun, G., Yuan, W., Zhang, L. and Zhang, X. (2019). Remote sensing of the terrestrial carbon cycle: A review of advances over 50 years. Remote Sensing of Environment, 233, 111383. doi:10.1016/j.rse.2019.111383

Yin, Y., Byrne, B., Liu, J., Wennberg, P., Davis, K. J., Magney, T., Koehler, P., He, L., Jeyaram, R., Humphrey, V., Gerken, T., Feng, S., Digangi, J. P. and Frankenberg, C. (2020). Cropland carbon uptake delayed and reduced by 2019 Midwest floods. *AGU Advances*, **1**, e2019AV000140. doi:10.1029/2019AV000140

Zavarsky, A. and Marandino, C. A. (2019). The influence of transformed Reynolds number suppression on gas transfer parameterizations and global DMS and CO_2 fluxes. *Atmospheric Chemistry and Physics*, **19**, 1819-1834. doi:10.5194/acp-19-1819-2019

Zeebe, R. and Wolf-Gladrow, D. (2001). CO_2 in seawater: Equilibrium, kinetics, isotopes. *Elsevier Oceanogr. Ser.*, **65**, Elsevier, Amsterdam.

Zeng, N., Zhao, F., Collatz, G. J., Kalnay, E., Salawitch, R., West, T. O. and Guanter, L. (2014). Agricultural Green Revolution as a driver of increasing atmospheric CO_2 seasonal amplitude. *Nature*, **515**, 394–397. doi: 10.1038/nature13893

Zickfeld, K., MacDougall, A. H., and Matthews, H. D. (2016). On the proportionality between global temperature change and cumulative CO_2 emissions during periods of net negative CO_2 emissions. *Environmental Research Letters*, **11**(5), 055006, doi:10.1088/1748-9326/11/5/055006